JPL CONTRACT NO. 951144/SSD 60374R/SEPTEMBER 1966

HUGHES
HUGHES AIRCRAFT COMPANY
SPACE SYSTEMS DIVISION

DEVELOPMENT AND TEST OF AN ION ENGINE SYSTEM EMPLOYING MODULAR POWER CONDITIONING PROJECT FINAL REPORT

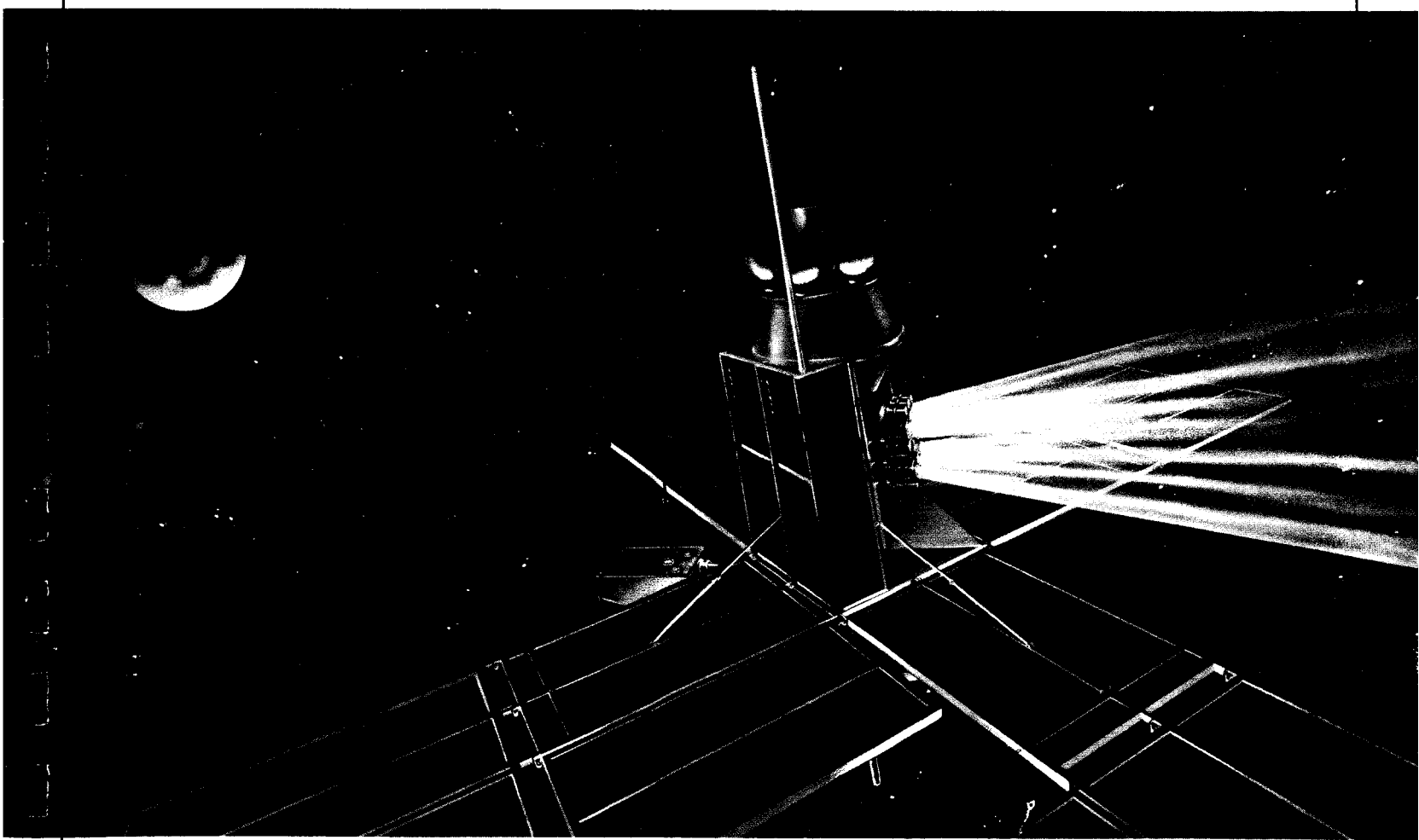

SOLAR POWERED ELECTRIC PROPULSION PROGRAM

DEVELOPMENT AND TEST OF AN ION ENGINE SYSTEM EMPLOYING MODULAR POWER CONDITIONING

Project Final Report

Approved: _____

J. H. Molitor, Project Manager
Hughes Research Laboratories

Approved: _____

R. N. Olson, Program Manager
Space Systems Division

JPL Contract No. 951144/August 1966

HUGHES

HUGHES AIRCRAFT COMPANY

This work was performed for the Jet Propulsion Laboratory, California Institute of Technology, sponsored by the National Aeronautics and Space Administration under Contract NAS7-100.

TABLE OF CONTENTS

LIST OF ILLUSTRATIONS

LIST OF TABLES

CONTRIBUTORS

The work to be reported in the following sections has been accomplished through the efforts of a number of people. These people have worked together as a closely coordinated team under the general supervision of the key personnel listed below. Although each of the persons noted were involved in the over-all system integration and test, an attempt is made to indicate the area of greatest participation in the subsystem development phase of the program.

Key Personnel

Mr. J. H. Molitor	Project Manager
Dr. H. J. King	Thruster and Feed System
Mr. W. J. Muldoon	Power Conditioning and Controls
Mr. D. G. Kovar	Power Conditioning and Controls.

SECTION I

INTRODUCTION

In February 1965 a program was initiated at Hughes Aircraft Company, under contract to the Jet Propulsion Laboratory, to determine the feasibility of solar powered electric propulsion systems for use in deep space missions of the near future. The over-all program was divided into a study phase and a hardware phase. The results of the initial study phase[1] indicated that solar-electric propulsion systems based on state-of-the-art technology and components could be developed at the present time for unmanned space exploration applications. Furthermore, it was shown that these systems, if properly designed, can be made highly reliable with minimal weight penalties and can meet the constraints imposed by spacecraft integration requirements. Finally, it was concluded that total ion propulsion system specific weights of 25 lb/kW or less were achievable and that these systems were potentially more attractive than all-chemical spacecraft, based on both mission performance and cost effectiveness.

During the study phase, analyses were conducted to establish the state of the art of the various components and subsystems associated with ion propulsion systems. Based on these analyses, choices were made on the types of thruster, feed system, engine control, and power conditioning to be considered for the spacecraft system design. (These comparative studies on feed and power conditioning systems are reviewed briefly in this report.) A major purpose of the hardware phase of the program was to verify experimentally the performance and designs established (and assumed) during the study effort. Therefore, the hardware verification effort was devoted to developing, integrating, and testing a complete ion engine system which would satisfy the requirements and constraints imposed by a solar powered, electrically propelled interplanetary spacecraft.

Specifically, the ultimate objective of the hardware program to be discussed in this report was to demonstrate in a 500 hour life test the operation of a complete engine system (including thruster, feed system, tankage, power conditioning, and engine controls) with a flight weight of less than 25 lb/kW. Initial power conditioning and control system designs were based on anticipated operation with a HRL 20 cm thruster. Later, at the request of the contracting agency, a 15 cm SERT-II type thruster was substituted. This substitution was made with some sacrifice in power conditioning operation and performance. Thus, the final system, which was to be operated completely closed loop in a space simulated vacuum and thermal environment, employed an oxide cathode mercury electron bombardment engine provided by NASA Lewis Research Center. The tankage, feed system, and power conditioning were designed and developed by Hughes. The primary control system was defined by NASA-LeRC and implemented by Hughes.

SECTION II

SUMMARY

The purpose of the effort reported herein was to establish the state of the art of ion propulsion technology and to show that ion propulsion systems can now be considered for near future unmanned interplanetary space missions. The hardware program included the development, integration, and test of a complete ion propulsion system. The system, which employed flight designed components and subsystems operated closed loop for 500 hours. The power conditioning and control system, as well as the thruster and feed system, was operated in a vacuum chamber which simulated the thermal environment of space.

The thruster employed was an oxide cathode mercury bombardment ion engine (weight ~7 lb) supplied to this program by NASA-LeRC. The oxide cathode used in the life test, however, was a "flower" cathode developed at HRL. With this cathode and other thruster modifications, the total input power required to operate the thruster and feed system was reduced from the original specification of approximately 1.5 kW to less than 1.2 kW.

The feed system developed for this program consists of a liquid mercury reservoir, a pressurizer, a solenoid valve, a vaporizer, and an isolator. The pressurizer and reservoir is essentially a single cylindrical unit in which the stored mercury is maintained at constant pressure by a movable piston driven by heating a small quantity of volatile liquid (in this case, water). Since the mercury pressure is directly related to the temperature of the pressurizer, no pressure sensor is required; a simple temperature regulation maintains constant (or controlled) mercury pressure. This system is readily scalable and can be expected to expel more than 95% of the liquid mercury contained in the reservoir. The vaporizer which separates the liquid and vapor phases of

the propellant, as well as controlling the vapor flowrate, is a tightly woven screen with nominal 2 μ apertures. The surface tension forces associated with these apertures will contain liquid mercury at pressures up to 1 atm; typical feed line pressures are 10 psi. Vapor flow to the thruster is obtained by temperature control of the vaporizer screen (i.e., control of the evaporation rate of mercury from the screen) with a dynamic response of 1% change per second at the operating point. The isolator which electrically decouples the high voltage thruster from the feed system consists of an insulating tube containing five electrodes separated by 1 cm gaps. As indicated by the Paschen curve, a mercury discharge will not occur for pressures of 10^{-1} Torr and voltages of 5000 V if the electrodes are separated by less than 3 cm. Although theoretically one gap is sufficient, four gaps in series were incorporated in the isolator design for additional safety. The necessity for this redundancy is questionable however. Integration tests on the complete feed system showed that the operational and controllability features were as desired. The total weight of the feed system was 4.5 lb with a typical operating power requirement of 20 to 30 W.

The power conditioning and control system developed for this program was mechanized using unique modular techniques. The electrical outputs of the various supplies required to operate the ion engine and feed system were generated by adding the outputs of individual low power, low voltage modules. Included in the over-all system are incremental (micrologic) and linear controllers which, by commanding and/or controlling the individual modules, provide (1) switching of redundant modules in case of a failure; (2) startup-shutdown-restart sequencing; and (3) linear control for closed loop engine operation. The micrologic control system can also provide incremental voltage regulation, as required by an interplanetary solar-electric propulsion system where the solar panel bus voltage changes with distance from the sun.

The modular approach to the power conditioning and control system was chosen over the more conventional technique because of its advantages for solar-electric propulsion systems. Along with weight,

efficiency, and reliability advantages, the multimodular approach fulfills many of the unique requirements placed on a power conditioning system by a solar-electric propulsion system (such as power and voltage matching).

One important consideration was system reliability. Although the parts count associated with the modular approach is greater than that of equivalent conventional systems, the reliability of the former is easily increased through the use of partial redundancy. For example, two additional (standby redundant) modules increase the reliability of a beam supply consisting of ten modules from 0.7 to > 0.99, with a weight penalty of only 20%. In a conventional system, complete supply substitution is required, with much greater weight penalties.

Table I summarizes the various power supplies and their gross characteristics as developed for the power conditioning and control system. This array of modules, which incorporates a flight design, is 36 in. by 24 in. by 3 in. and weighs 25 lb, including redundant modules and the structure which provides mechanical support as well as radiation cooling. Although the original design specification on the SERT-II thruster was $\sim$1500 W, the total power supply capability is 2400 W.

The additional capability resulted from a design philosophy which required that all circuit techniques which might be employed in higher power solar-electric propulsion systems be demonstrated in the present design. Accordingly, the following circuits and circuit techniques were included: (1) basic inverter module; (2) dc adding of module outputs; (3) ac adding of module outputs; (4) inverter start-stop circuitry; (5) thermistor bridge temperature regulator; (6) magnetic modulator current regulator; (7) micrologic startup-shutdown-restart progammer; (8) micrologic incremental voltage control; and (9) closed loop linear engine control. With the substitution of the HRL cathode and other thruster modifications, the system operated at 1200 W. A power conditioning system and control system design employing the modular approach and optimized for 1200 W is described in the Appendix.

TABLE I

Power Supply Characteristics

Supply	Power,[a] W	Percent of System Power	Basic Weight, lb	Redundant Weight, lb	Total Weight, lb	Percent of System Weight
Beam	875	59.7	7.3	1.9	9.2	36.8
Arc	252	17.2	3.4	1.1	4.5	18.0
Cathode Heater	162	11.1	1.1	0.5	1.6	6.4
Magnet	60	4.1	2.0	1.0	3.0	12.0
Accelerator	20	1.4				
Feed System/ Neutralizer	96	6.5	2.2	1.1	3.3	13.2
Control	—	—	0.9	—	0.9	3.6
Frame and Wiring	—	—	2.5	—	2.5	
Totals	1465	100	19.4	5.6	25.0	100.0

[a]This column represents the SERT-II thruster specifications rather than individual supply capabilities, which total 2400 W.

This optimized array would be 21 in. by 25 in. by 3 in. and would weigh 15.5 lb or 12.9 lb/kW, again including redundancy and structure for support and radiation cooling. The specific weight of the modular type power conditioning and control systems will decrease as the power requirement (i.e., thruster size) increases. For example, design analyses have indicated specific weight values of 7 lb/kW and 6 lb/kW for system sizes of 3 kW and 6 kW, respectively.

A 500 hour test of the above power conditioning and feed systems and the modified SERT-II thruster was conducted to demonstrate system performance. At the nominal thruster operating point, a propellant efficiency of 80% and an ion source energy (discharge plus cathode) of approximately 600 eV/ion was achieved. Other components, notably the electromagnet, consumed 400 eV/ion. No power supply failures were incurred during the test; however, during the integration phase the ability of the redundant switching circuitry to substitute operational modules for failed modules was demonstrated by manually simulating the loss of a module. The feed system also operated stably during the 500 hours.

Two anomalies were observed during the test. The first was a vacuum failure caused by a cold leak developing in the cryowall; this failure interrupted the test at approximately 250 hours. The second was a gradually increasing arcing rate which became excessive at 400 hours. This problem was solved by increasing the output capacitance of the beam supply; this provided sufficient energy in the arcs to burn away the low resistance path which caused the arcs. The test was then completed normally. When the system was disassembled, it was found that the arcing had occurred along the inner surface of the isolator. Improved isolator designs (discussed below) which were developed subsequently and tested for 1000 hours do not suffer from this problem.

The test served as a conclusive demonstration that all components and subsystems required to construct an ion engine system for solar powered spacecraft are currently available as part of the state of the art technology.

SECTION III

SYSTEM SPECIFICATIONS

Basically, the system to be tested included a thruster, feed system, and power conditioning and controls; the characteristics and performance of the system were to be similar to those assumed in the study and design phase of the program. The thruster and its nominal operating characteristics were furnished by NASA-LeRC midway through the program. This thruster was of a nominal 1 kW size and is representative of those anticipated for use on the proposed SERT-II flight test. The characteristics as specified in Ref. 2 are given below:

1. Solar Cell Array Power Source

   The NASA-LeRC SERT-II power source will be a solar cell array consisting of a series-parallel combination of 10 Ω-cm n-on-p silicon solar cells. Thermal calculations show that 55 to 65°C solar cell temperatures are expected for the orbital conditions. The electrical degradation is equivalent to 10^{15} electrons/cm^2 irradiation of 1 MeV electrons. Figure 1 shows typical solar cell characteristics; for design purposes assume that there are 135 solar cells in series in each parallel string making up the array. Design point A in Fig. 1 is considered the loaded "end-of-life" input voltage for the steady-state load requirement of 1 kW thruster load plus the power conditioning and control system inefficiencies. This design point A represents 40 V dc. For test purposes, a simulated solar cell array power source should be used which will duplicate as closely as possible the static and dynamic characteristics of an actual solar cell array. The simulated solar cell array power source shall have sufficient control range to permit matching of the array's output characteristics which result from the long term radiation damage.

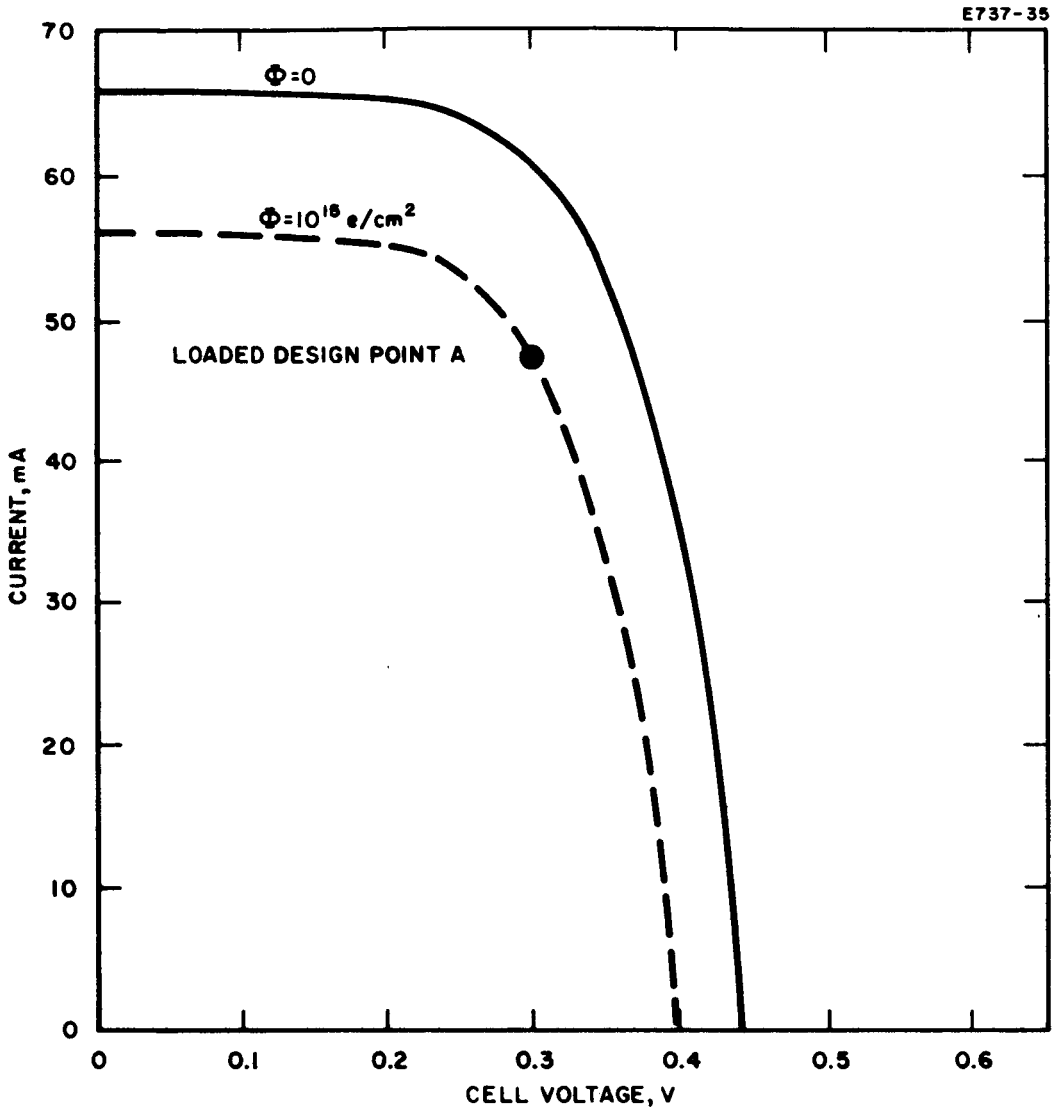

Fig. 1. Current versus voltage curves for n-p 10 Ω-cm silicon solar cells at 70°C temperature before and after 1 MeV electron irradiation.

The power conditioning and control system shall be designed to be compatible with the solar cell array characteristics and to provide stable regulated operation of the thruster at maximum efficiency.

2. Power Conditioning Output

The power conditioning output requirements shall be a function of the thruster requirements and its operating characteristics. Table II represents the maximum thruster power conditioning at 45 V ac input:

The basic power conditioning and control system specifications were subsequently amended by a JPL technical memorandum,[3] as follows:

1. The power conditioning shall be designed for operation with the NASA-LeRC engine.
2. The solar simulator output characteristic shall be as shown in Fig. 2.
3. The beam current shall at no time exceed 255 mA.
4. The main drive voltage shall be between 3000 and 4000 V.
5. The accel voltage shall be 2500 V under load, and the supply will be unregulated.
6. The magnet should carry 15 A under load, and this supply will be unregulated
7. The discharge current shall at no time exceed 7.0 A.
8. The discharge voltage shall be between 30 and 36 V during normal operation, but shall rise to 108 V when the discharge current is less than 10 mA.
9. The load line of the discharge power supply is at the discretion of the contractor, subject to the above constraints.

TABLE II

Thruster Power Conditioning Parameters

Supply	Output[a]		Relationship to Ground	Regulation[b]		Peak Ripple, %
	Voltage, V	Current, A		Line, %	Load, %	
Magnetic field	4 dc	15 dc	+3 kV dc	±10	5	—
Feed	6 ac (3 V tap)	3 ac (6 A tap)	+3 kV dc	2	2	—
Cathode	3 ac rms	50 ac rms	+3 kV dc	2	2	—
Anode	36 dc	7 dc	+3 kV dc	2	2	10
Screen	3000 dc	0.25 dc	+ to ground	±10	5	10
Accel[c]	2000 dc	0.05 dc	+ to ground	+10	2	10
Neutralizer[d]	3 ac rms	15 ac rms	ground	2	2	—

[a]AC outputs shall be rms values.

[b]Regulation for 40 to 60 V input and zero to full output load.

[c]Shall share transient surge capacity of screen supply.

[d]Provide for transfer of this power to an alternative neutralizer if the primary neutralizer open circuits, and also by external command.

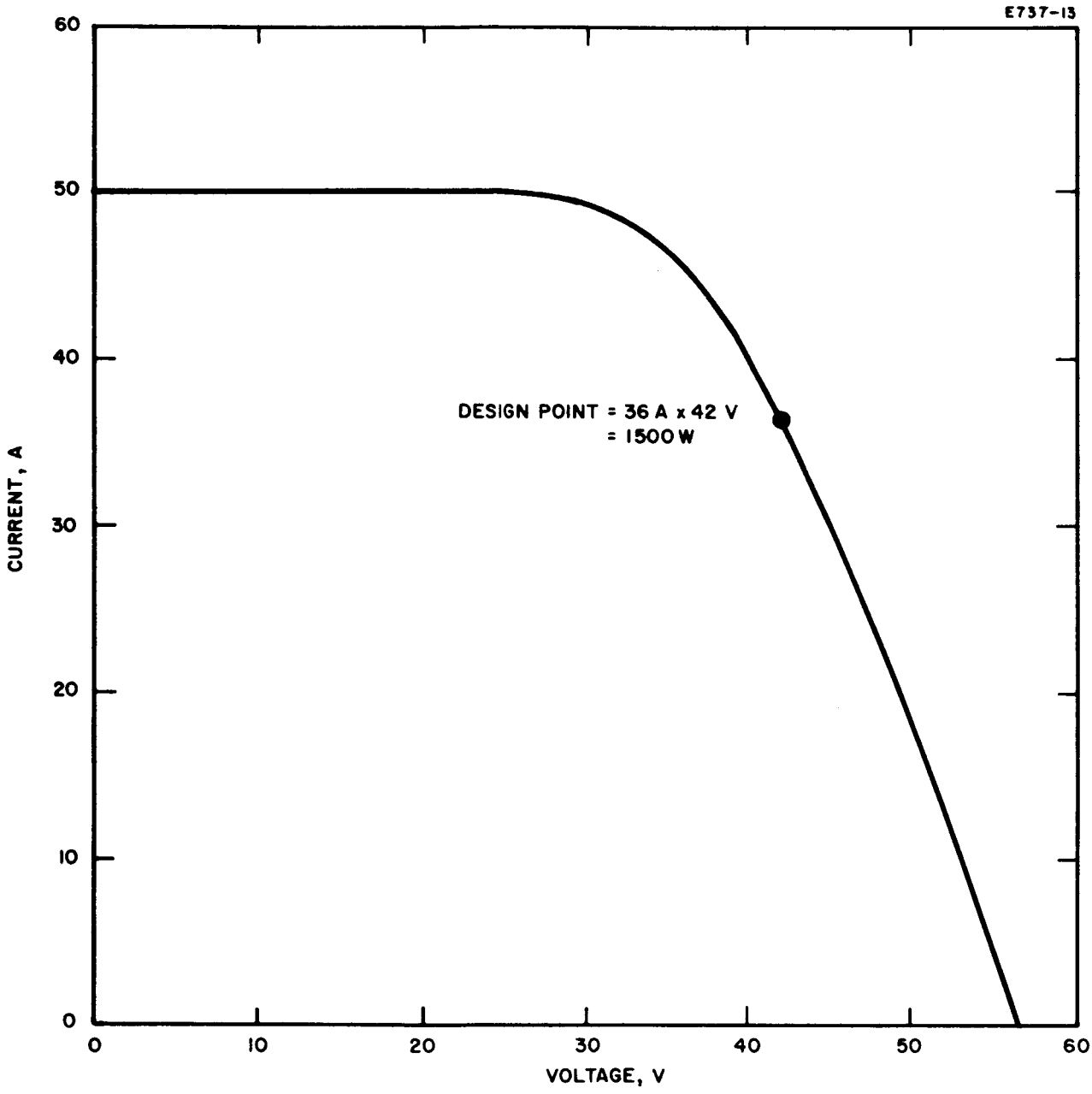

Fig. 2. Solar cell simulator characteristics.

10. All heater currents shall be rms sensed.

11. The cathode heater current shall at no time exceed 50 A rms, and shall have a minimum set point of 25 A.

12. The neutralizer heater current shall be variable over a range from 5 to 15 A.

13. The feed system heaters are at the discretion of the contractor.*

14. The following control loops shall be provided:

    a. A closed loop shall be established between the beam current and the cathode heater current, which will command the cathode heater current to vary (from 25 to 50 A rms) to maintain the beam current at some reference value.

    b. A closed loop shall be established between the accel current and the feed system power; this will command the feed system power to vary to maintain the accel drain initially at some reference value.

    c. An override shall be provided on the cathode heater current control so that the cathode heater current shall decrease linearly to 0 A as the discharge current increases from 6.5 to 7.0 A.

*Both the vaporizer and pressurizer were allotted 25 W of power and isolated from ground. The final design required less than half this power at ground potential; thus the weight of these supplies can be considerably reduced.

d. A control loop shall be provided which reduces the discharge voltage linearly to 5 V as the cathode heater decreases from 25 to 23 A.

15. Minimum and maximum set points on the heater currents, and reference values cited above, should be discretely adjustable by external command.

16. Telemetry outputs shall be provided as specified by NASA-LeRC for power conditioning for SERT-II.

These specifications (along with certain thruster modifications) resulted in two major changes from the original system design, which was based entirely on the results of the study phase of the JPL program. These changes were as follows:

a. Solar cell output voltage was reduced from 90 to 45 V.

b. Engine power requirement was reduced from 1.6 to 1.2 kW.

With these changes incorporated the demonstration system was made compatible with both the SEP designs and the tentative SERT-II flight specifications. As a result, however, the 500 hour test could not be conducted with the power conditioning operating at the minimum specific weight capability. (At the conclusion of the 500 hour test the thruster power was increased to approximately 1.8 kW to demonstrate the power conditioning capabilities more fully.)

The original startup sequence as specified by NASA-LeRC was simply the simultaneous turnon of all supplies. (This was later modified after joint discussion between JPL, NASA-LeRC, and HAC personnel; three distinct groups of supplies should be turned on in sequence.

During the final integration phase, it was found necessary to further modify the system so that the magnetic field rose to full value over a time period of a few milliseconds — rather than being pulsed on — to avoid overloading the accel supply.)

SECTION IV

SYSTEM DESIGN APPROACHES

A. FEED SYSTEM

The mercury vapor propellant feed system developed for this program consists of the following major components:

- a liquid mercury storage reservoir
- a pressurizer which maintains the liquid mercury in the reservoir and feed lines under constant pressure
- a solenoid valve
- a vaporizer which separates the liquid and vapor phases and controls the vapor flow rate
- an isolator which provides electrical isolation between the thruster which operates at the high voltage and the electrically grounded feed system and reservoir.

The conventional approach to the design of liquid mercury expulsion systems has been to use gas pressure to drive the mercury from some type of collapsible reservoir (bellows, bladder type, or a system incorporating metal or elastometric diaphragms). In these systems the gas is stored at high pressure and is passed through a reducing valve into the pressurizing chamber. Because neither the pressure reducer nor the pressure sensing unit specifically required for this approach was available as an "off the shelf" item, a system requiring only stock components and a thermistor bridge temperature control-sensor was designed. In this system the pressurizer-reservoir is essentially a

single cylindrical unit in which the stored mercury is maintained at a constant pressure by a movable piston driven by heating a small quantity of volatile liquid (in this case, water). Since the mercury pressure is directly related to the temperature of the pressurizer, no pressure sensor is required; a simple temperature regulator maintains constant (or controlled) mercury pressure. The vapor type pressurizer has several distinct advantages:

1. It has a low operating power.
2. There are no Hook's law forces, such as would exist if a metal diaphragm were employed.
3. No pressure sensor is required.
4. No gas bottle or regulator is required.
5. The system is readily scalable.
6. More than 95% of the mercury in the reservoir can be expelled.
7. The system can be readily cycled and refilled.

The valve used was developed by HAC for use in the cesium vapor line of the SERT-I ion engine test. It was used here primarily because of its availability and because it performed well during the tests. Newer commercial valves are now available which have a magnetic latching characteristic, so that no electrical power other than a current pulse is required to open or close them. Because of the power saving involved, their use should be investigated for future systems.

The vaporizer was simply a fine mesh stainless steel screen which separated the liquid and vapor phases by surface tension. Because of the very low mass and relatively low operating temperature ($\sim 200^{\circ}C$), the power consumption was low and the response was very good. The propellant flow rate follows the vapor pressure curve directly, and hence is strongly dependent on temperature. This relationship does not present a thermal problem, however, since it can be readily compensated by a tight electrical control loop.

The isolator consists basically of an insulating section of feed line with size and temperature designed to maintain the pressure at the appropriate point on the Paschen curve. The design used here had a series of sections to provide a safety factor.

B. POWER CONDITIONING

An ion engine power conditioning system for a solar powered electric propulsion system must perform several functions. First, the system must be able to convert solar panel output voltage to usable ion engine voltages. Second, the system must be able to control and regulate the ion engine operating voltages and currents as the solar panel output changes. Third, the system must provide a power and impedance match between the solar cell source and the ion engine loads. Finally, this must be accomplished with power conditioning circuitry and components which have the following system characteristics.

Low specific weight	< 15 lb/kW
High power efficiency	> 90%
Long operating life	> 10,000 hours
High system reliability	> 0.97.

In attempting to provide the above characteristics, it is desirable that over-all circuit simplicity (i.e., minimum electronic part count) be maintained and that the circuit design be amenable to redundancy techniques. It is also desirable that the circuit design be compatible with spacecraft mounting and heat rejection systems, preferably completely free of the need for supplementary heat radiators and their associated heat conduction systems.

Using the above design criteria, two possible power conditioning design approaches were considered and evaluated at the outset of this program. The first, or conventional, method consists of a single high power level circuit for each of the required power blocks. In analyzing

this approach, the power, voltage, and current ratings of the various power supplies were established. These requirements then determined the type of circuitry which would be employed and the electronic components which would be used to perform the various circuit functions. A major drawback to this approach is the limit in component selection. For example, high power systems require high current transistors. Because of their low switching speeds, these transistors place a design limit on the upper frequency of the inverter system, thereby increasing the weight of the magnetic components above a frequency limited minimum. (This problem may be alleviated to some degree by the development of high power, high frequency transistors.)

In the second approach the design analysis procedure was reversed. That is, the initial step was to select transistors for the inverter circuit which had high switching speeds and high voltage ratings, permitting high efficiency at high frequency. The transistor voltage and current ratings were used to establish the power handling capability of an individual power conditioning module. The complete power conditioning system was then designed using these modules as the basic building block. As described below, a more detailed analysis of the modular approach to ion engine power conditioning indicated numerous advantages over the more conventional methods. Therefore, the modular approach was chosen for this program.

1. Modular System Design Advantages

In a detailed comparison, the low power module approach shows a substantial improvement in weight and efficiency over the conventional high power circuit approach. For example, a 6 kW power conditioning system consisting of a series of low power modules would weigh 36 lb (i.e., 6 lb/kW) and have a 93% power efficiency. An equivalent conventional system is estimated to weigh 120 lb (i.e., 20 lb/kW) and have a power efficiency of 88%.[4] The weight figures quoted here include the structure and radiating surfaces necessary to dissipate

the power losses. The weight and efficiency advantages shown by the modularized system accrue for several reasons. For example, substantial reductions in structural (both chassis and heat radiator) weight are inherent in the modular approach, since the low power dissipation per component permits direct heat radiation to space, utilizing only the area used to mount the components. That is, the power density is so low that no thermal conduction or liquid coolant radiator heat exchange type of cooling system is required. A further reason for weight reduction in the modular system is the low weight density per mounting area, which permits a very low weight supporting structure.

The low weight of the modular system, however, derives principally from the use of a high inverter operating frequency. The high operating frequency has been made possible by recent improvements in power transistors, which are characterized by switching speeds of 1/4 μsec. Such speeds permit square-wave frequencies of the order of 10 to 20 kc with high efficiency switching. These silicon devices also permit switching of relatively high dc supply voltage, permitting a further increase in efficiency by operating at a low ratio of V_{ce} saturation drop to line voltage. Transistors with 400 V ratings permit high efficiency operation at a power level of 200 W per pair, with voltage safety factors of two, current safety factors of two, and power safety factors of four.

The high switching frequency also results in weight and efficiency rewards in magnetic components (such as transformers, magamps, and filters). Transformer power efficiencies of 98% are easily obtainable at low temperature rise (high reliability) with typical weights of 3 oz for a 200 W transformer (i.e., 1 lb/kW). This figure compares with about 4 lb/kW for a 1000 cycle transformer, typical of the high-power circuit approach.

High frequency operation also permits substantial reductions in filter weights because of the lower inductance and capacity required. Furthermore, operating modules in series with staggered frequency or phase results in low output ripple.

Although the conventional type system will typically employ a lesser part count, the modular concept lends itself to partial redundancy techniques. Thus, in order to achieve the desired overall system reliability (e.g., > 0.97), the weight penalty for the modular system would be approximately 25%, while a 100% increase in system weight would be required with the conventional approach. It may also be shown on the basis of stress factor that the reliability of individual power semiconductors in the modular approach is substantially greater because of the lower operating temperatures obtainable with this design. Transistor junctions typically are only $5^{\circ}C$ higher than the chassis mounting, compared with the $40^{\circ}C$ common with the high power circuit.

In addition to its weight, efficiency, and reliability advantages, the multimodule approach fulfills many of the unique requirements placed on a power conditioning system by a solar-electric propulsion system. For example, the multimodule power conditioning concept is more versatile than the conventional system in matching solar cell loads and voltages to the ion engine. In the modular system, loads and voltages are matched by varying the number of modules operating in series in a given supply. Module switching is equivalent to changing the primary to secondary turns ratio of the power output transformer in a conventional circuit. The module system has the advantage that the switching process required to change the effective turns ratio can be performed in the low power portion of the inverter circuit. Switching is performed by turning the inverter feedback transformer on or off with the micrologic circuitry. In the switching process, a step change in the output voltage results without the supply output voltage interruption which would occur in tap switching the power output transformer in a conventional system.

Another advantage of the multimodule circuit concept is the possibility of interrogating the solar cell power source to determine whether the system is operating at the maximum power point. In any interplanetary mission, the solar cell voltage-current characteristics will change continuously. To derive the maximum power available from the solar cell system, the load resistance presented to the solar cells must also change with time. By switching an additional power conditioning module in or out and monitoring the change in solar cell power output, it would be possible to determine whether the ion engine load should be either increased or decreased. To insure operation at the maximum power point, the ion engine load could then be varied by changing the mercury flow rate to the engine system.

Along with the decrease in power available during a typical Mars mission, the solar panel bus voltage will increase approximately 30% during the flight. If uncompensated, this increase in solar panel output voltage would result in a direct increase of 30% in the main beam voltage. The multimodule approach easily compensates for this voltage rise by switching out inverter modules at the same rate the input voltage increases. By this technique, the main beam voltage is effectively regulated with zero power loss. This technique has two further advantages. First, the system would have a built-in redundancy. As a module is switched out, it can be used as a standby for the remainder of the mission. Switching-out of inverter modules increases the overall system power efficiency. The increase in efficiency is a direct result of operating fewer modules at higher individual efficiencies because of higher line voltage.

Finally, the multimodule system has startup advantages over the conventional system. The solar cell power source is a soft power system, i.e., the output voltage is very dependent on the electrical load. A high powered inverter system, if turned on fully, would initially present a very low impedance to the solar cell system. To avoid this condition, the high power inverter system employs slow turn-on

procedure, which requires additional circuitry and complexity. The multimodule system has an inherent slow turn-on capability simply by programming the switching circuitry to turn on one module at a time.

2. General Circuit Considerations

Since the modular approach employs a number of modules in series, connection techniques have been devised so that for any type of module failure, the total output is not interrupted except for a voltage drop equal to a single module's voltage output. This drop in voltage is then automatically corrected by turning on a standby module.

Furthermore, voltage regulation is obtained in the series module system with the same control logic used to detect a failed module and replace it with a standby module. With 20 series modules, the regulation band is 5% or ± 2.5%. Similarly with 10 modules in a series string, ± 5% from nominal is the limit of regulation. This degree of regulation will be adequate for the bulk of the power in the ion engine, i.e., positive and negative high voltage supplies.

As indicated earlier, studies have established power conditioning and control system requirements for a wide range of ion engine sizes (i.e., power levels) for various unmanned interplanetary missions. Therefore, in order to solve the power conditioning problems associated with these requirements, the techniques which should be proven early in the development (i.e., design verification of the hardware system under consideration here) are those which are applicable to various future missions. With this philosophy, the design of the relatively low power demonstration model power conditioning system would have to employ all the circuit techniques which would be required in the development of a higher power system. Because the use of this approach would not result in an optimized 1.2 kW system (for example, ac adding and power modulation by magnetic means) some performance

penalty (i.e., weight) must be expected (and accepted). As a result, however, no extrapolation of technology will be required for scaling to a larger system. (The modular power conditioning and control system weight and efficiency when optimized for 1200 W total output is estimated in the Appendix. These estimates are based on the results of the development and test program described in this report and also reflect recent improvements in power transistors.)

On this basis, the demonstration system must provide design verification of the following circuits and circuit techniques:

1. basic inverter module
2. dc adding of module outputs
3. ac adding of module outputs
4. inverter start-stop circuitry
5. thermistor bridge temperature regulator
6. magnetic modulator current regulator
7. micrologic startup-shutdown-restart programmer
8. micrologic incremental voltage control
9. closed loop linear engine control.

SECTION V

SUBSYSTEM DEVELOPMENT AND TESTING

A. THRUSTER

The thruster employed in this program was supplied GFE by NASA-LeRC. The thruster, which was designed to produce a 15 cm diameter beam weighed 7 lb. Oxide cathodes manufactured at NASA-LeRC (designated as "brush" cathodes) were to serve as both the neutralizer and primary electron source for the discharge chamber of the engine. The operating parameters for this engine were provided by NASA-LeRC in Ref. 2.

1. Modifications

When the thruster was received, a series of test runs were conducted with laboratory type supplies to assure that the thruster met specifications and that it was compatible with the Hughes feed system. During these tests, several discrepancies were noted.

a. Optical System

The acceleration drain currents were as specified (~5 mA at 250 mA beam) for the ion optical system as it was received (see Fig. 3(a)). However, a total accelerating voltage of 7 kV was required to draw the 250 mA beam. Because the perveance was lower than anticipated, only 170 mA of beam could be drawn at the designated operating point (i.e., 5 kV total accelerating voltage). Several steps were required before this problem was alleviated. First the necessary parts were fabricated to move the two electrodes closer together, producing curve 2 in Fig. 3(b). The perveance was still too low; therefore, the screen electrode was countersunk on the plasma side to further increase the perveance, as shown as curve 3 in Fig. 3(b). This gave

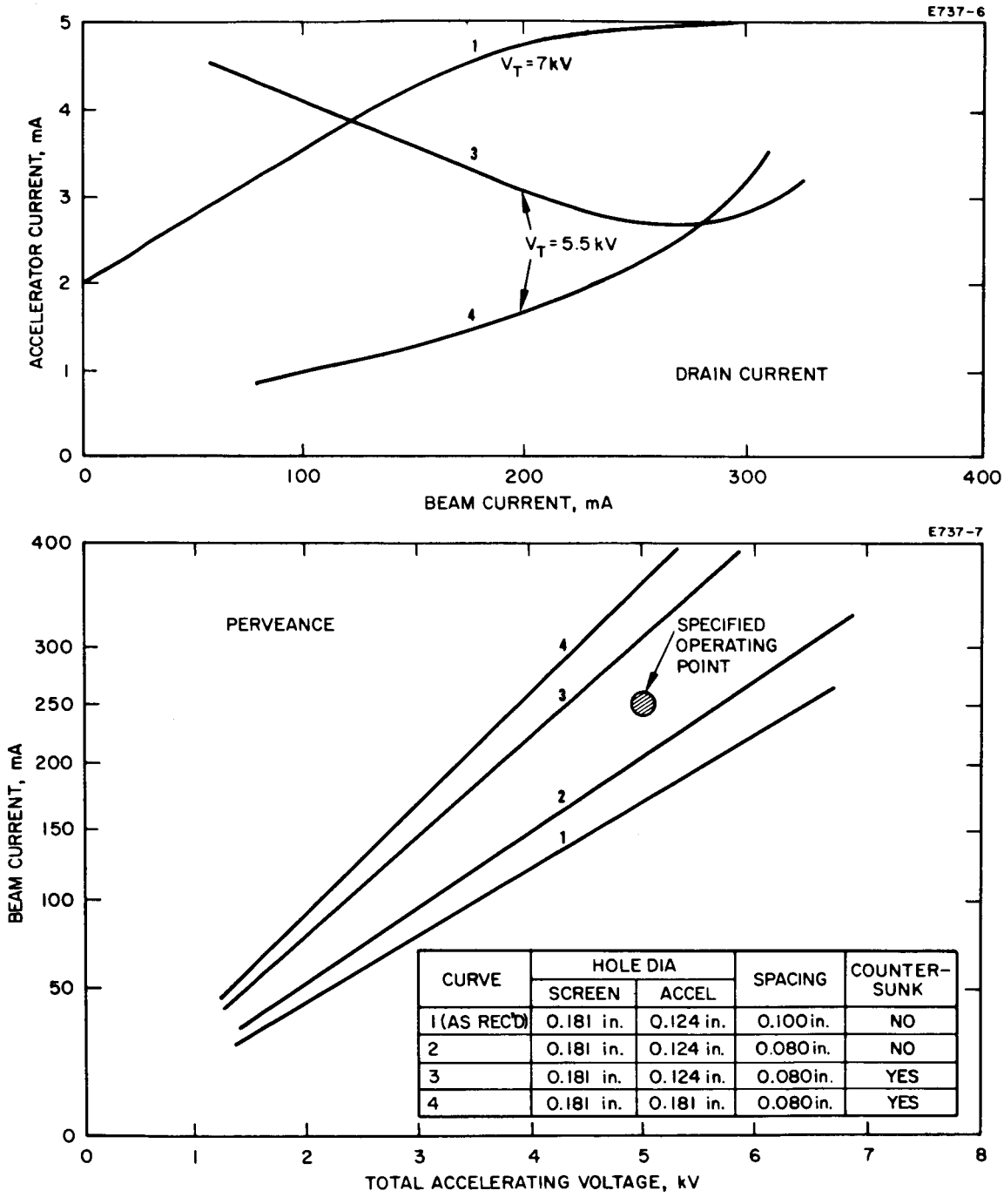

Fig. 3. Performance of ion optical system.

a sufficiently high perveance but produced an accelerator drain current which had a minimum (e.g., Fig. 3(a), curve 3) rather than being a monotonic function of the beam current. This situation was incompatible with the control system defined by NASA-LeRC, which required that the accelerator current be a single valued function of the beam current. The final modification involved enlarging the accelerator electrode holes to equal those of the screen electrode. This modification produced curve 4, which has the desired high perveance and almost linear accelerator drain curve. The final configuration used has a perveance which is a factor of two higher than the "as received" design, while the associated accelerator drain current is a factor of two lower than the original value.

The final operating point was a beam current of 250 mA at a drain current of approximately 2.2 mA. This lower drain current value required a change in the set points in the flow control circuit. These adjustments were made during the integration phase of the program.

b. Cathode

The cathode power supply was designed to operate at a maximum of 50 A and 3 V, as specified. During the three month test period preceding the actual life test, 12 brush cathodes of five different physical sizes were delivered GFE and tested at Hughes. All required in excess of 60 A to reach operating temperature. Since this level of current was beyond the capability of the previously specified and developed heater supply, these cathodes were unsuitable for the system test. However, they were used during the preliminary testing to establish the thruster operating characteristics.

As result of a change work order, a suitable cathode was designed, fabricated, and tested at Hughes. A photograph of this unit is shown in Fig. 4. Construction techniques are similar to those of the "flower" cathode tested over the past year at Hughes,[5] although the small size required that the nickel screen upon which the emissive material is sprayed be formed into a spiral rather than the characteristic flower petal geometry. Typical operating characteristics of this cathode are shown in Fig. 5.

M 4830

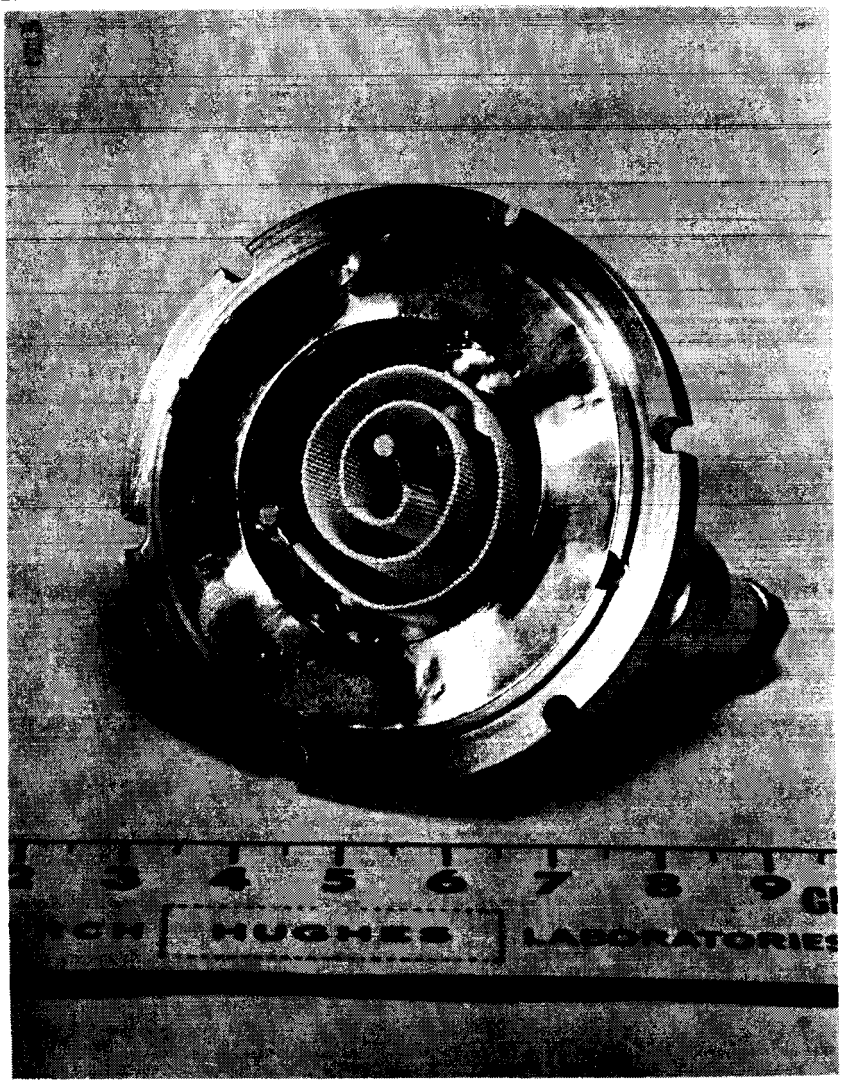

Fig. 4. Hughes-designed cathode.

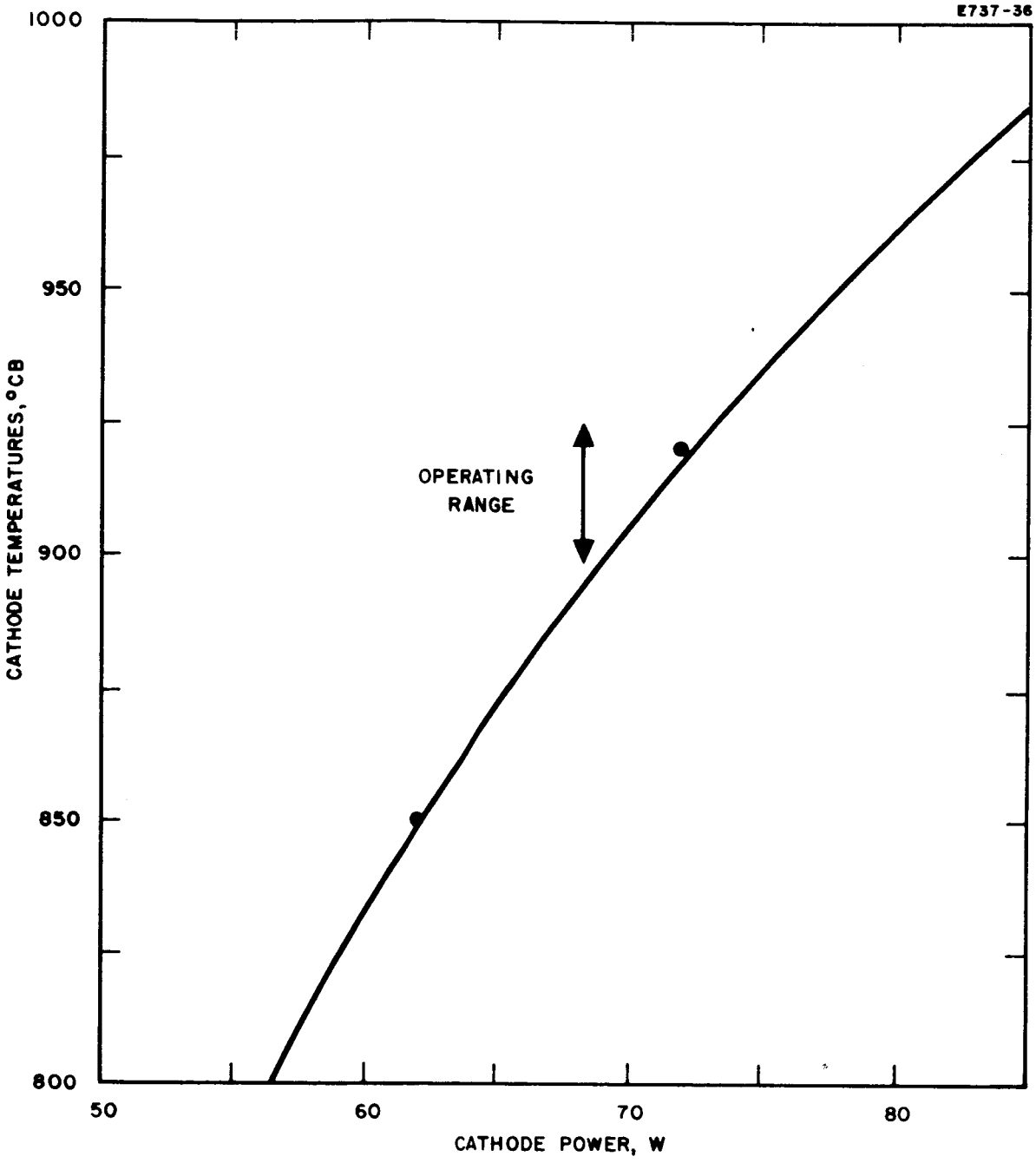

Fig. 5. Typical operating characteristics of Hughes-designed cathodes.

c. Discharge Current

As specified, the discharge power supply was to be capable of 7 A continuous operation. In the final engine configuration test the discharge current never rose above 2.6 A and no autocathoding was observed. Thus the discharge supply was considerably overdesigned and accounted in part for the relatively high weight to operating power of the power conditioning subsystem.

2. Operating Characteristics

During the thruster test period, when the above changes were being made, a number of parametric data pertaining to thruster performance were obtained. The data to be reported here were taken employing the optics design 3 of Fig. 3(b) and one of the several "brush" cathode designs tested. The general procedure was to allow the feed system to run overnight to calibrate and stabilize the feed rate, to run the thruster at a high power level to drive off excess mercury which might have accumulated, and finally to vary the desired electrical parameters to obtain the necessary data.

Two neutral mercury flow rates were established, each known to an accuracy of approximately ±5%. These flows bracket the feed rate used in the final life test. The pertinent data are shown in Fig. 6. The specified operating points for magnet current and discharge voltage are a good compromise between performance and power consumption. The position of the knee of the curve in Fig. 6(c) is interesting because it occurs at a lower cathode power for the higher beam current. This is attributed to cathode heating resulting from ion bombardment from the plasma, which is large for the higher plasma density associated with the high beam current. Thus this arc power is sufficient to maintain parts of the cathode at emitter temperature even though the power to the cathode heater is significantly reduced. This phenomenon was also apparent as a hysteresis in the beam current as the cathode power was varied.

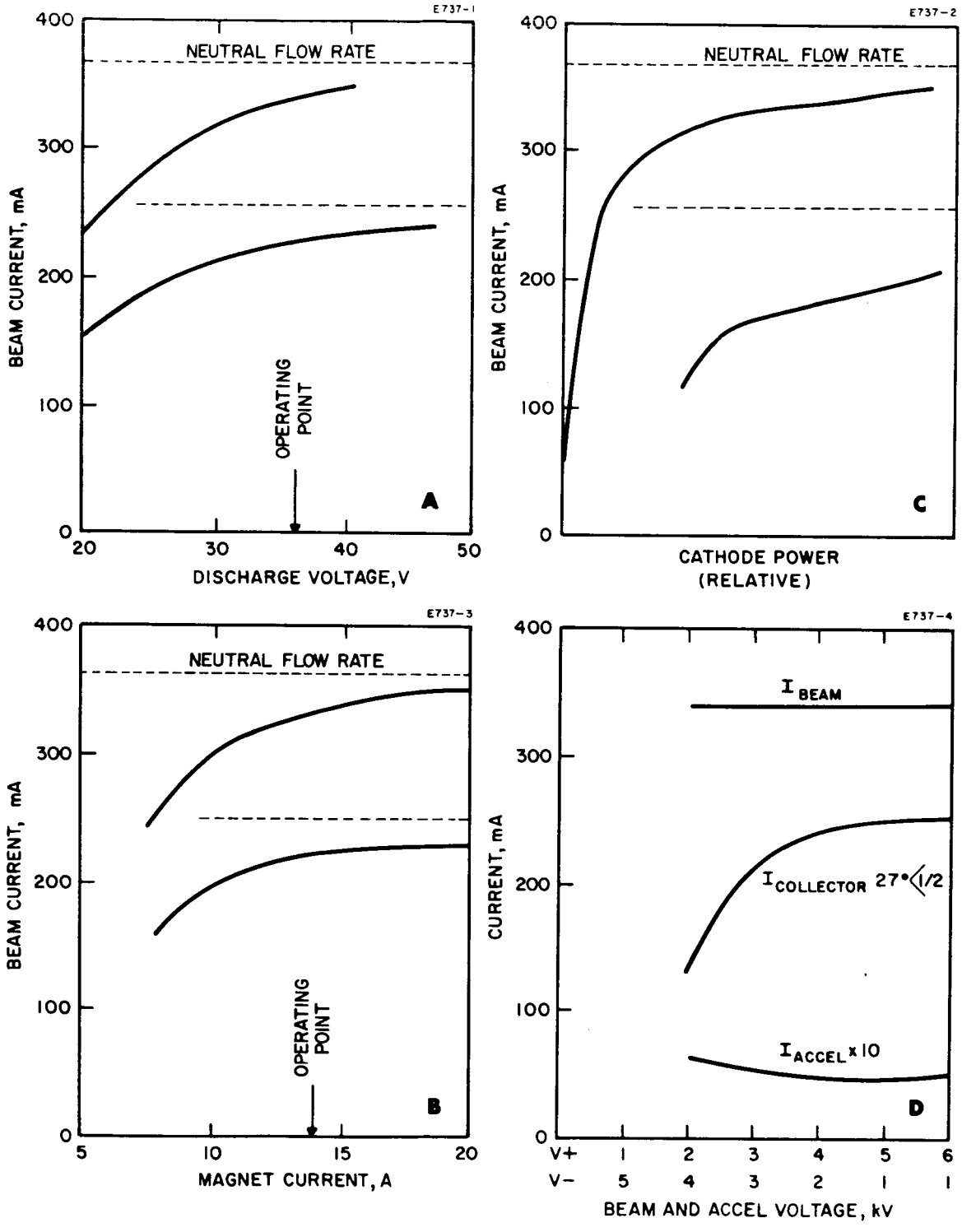

Fig. 6. Data for neutral mercury flow.

Figure 6(d) shows the current to the collector as a function of voltage and accel-decel ratio $[(V_+ + V_-)/V_+]$. These data are of interest in the design of a final system where it is desirable to minimize beam impingement on the solar panels. Note that as the accel-decel ratio is reduced, the collector current increases until approximately 75% of the beam current is collected in a 27° half angle. Crude calculations based on neutral efflux from the discharge chamber indicate that charge exchange collisions along the 14 ft beam path can account for most of the remaining 25%.

As a result of the above studies of thruster performance and because of the mechanical modifications described, the final operating point for the system life test was established as follows:

Beam current	250 mA
Beam voltage	3.5 ± 0.5 kV
Accelerator current	~2.2 mA
Accelerator voltage	2.5 kV
Discharge current	~2.5 A
Discharge voltage	36 V
Cathode current	50 A max
Cathode voltage	3 V max
Magnet current	15 A max
Magnet voltage	4 V
Feed system	20 W
Neutralizer current	10 A
Neutralizer voltage	3 V

B. FEED SYSTEM

1. Pressurizer-Reservoir-Valve

The reservoir and the expulsion system used in this program are shown in Fig. 7. The mercury is contained in a cylinder and pressure is applied by a movable piston. The seal between the piston and cylinder is made by a "rolling diaphragm"* to reduce friction and contamination. The pressurizer is an equivalent unit except that the mercury is replaced by a small quantity of volatile liquid — in this case, water. The vapor pressure of the liquid in the pressurizer is directly related to the temperature; thus the force on the mercury may be controlled by controlling pressurizer temperature. By thermally isolating the pressurizer from the reservoir, it is possible to effect rapid pressure changes at low input power levels, since the relatively small pressurizer mass is thermally decoupled from the large mercury mass in the reservoir. With the particular design used here, the pressurizer operating temperature of 95°C is maintained with 5 W of input power.

While the water vapor type of pressurizer described above is simple and reliable, it requires both a small power supply and a temperature controller. A different concept employing constant force springs is currently being investigated and shows promise of performing the same function with no power input and possibly an over-all reduction in system weight.

To provide smooth operation, some clearance must be left between the cylinder wall and the Bellofram. Therefore, 100% expulsion of the mercury is not possible. With reference to Fig. 7, the percentage of mercury remaining when the piston has fully bottomed is

*Commercial units fabricated by Bellofram Corporation, Lexington, Massachusetts. The unique features are essentially zero dynamic friction of Hook's law forces.

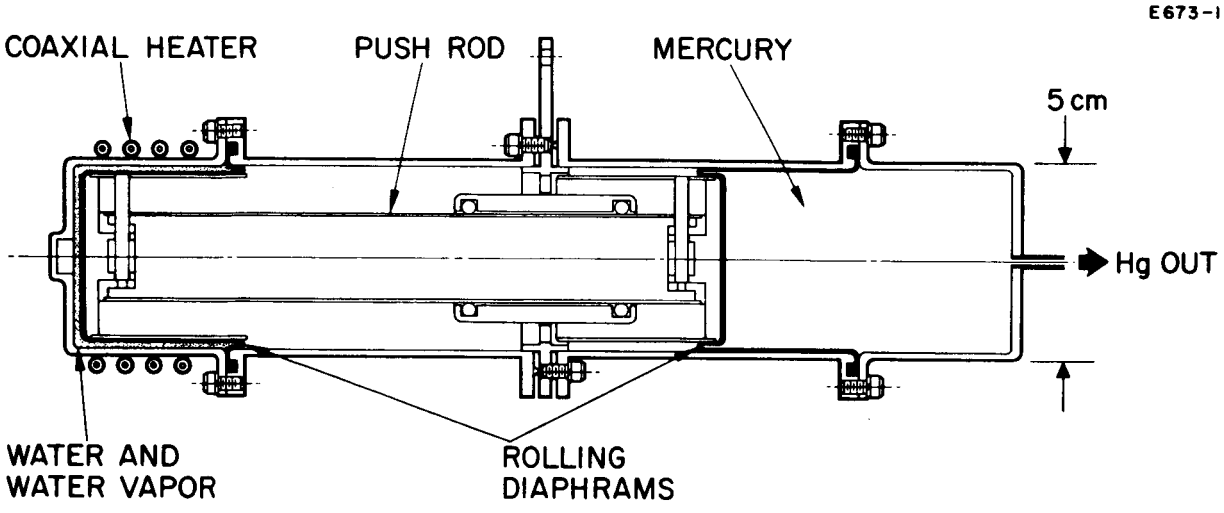

Fig. 7. Mercury reservoir and expulsion system.

$$100\,\frac{\Delta V}{V} \cong \frac{100}{2}\left(\frac{2\pi r\delta}{\pi r^2}\right) = \frac{100\delta}{r}$$

where

$r \equiv$ cylinder radius

$\delta \equiv$ clearance between cylinder and diaphragm

and the factor 1/2 occurs because the elastomer extends along only half the length of the cylinder.

The percentages of mercury recoverable for a typical value of $\delta = 0.1$ cm are shown in Table III for various reservoir sizes (where in each case the length of the cylinder is four times the radius).

TABLE III

Mercury Recovery

Radius, cm	Volume, cm^3	Capacity, A/hour	Recovery, %
2.5	208	387	96
5	1570	2920	98
10	12600	23400	99
15	42500	79000	99

During development tests, a machinists dial indicator was attached to the piston with a taut metal band to monitor the piston travel. A calibration run was then made in which the mercury from the feed system was expelled into a beaker on a direct reading balance. The weight of the accumulated mercury was recorded as a function of piston motion. This direct calibration of the system (see Fig. 8) showed that 0.001 in./hour of piston travel equals 84.8 mA equivalent of neutral mercury flow.

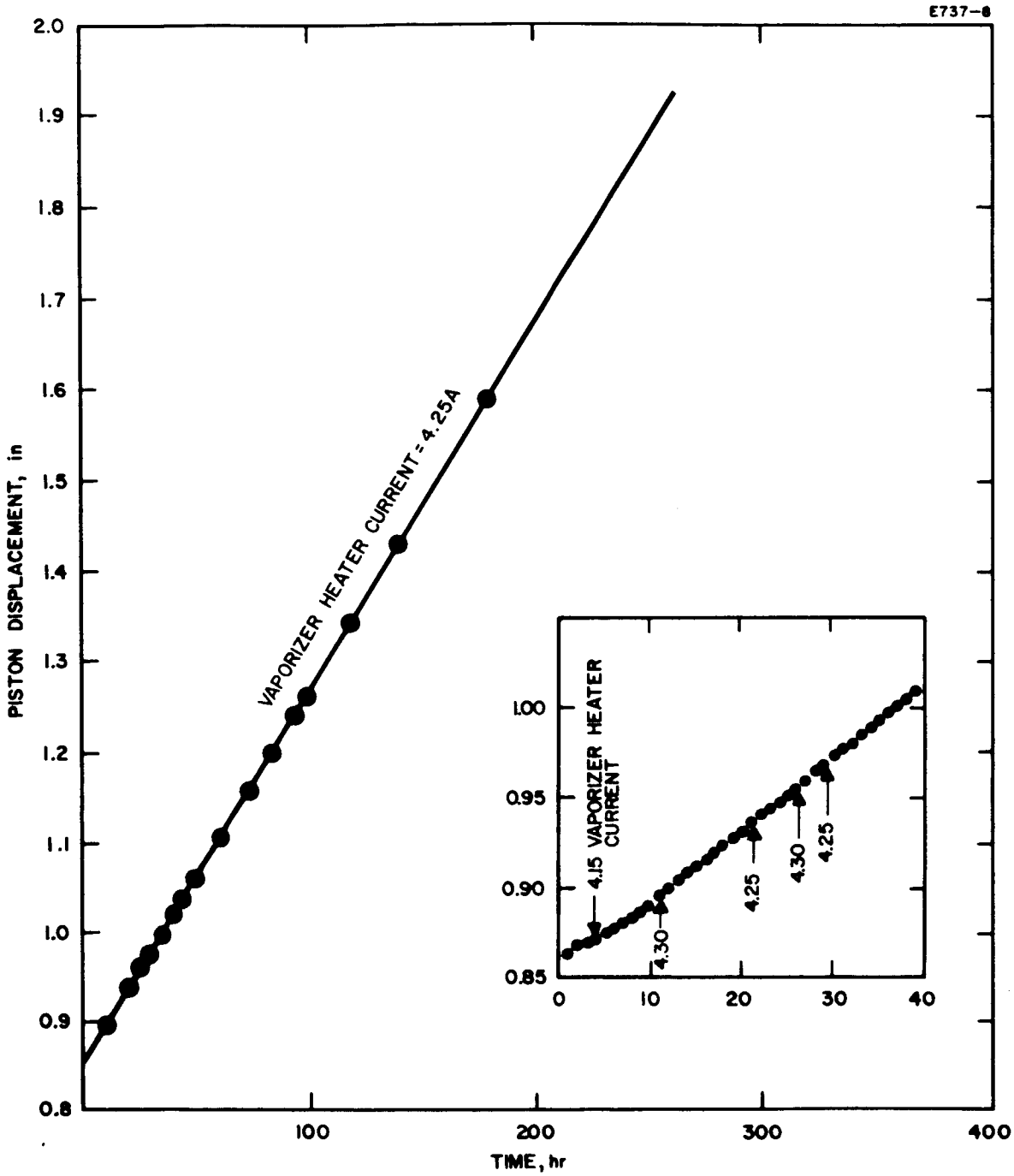

Fig. 8. Neutral mercury flowrate (piston displacement as a function of time).

When in use, this dial indicator is situated so that it may be seen through a window in the vacuum system. The indicator reading is recorded as a function of time and is used to establish the neutral mercury flowrate.

The solenoid value employed in this system uses a design developed for the high temperature cesium vapor line of the SERT-I system. It is used here primarily because of its immediate availability at no design cost. In the final system a lighter, smaller unit could be developed to meet the lower temperature, low flow requirements of this application.

2. Vaporizer

A tightly woven stainless steel screen with nominal 2 μ apertures is both used as a phase separator and a flow controller in the feed line. When properly processed it was experimentally established that the surface tension forces associated with the small apertures will hold back liquid mercury at pressures up to at least 1 atm. Typically the feed line pressure is maintained at 10 psi during operation. The section of feed line containing the vaporizer is temperature controlled to provide control over the evaporation rate of the mercury from the exposed surface. A typical plot of flowrate versus temperature for the system used is shown in Fig. 9.

Compromise is obviously necessary between speed of response and power input. In the present system the nominal operating power was chosen as 10 W, and the feed line and support structure were sized to accommodate this value. This design produced a dynamic response of approximately 1 % change in flowrate per second when the power was switched fully on or off. The heater, which maintains the vapor feed line and the upstream end of the isolator above condensation temperature, was operated in parallel with the vaporizer heater to eliminate the need for an extra power supply. It was sized to consume two thirds the power of the vaporizer.

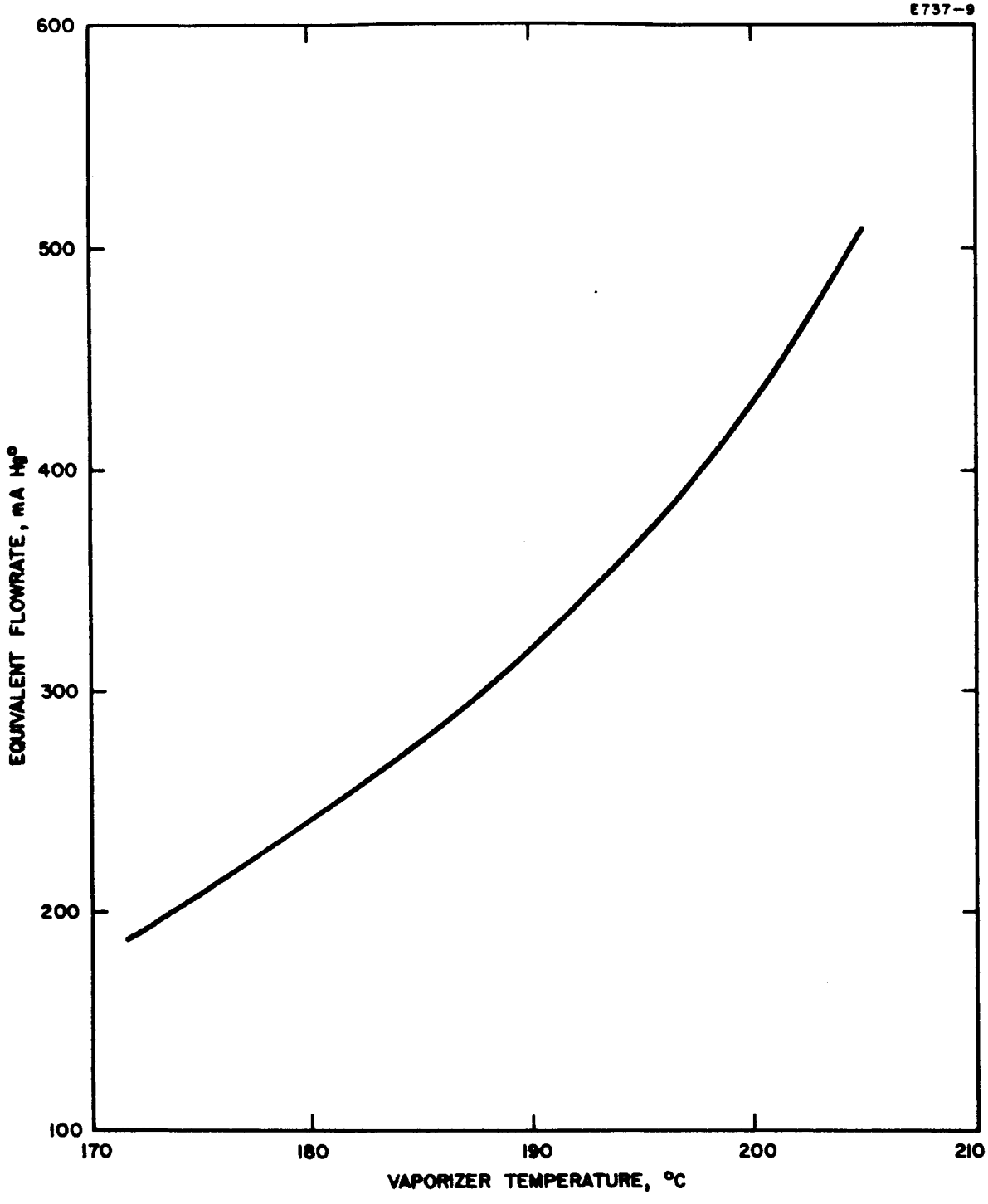

Fig. 9. Typical plot of flowrate versus temperature.

Several test runs were made to calibrate the vaporizer against the piston motion in the reservoir and against a vapor flow meter (which was not part of the final system). The dynamic response, stability, and reproducibility were also demonstrated at this time. The longest continuous run under well controlled conditions was the life test itself. The data of Fig. 8 taken during this period show the stability and control possible with this system. The unit is easily incorporated as part of a closed loop control system to provide accurate control of the propellant flow.

3. Isolator

After vaporization, the mercury streams through an isolator (Fig. 10) before it enters the thruster. This isolator permits operation of the reservoir and feed system at ground potential while the thruster is at positive high voltage. Basically, the isolator consists of an insulating section in the feed line. This section must be dimensioned so that a gas discharge cannot be ignited between the conducting pieces of feed line on both sides of the insulating tube.

The presence or absence of a discharge can be predicted from the Paschen curve, which describes the breakdown potential as a function of the product of pressure and electrode gap width (see Fig. 11). For a feed line pressure of 10^{-1} Torr and a high voltage of 5000 V, the gap width should be smaller than 3 cm if a mercury discharge is to be prevented. In the present isolator configuration the gap electrodes are separated by 1 cm; for additional safety, four sets of electrodes are arranged in series. An isolator of this design readily withstands a voltage of 5000 V at a flowrate corresponding to 1 A equivalent neutral mercury flow.

The isolator must be maintained above the condensation temperature for mercury at the vapor pressure present in the feed line. This is less than 80°C for typical feed line pressures of less than 0.1 Torr. A copper tube is provided to conduct heat from the discharge chamber and

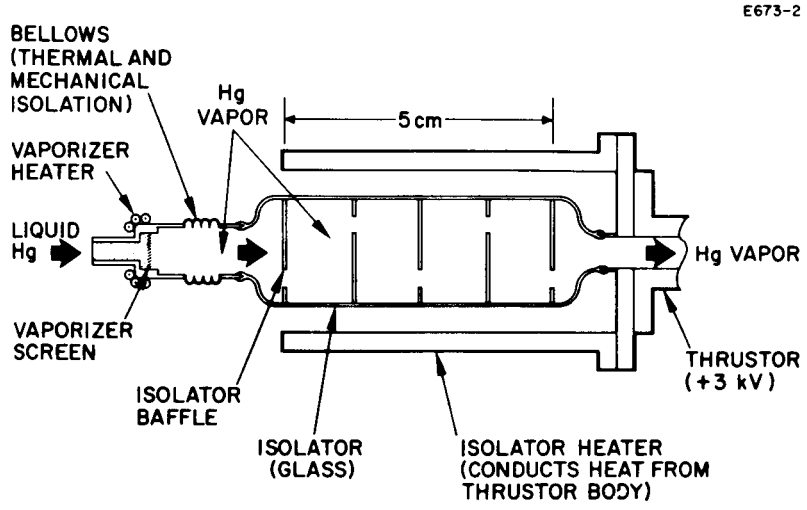

Fig. 10. Mercury vaporizer and high voltage feed line isolator.

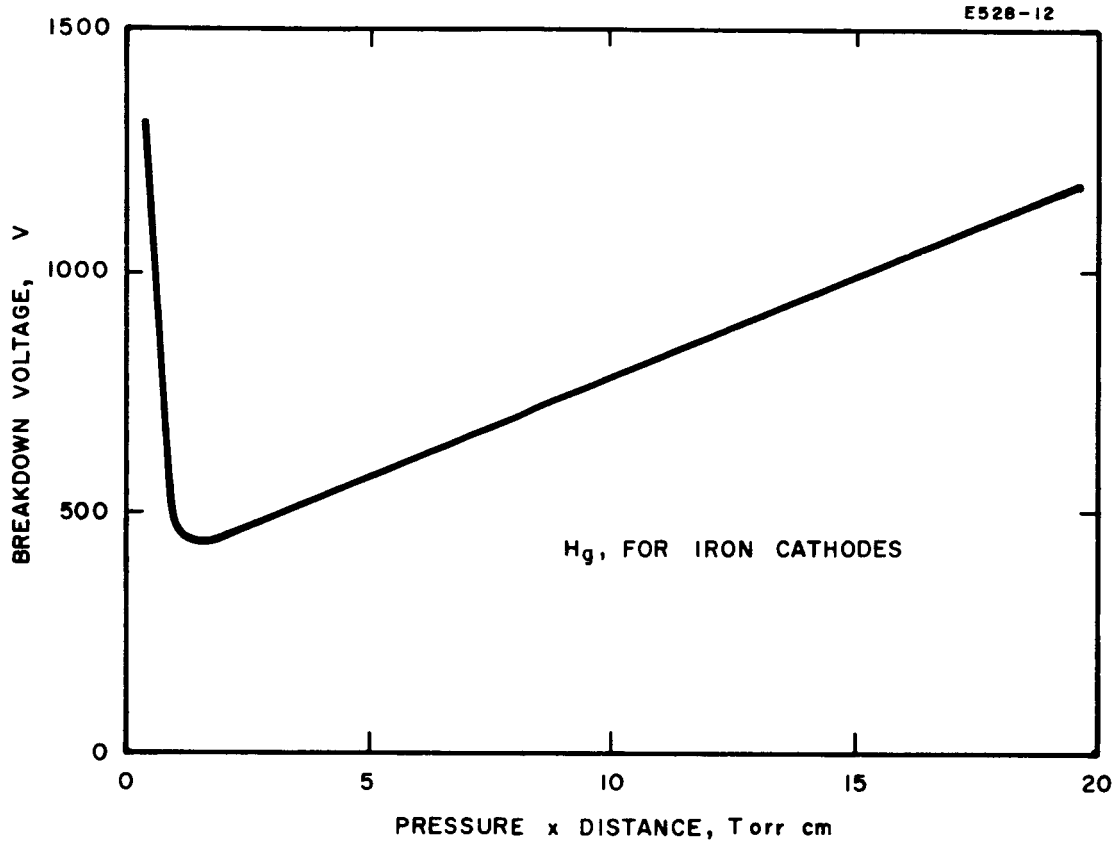

Fig. 11. Breakdown potential as a function of the product of pressure and electrode gap width.

radiantly heat the isolator. From a cold start it is necessary to apply cathode power for approximately 1 hour before the isolator is at operating temperature.

The insulating tube used in the present isolator is made of glass for convenience in fabrication. An all ceramic and metal model has been fabricated and performs well on another system. This type of design should be used for future systems because it is more rugged and because it is conductively heated from the discharge chamber, rather than radiantly heated, and thus will reach operating temperature more rapidly.

4. Integration and Operating Characteristics

The final integration of all components was performed in conjunction with the preliminary thruster tests. During these initial tests the individual components operated as specified, providing the desired constant feed rate, as shown in Fig. 8. Typical operating power was 20 to 30 W for the complete system, the exact number depending on the thermal environment.

C. POWER CONDITIONING AND CONTROL SYSTEM

The initial specifications for the various power supplies and controls are presented in Section III and the design philosophy is given in Section IV. The implementation based on the above is discussed here.

1. Power Supplies and Controls

As discussed earlier, the power conditioning subsystem was mechanized using modular techniques. Photographs of the complete system prior to test are shown in Fig. 12(a) and 12(b). (Thermocouples are provided to monitor component temperatures during the run (see Section VII)). The modular array may be clearly seen from

M 4790

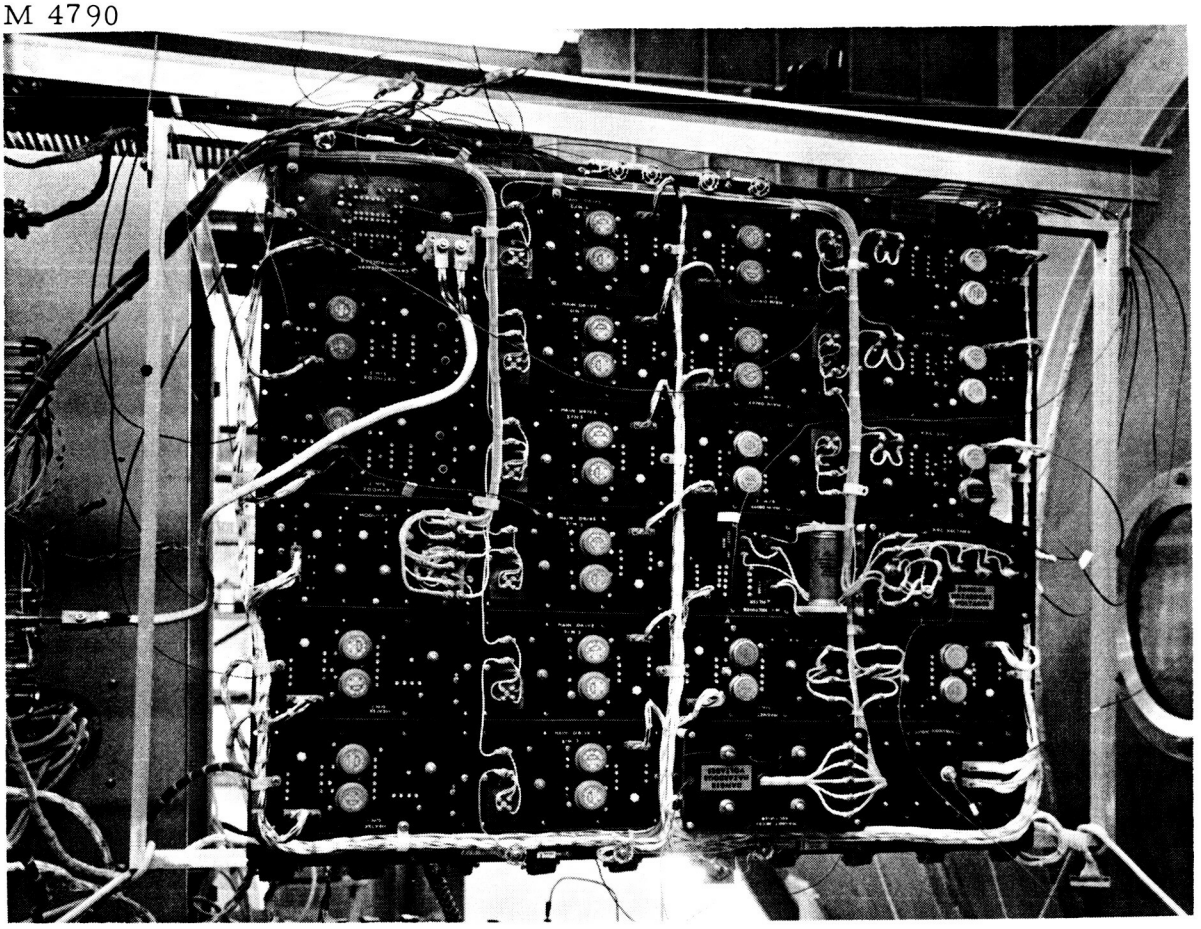

(a) Front view.

Fig. 12. Power conditioning and control system prior to test.

M 4791

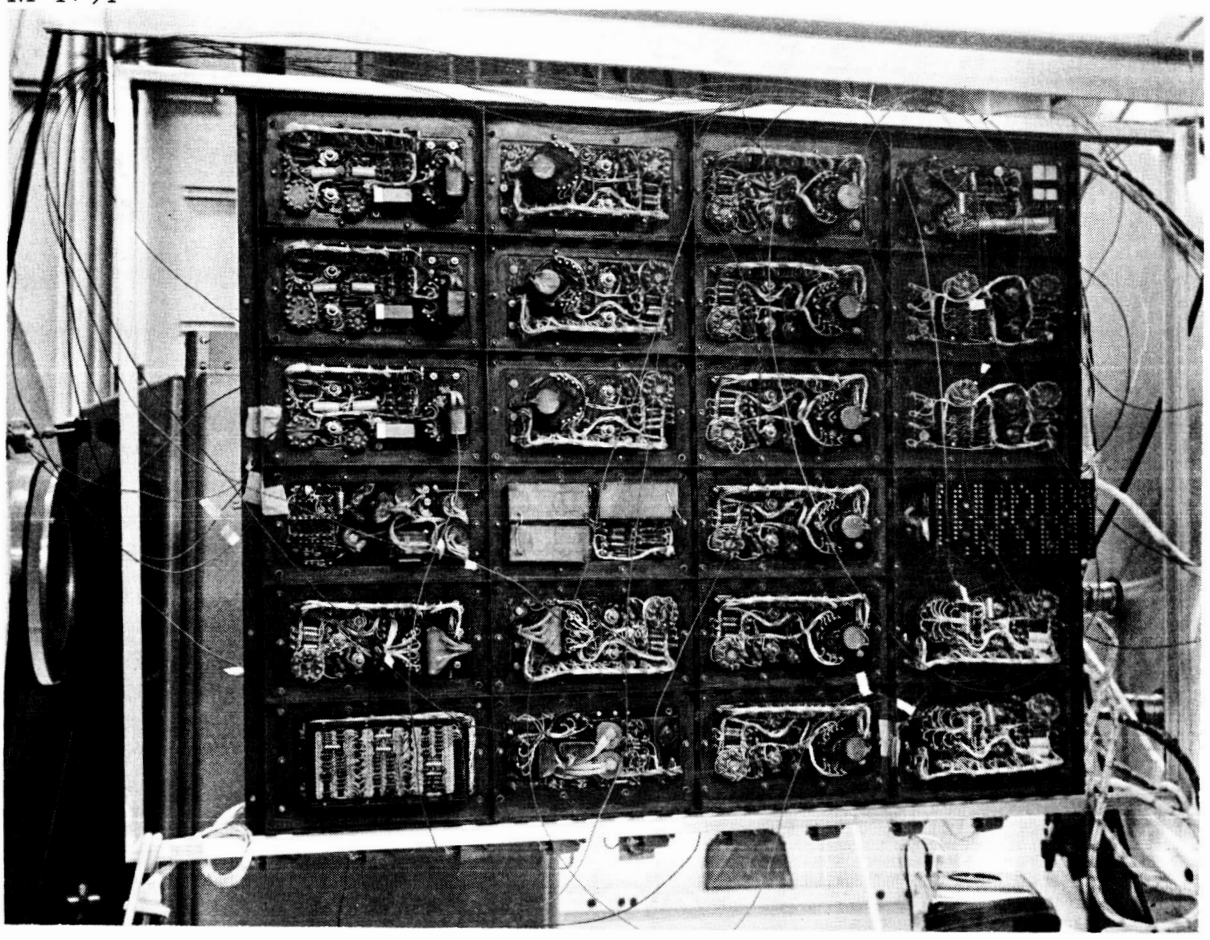

(b) Rear view.

Fig. 12. (Cont'd).

these photographs. The various outputs (beam, accel, etc.) are generated by adding the outputs from the modules, as described in detail in this section. The modules are individually commanded by a micro-circuit control system which accomplishes redundant switching, sequencing, and linear control for closed loop engine operation.

A detailed breakdown of the power conditioning system is presented in Table IV. The table gives the number and types of modules, along with their power, voltage, and current rating. Also included is a specification of salient system parameters, such as over-all-efficiency, size, and weight.

Figure 13 shows the functional diagram of the power conditioning system. It may be seen that both dc and ac adding techniques are employed. The functional diagram shows the incremental and linear control systems which automatically start the engine and maintain its operating point. This system also provides automatic engine restart and shutdown control capability. The micrologic control system is employed to accomplish all digital type functions, such as sequencing, redundant switching, etc. The linear control system, on the other hand, controls the engine heater systems and maintains the ion engine operating current at programmed or set levels. Voltage and current telemetry outputs are provided for each supply, although this is not shown. The individual modules listed in Table IV are described below.

a. Beam Supply

The beam supply must furnish power at 3500 V dc. Seven operating and two standby 125 W self-oscillating inverter modules are employed. A tenth module which contains the high voltage filters and bleeders (for both the positive and negative high voltage supplies) is also required. This tenth module also contains the sampling resistors and voltage dividers used to provide both beam and accel telemetering. The inverter inputs are connected in parallel, and their outputs are connected in series. The micrologic system monitors the seven operating modules for failures and turns on the standbys, as required. All

TABLE IV

Details of Power Conditioning Modules

Function	Design Specifications			Operating Modules		Standby Inverter Modules	Total Modules	Supply Maximum Capability (200 W/inv)	Total Weight, lb	Efficiency, %	Power Loss, W	Semiconductor Type
	W	V	A	Inverters	Other							
Beam	875	3500	0.25	7	1 (Filter)	2	10	1400	9.2	94	55	2N2580
Accel/Magnet	20 60	2000 4	0.01 0.05	1	1 (Rect)	1	3	200	3.0	75	25	2N2580
Arc	252	36	7	2	1 (Rect)	1	4	400	4.5	87	37	2N2580
Cathode Heater	162	3.25	50	1	1 (Controller)	1	3	200	1.6	90	18	2N2581
Feed/Neutralizer Heaters	45 25 25 1.0	3 5 5 10	15 5 5 0.1	1	1 (Modulation)	1	3	200	3.3	85	19	2N2580
Logic and Control	—	—	—	–	1	–	1	—	0.9	—	1	DTμL and μA 709
Frame (structure)	—	—	—	–	–	–	–	—	2.5	—	—	—
Totals	1465			12	6	6	24	2400	25.0	90	155	

Notes
Weight of standby modules = 5.13 lb
Weight of system excluding standbys = 19.87 lb
Weight shown includes all support structures and radiation cooling required for space applications.

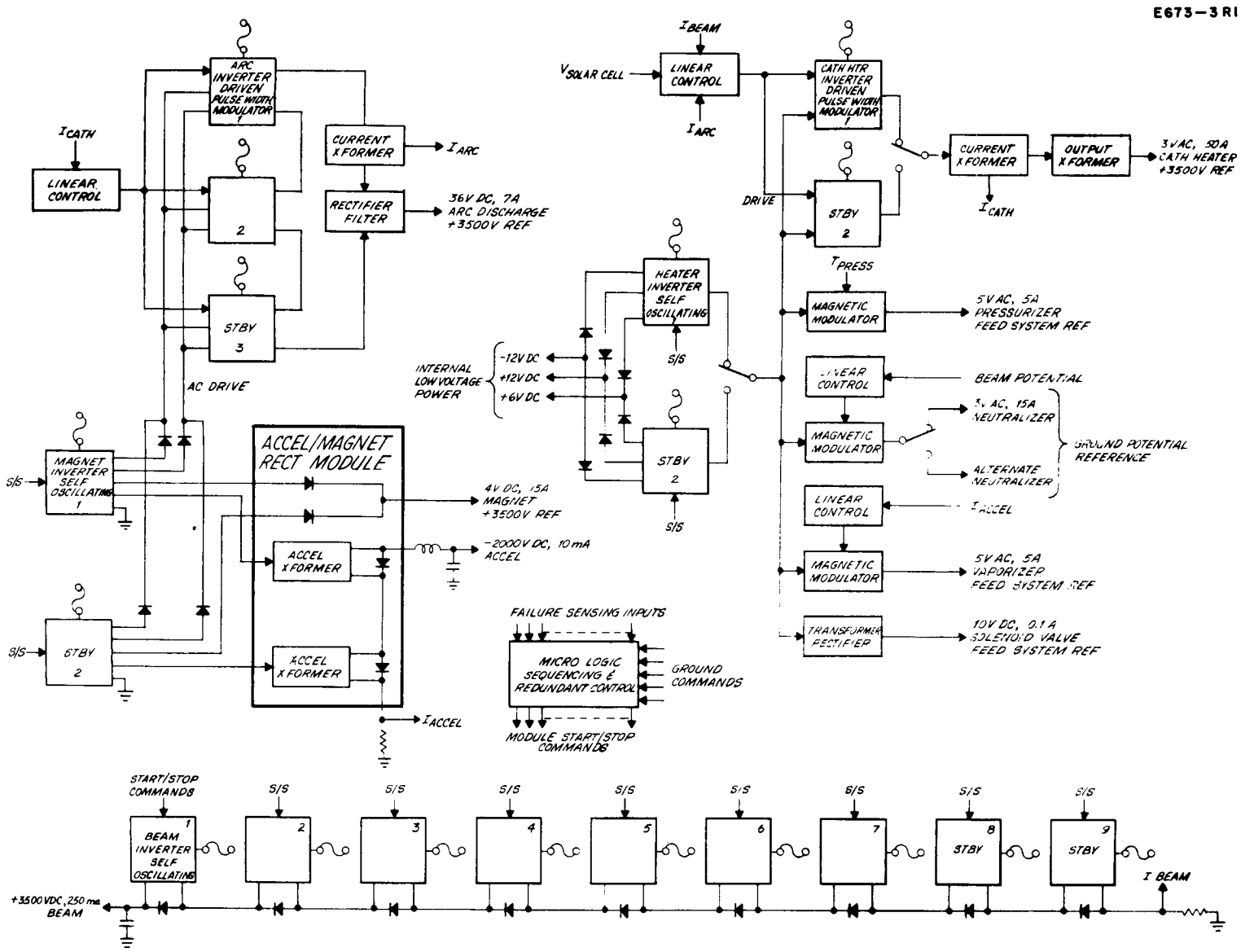

Fig. 13. Power conditioning functional diagram.

inverter modules are fused at the power inputs and employ bypass diodes in the output circuits. If an inverter module short circuits, the fuse opens. If the inverter stops oscillating, or a transistor malfunctions, the bypass diode prevents an opening of the inverter output series circuit. Each inverter module has its own individual micrologic start/stop circuit to control inverter oscillation. This circuit accepts logic commands from the main micrologic system. In the event of an engine arc, the modules will be shut down and restarted via the micrologic system. The inverters are shut down during arcing to prevent circuit damage.

The basic circuit of the self-oscillating inverter (minus the start/stop circuit) is shown in Fig. 14.

This circuit is a magnetically coupled oscillator which employs a separate saturating feedback transformer for timing. The output transformer does not saturate; therefore, no large transistor collector current spikes occur at the switching moment (as is the case with the more conventional single transformer circuit). These current spikes would represent a high transient collector dissipation. Therefore, two transformer circuits are employed to reduce transistor dissipation.

Conventional inverter start/stop circuits, which rely on a transient or a bias supplied by the application of E_{line} for starting and the removal of E_{line} for stopping, are not applicable here. It is undesirable to insert a switch in series with the line to exercise this type of start/stop circuit because such a switch sacrifices efficiency if a semiconductor is used or sacrifices turnoff speed if a relay is used. Turnoff speed is essential here in order to accomplish a high speed shutdown in the event of a load transient (typical with ion engines). Therefore, the prime source voltage remains connected to the inverter circuit at all times, and the start/stop function is accomplished in other ways.

The basic start/stop function is shown in Fig. 15.

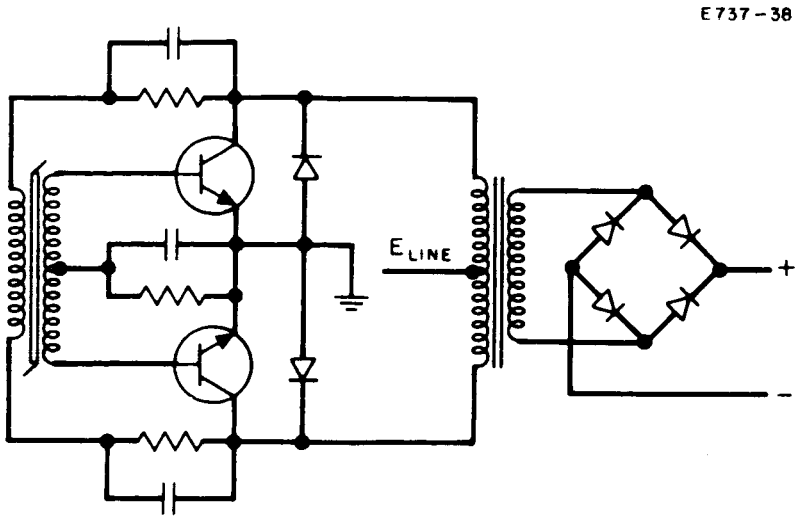

Fig. 14. Basic self-oscillator.

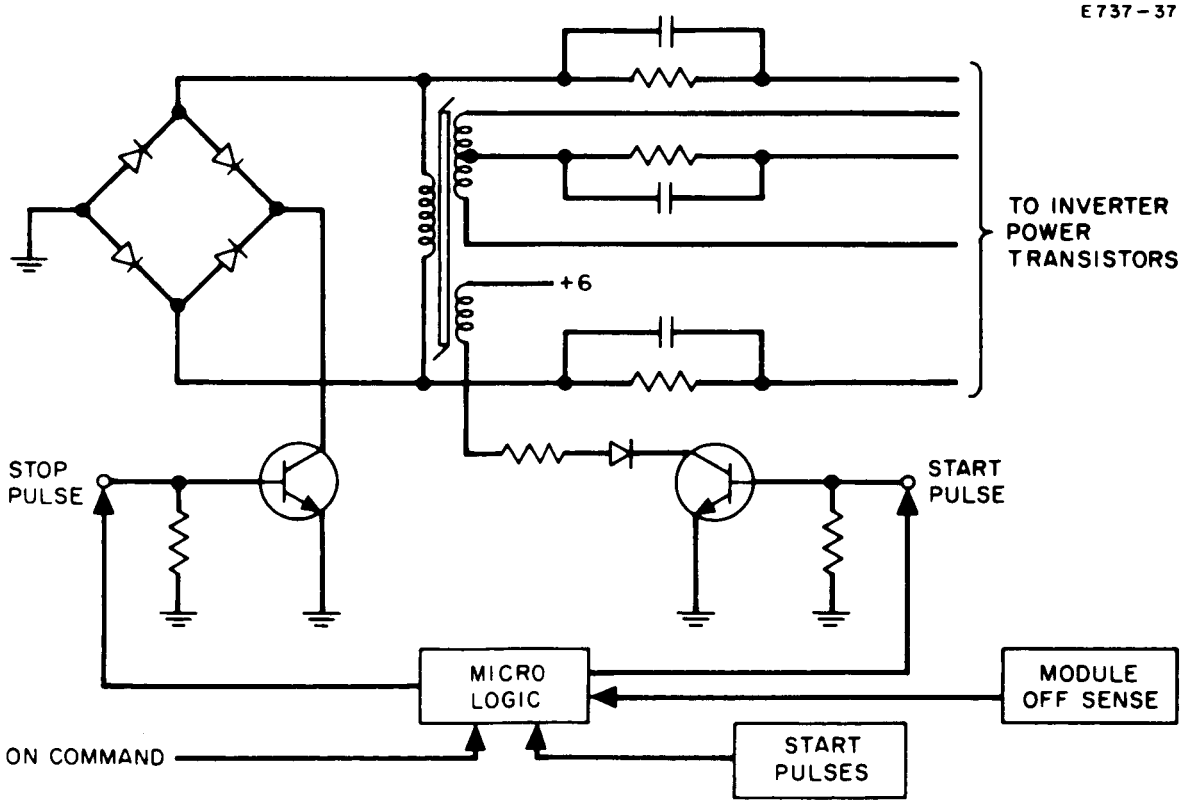

Fig. 15. Start/stop circuitry.

The inverter will not oscillate with the line voltage applied as shown in Fig. 14. Some external energy must be delivered to the circuit to "set it in motion." In the circuit of Fig. 15, the start circuit delivers a pulse of energy to the inverter via the feedback transformer, as shown. The micrologic circuitry passes the train of 1% duty cycle start pulses to the start circuit if the "ON" command is present and the inverter is not operating (as indicated by the "off sense" circuitry which derives its output from an auxiliary winding on the output transformer). The micrologic circuitry will not pass the train of start pulses if the "ON" command is absent or the inverter is operating.

Thus, the starting logic receives the "ON" command, applies the start pulse to the inverter, observes that the module has started, and then inhibits further start pulses from being passed to the module. If for any reason the module should stop (by a mechanism of some random transient, for example) and "ON" command is still present, the micrologic will again apply start pulses until starting occurs. This level of sophisitication is employed in the start circuit to provide for reliable starting under all conditions which might develop during the course of a 10,000 hour mission. Since some unknowns are necessarily involved in a mission of this length, it is necessary that the control logic be as "foolproof" as possible.

Note that only one start pulse generator is necessary for all modules. Furthermore, it should be noted that the start circuit is essentially disconnected from the module when starting has occurred. This insures that the high efficiency operation of the basic module is not affected by the presence of the starting circuit. This same philosophy is carried over into the design of the stop circuit. That is, it is disconnected from the module once oscillation has ceased, and therefore there is no standby dissipation in the stop circuit during the period when the module is off.

The stop circuit functions by shorting out the feedback circuit and thus quenching the oscillation. The micrologic circuit turns on the stop transistor whenever the "ON" command is absent and the module is operating. The stop transistor will not be turned on whenever the "ON" command is present or when the module is not operating. Thus, the stopping circuit operates on the absence of the "ON", turns on the stop transistor, which shorts out the feedback circuit, and then turns this transistor back off when the module ceases operation. If for any reason the module should start (via some random transient, for example) and the "ON" command is absent, the stop transistor will be turned on and the module will be stopped. Thus, the same "foolproof" philosophy used in the start circuit is used in the stop circuit.

A diagram of the logic circuitry is shown in Fig. 16. This diagram is simply a "Nand Gate" mechanization of the function described above, and the techniques are standard. Currently available hardware allows this circuitry to be packaged in three small "flat packs" and provides the reliability equivalent to that of three transistors. Thus, small size and high reliability are features of this circuit. This circuit is then packaged in the self-oscillating inverter module and is considered to be a part of the module circuit.

b. Magnet/Accel Supplies

The magnet inverters (one operating, one standby) are self oscillating circuits which supply ac power to the magnet rectifiers, the accel output transformers (located in the accel/magnet rectifier module), and the arc driven inverter. Micrologic start/stop is employed here in a manner identical to that of the main beam supply. The magnet rectifiers (one operating, one standby) and the accel output transformer-rectifier combinations (one operating, one standby) are contained in a separate module. This module contains current transformers for providing magnet current telemetry.

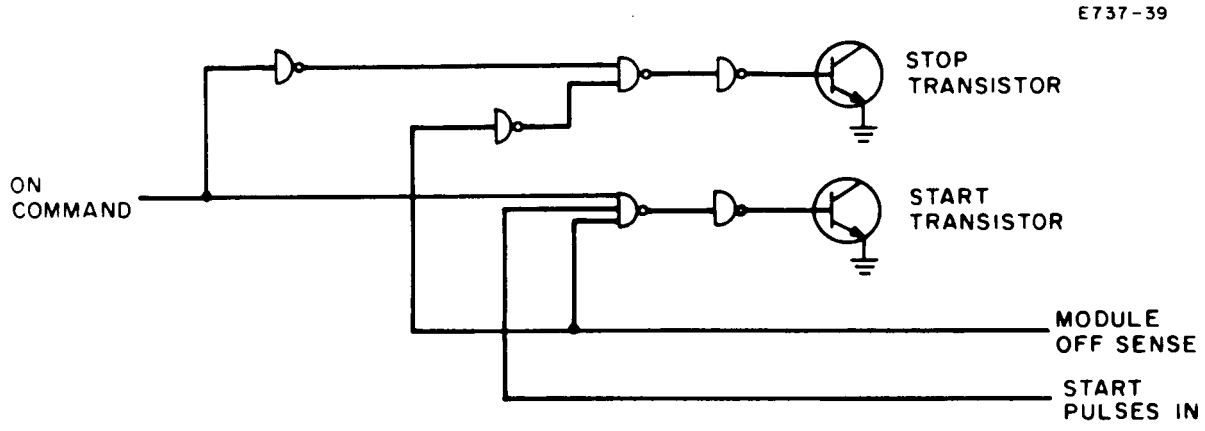

Fig. 16. Start/stop micrologic.

c. Arc Supply

The arc inverters (two operating, one standby) are driven, pulse-width modulated circuits which supply ac power to the arc rectifier-filter module. The module outputs are ac series added (made possible by the driven operating mode) to form the total. The module which is not in use has its transformer primary shorted out by a relay. Drive power is received from the magnet inverters, and the pulse width modulation is governed by circuitry located in the arc rectifier-filter module. The rectifier-filter module also contains sensing transformers for arc voltage and current telemetry.

The basic circuit of the driven inverter is shown in Fig. 17. For the sake of simplicity, pulse width modulation is not shown. With the exception of the control logic, the operation of the circuit is quite straightforward. The relay is energized during normal operation; its primary function is to short out the transformer in the event of a module failure. If only half of the primary is shorted, only one relay pole is needed either to connect to E_{line} or to accomplish shorting. The transistor which operates the relay is also used to connect or disconnect the drive to the inverter and is used to provide rapid turnoff of the inverter in the event of transient overload.

The control logic for this module is different from that for the self-oscillating case. Here the on-off control is primarily dc rather than pulse type. In addition, it is necessary to determine whether the module has failed, so that the relay may be deenergized even though the "ON" command is present. In contrast to the self-oscillating inverter modules which are used in the dc adding technique, it is not only necessary to sense that a failure has occurred, but it is also necessary to determine which module has failed, so that its relay may be closed.

Micrologic is used to perform the failure sensing mechanism; this decision is based on the following logic:

Module Failure = (Delayed Command On) · (Module Not Operating)

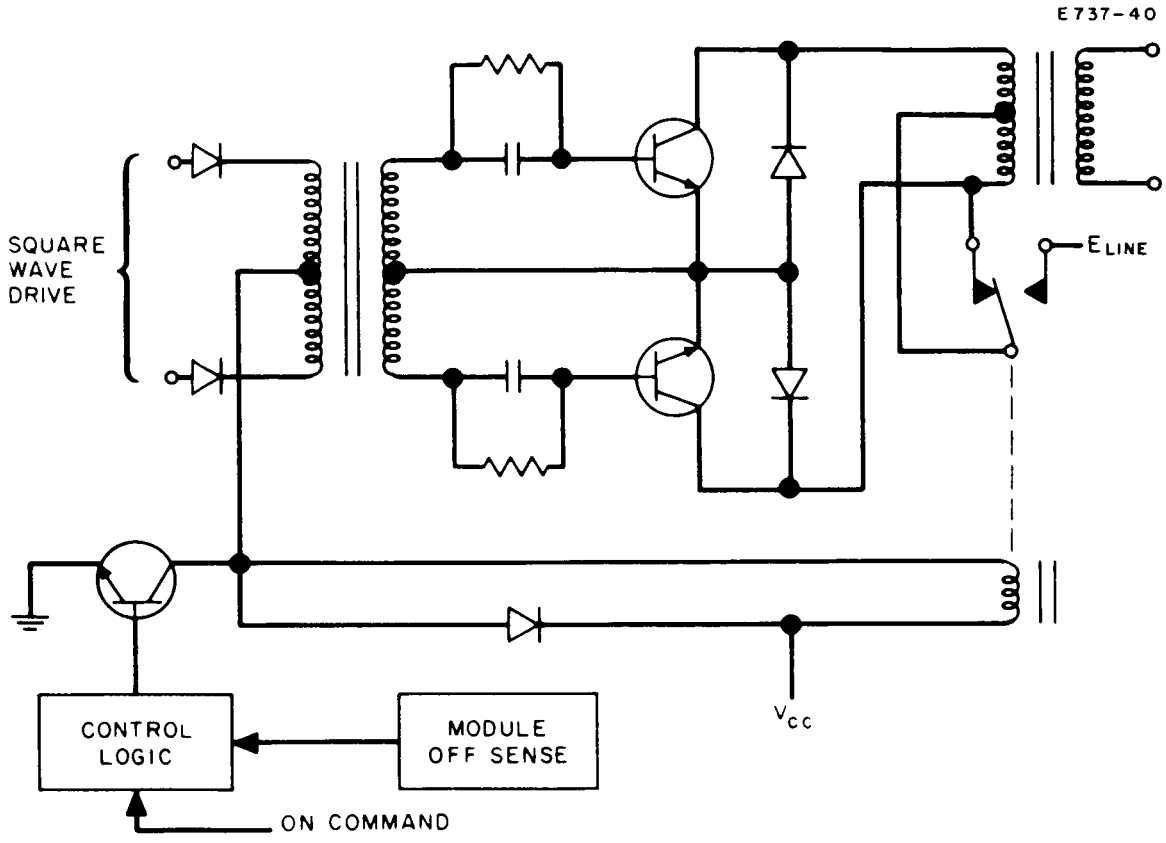

Fig. 17. Driven inverter circuit.

failure signals in the correct Boolean form to derive a signal which indicates whether two failures have occurred. The circuitry to generate the commands for both standbys requires eight "flat packs" and is packaged in an encapsulated block which has the approximate dimensions of 3-1/2 in. by 5/8 in. by 3/16 in. Thus, the physical size of the hardware required to perform this task is made very small through the use of microelectronics.

Failure sensing and switching for the other supplies is as described above. However, since the remaining supplies consist of, at most, three modules (arc supply), the situation is not as complex. For example, the magnet/accel supply has only one operating and one standby module. Therefore, it is necessary to determine only if the one module has failed in order to command the standby.

(3) Linear Controller – The linear controller maintains the engine operation within prescribed limits by sensing various parameters, and generating signals which control the four variable supplies. The nature of the control function may be changed in discrete steps by digital commands from ground control. The four variable supplies which are involved in the linear control are listed below:

1. Vaporizer
2. Cathode Heater
3. Arc
4. Neutralizer.

The interpretation of the control characteristics given in Section III is described in Figs. 20, 21, 22, and 23 and Table V. Note that in the case of the vaporizer and cathode heater control, a family of curves is available. These discrete families are selected by ground command. Note also that the cathode heater is controlled by more than one parameter. In this case, the control function which demands the greatest amount of power reduction is used (for example Fig. 24).

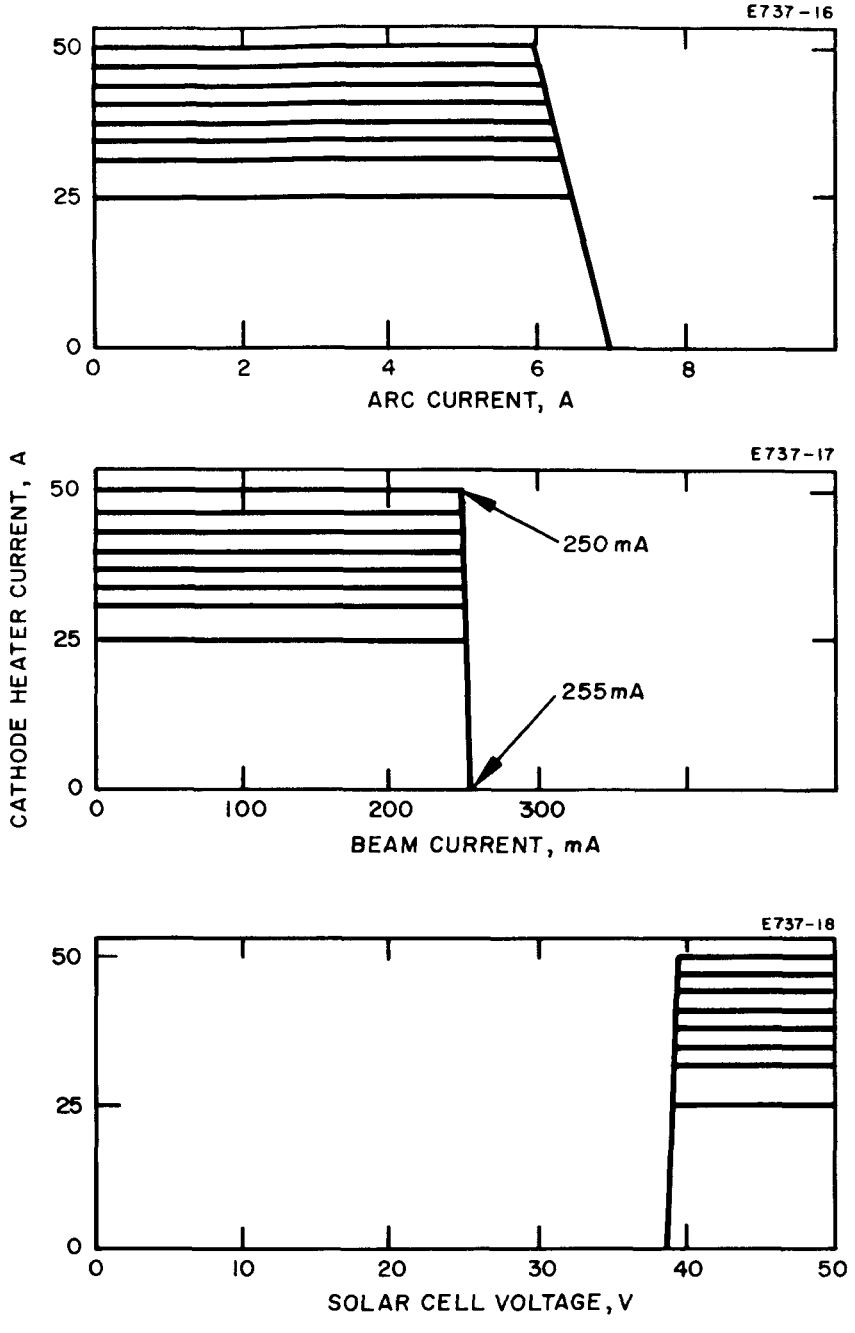

Fig. 20. Cathode heater control characteristics.

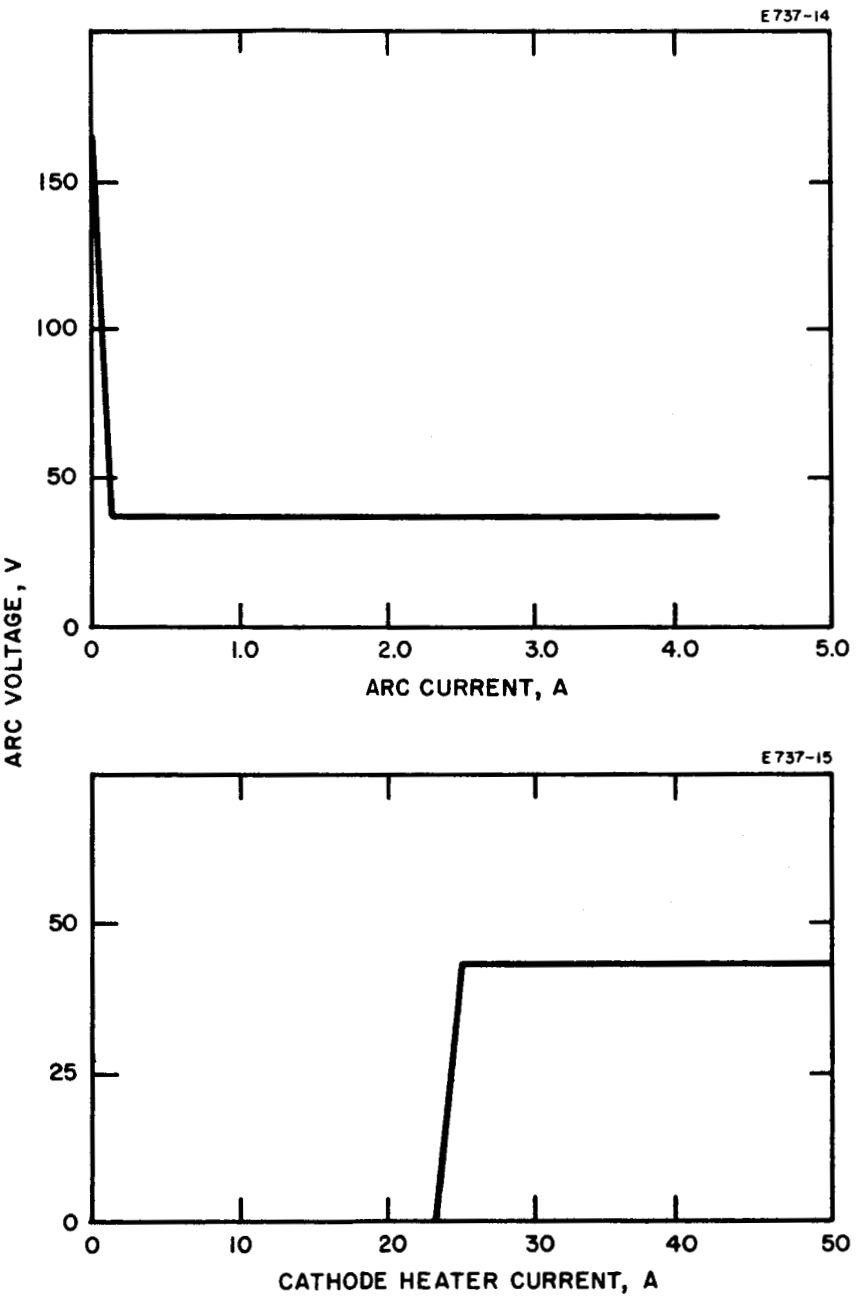

Fig. 21. Arc control characteristics.

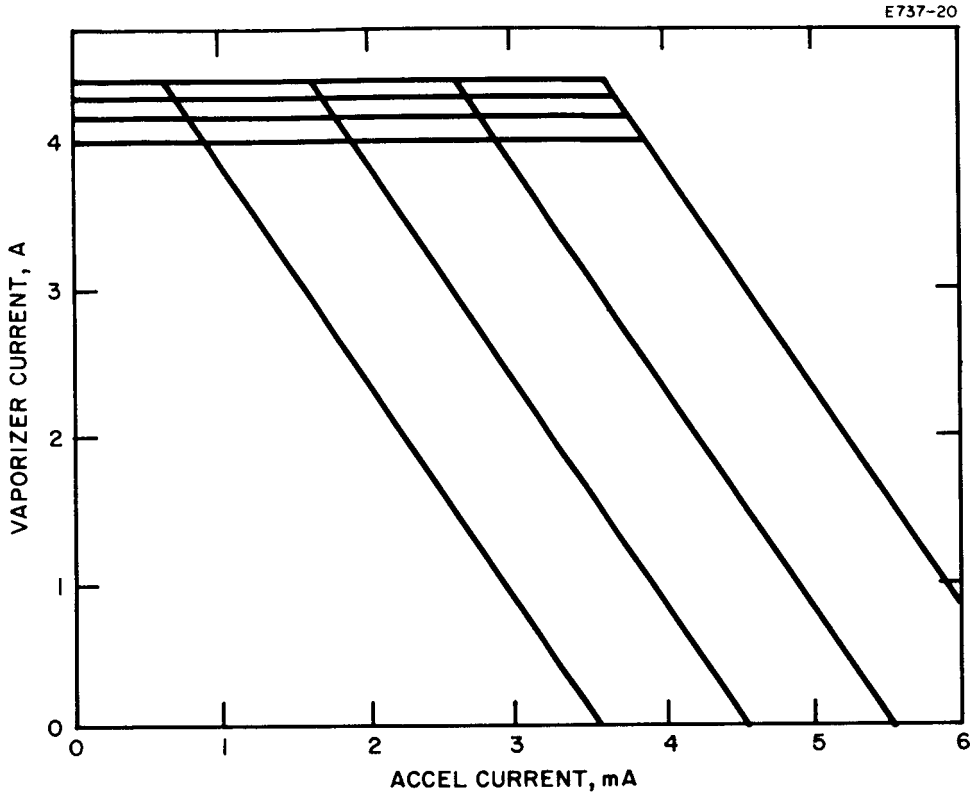

Fig. 22. Vaporizer control characteristics.

TABLE IX

Weights and Powers for Various Supplies

Supply	Power, W	Percent of Power	Basic Weight, lb	Redundant Weight, lb	Total Weight, lb	Percent of Weight
Beam	875	73.0	4.18	1.84	6.02	38.6
Arc	90	7.5	1.30	0.80	2.10	13.5
Cathode Heater	150	12.5	0.60	0.60	1.20	7.7
Magnet	45	3.7	0.90	0.60	1.50	9.6
Accelerator	5	0.4	0.50	0.30	0.80	5.1
Feed	35	2.9	0.30	0.20	0.50	3.2
Control			0.90		0.90	5.8
Frame and Wiring			2.50		2.50	16.1
Total	1200	100.0	11.18	4.34	15.52	100.0

in any assessment of power conditioning weight; with a solar array weight of 50 lb/kW it is apparent that a 5% lower efficiency would result in 2.5 lb/kW addition in solar array weight, a significant fraction of the power conditioning weight at 12.9 lb/kW.

REFERENCES

1. "Solar Powered Electric Propulsion Spacecraft Study," Final Report, JPL Contract No. 951144, December 1965 (SSD 50094R).
2. Letter from B. L. Sater (NASA-LeRC) to J. Stearns (JPL), dated 4 October 1965.
3. JPL Technical Memorandum, signed D. Kerrisk, dated 27 October 1965.
4. These numbers are extrapolated from data presented by Westinghouse Electric Corporation, NASA Reports CR-54216 and CR-54217, dated May and March 1965, and Wilmore Electronics, NASA Report CR-54408, dated December 1965.
5. H. E. Gallagher, "Low Work Function Cathode Development," Hughes Research Laboratories Final Report on Contract NAS 3-7114.

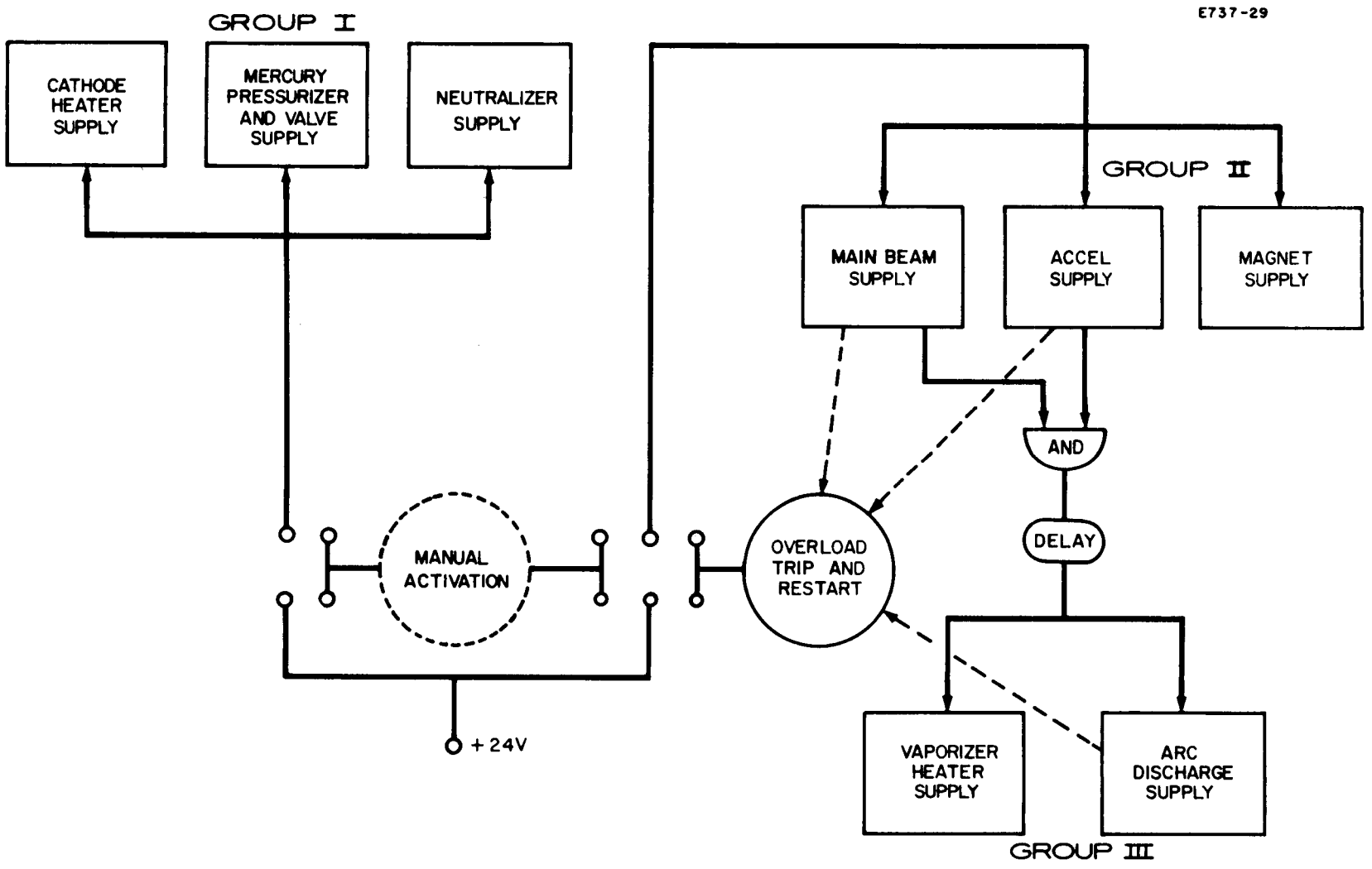

Fig. 19. Startup sequence for ion engine system test.

event of an engine arc, block 2 and block 3 are simultaneously turned off. Within 1/2 sec, block 2 is restarted and block 3 follows by the 5 sec delay. This automatic turn off and restart occurs each time an engine arc takes place. (During system integration tests, it was found necessary to alter this sequence slightly, as discussed in the next section.)

(2) Failure Sensing and Redundant Switching – This portion of the logic system essentially controls the standby modules. In order to illustrate how this is mechanized, the main drive switching will be described. There are seven operating and two standby modules in the main drive supply. When block 2 is commanded on by the sequencer, the seven operating modules are commanded on and the two standbys are held off unless there has been a failure in the first seven.

The first step in redundant switching is the determination of a failure. A failure is sensed by comparing the module "ON" command with a signal which defines the state (on or off) of the module. This signal is derived directly from the module output transformer and provides a digital indication as to whether the module is producing power. A module failure signal is derived by the following logic:

$$\text{Module Failure} = (\text{Delayed Command On}) \cdot (\text{Module Off}) \cdot$$

The delay is used to remove the ambiguity which would exist at the moment of turnon if the delay were not used.

If a failure is detected in one of the seven operating modules, the first standby is commanded "ON." It is not necessary to determine which module has failed because the dc adding technique provides for bypassing a failed module through its own output rectifier. Thus the "ON" command for the first standby is generated by "OR"ing the failure sense signals of each of the first seven modules. If any two failures should occur in the first seven plus the first standby, the second standby is commanded "ON." This command is generated by combining the module

d. Cathode Heater

The cathode heater inverters (one operating, one standby) are driven, pulse-width modulated circuits which supply ac power to the cathode heater output transformer located in the cathode controller module. Drive power is received from the heater inverters and the pulse width modulation is governed by the cathode controller module which contains the cathode heater output transformer and the circuitry required to control the pulse-width modulation of the cathode heater inverter. The control is such that an rms current regulator is mechanized. The regulation point is controlled by an external analog voltage. The controller module also contains the cathode heater telemetry circuits.

e. Neutralizer/Feed Heater

The heater inverters (one operating, one standby) are self-oscillating circuits which supply ac power to the neutralizer, vaporizer, pressurizer, and solenoid valve modulators. AC power is also supplied to the cathode heater driven inverters, and low voltage (+ 6, ± 12 V) dc power is distributed throughout the system for use as control voltage, logic power, etc. Since low voltage is not present for micrologic operation prior to starting the heater inverters, these are started directly from ground command. The heater modulator module contains the magnetic modulators for controlling the neutralizer, vaporizer, pressurizer, and solenoid outputs. The neutralizer and vaporizer supplies are rms current regulators with outputs controllable by an external analog signal. The pressurizer is a temperature regulator employing a thermistor-bridge detector and the solenoid is merely a constant output supply. The modulator module contains the telemetry circuits for all of these supplies.

f. Control and Logic

The control and logic functions are mechanized using both analog and digital techniques. Digital techniques are used primarily for failure sensing, redundant switching, and start/stop sequencing. Integrated microcircuitry in flat-pack form is employed throughout. Analog

techniques are used to generate the linear control functions. Integrated circuit operational amplifiers (packaged in TO-5 cans) sense engine performance and generate the analog voltages which control the adjustable supplies. Key digital logic signals are also made available for telemetry.

In addition to supplying the engine with the basic power forms required for operation, the power conditioning subsystem must provide for automatic system control. This can be broken into three categories: start sequence, failure sensing and redundant switching, and linear engine control.

(1) Start Sequence – The initial startup sequence specified by NASA-LeRC was a simultaneous turn onof all supplies. This specification was later redefined by agreement between NASA-LeRC, JPL, and HAC to require a sequence of three basic steps. That is, during the sequence, power is applied to the engine in blocks. These are listed below and shown in Fig. 19.

Block 1 – Cathode Heater, Pressurizer, Neutralizer, Valve

Block 2 – Beam, Accel, Magnet

Block 3 – Vaporizer, Arc

The block 1 group is started on ground command by sending a pulse to the heater inverter which operates these supplies. This signal causes the cathode heater, plus all supples in the modulator module (except the vaporizer), to begin operation. The vaporizer supply is inhibited at this time by a bias signal which is not removed until block 3 starts.

After allowing sufficient time for engine warmup (this time is determined by ground control), a ground command is sent to the logic system, which in turn sequences block 2 and block 3 automatically. The logic system starts block 2 as soon as the ground command is received. After an atuomatic 5 sec delay, the logic system starts block 3. In the

This logic is self-explanatory. Note that the "ON" command is delayed slightly to eliminate the ambiguity which would exist at initial turnon if the "ON" command were used directly. Only one delayed command "ON" signal is needed for the series string, and this signal is generated by simply applying the "ON" command signal to an R-S flip-flop and using the delay of one clock pulse. This signal is "anded" with the Module Not Operating signal to generate a Module Failure signal which is used in the relay logic. The relay micrologic operates the transistor which controls the relay. The relay logic is as follows:

$$\text{Relay On} = (\text{Command On}) \cdot (\text{Module Not Failed}) \quad .$$

This logic is again self-explanatory and it can be seen that the relay is deenergized if the module fails, even though the command "ON" signal is still present. The relay and module failure logic may be mechanized with only three "flat packs"; therefore, the hardware is no more complex than that for the self-oscillating modules.

The incorporation of the pulse width modulator in the driven inverter circuit is shown in Fig. 18. The arc inverter modules employ the circuit of Fig. 17 along with the modification shown in Fig. 18.

A separate module contains the arc supply rectifier-filter and the circuitry required to control the pulse-width modulation of the arc inverters. The rectifier-filter consists of two basic circuits. One is a low voltage (36 V dc), low impedance circuit and the other is a high voltage (108 V dc), high impedance circuit. The outputs of these two are "or'd" together through diodes. This provides the necessary boost to start the arc when the output current is low, while supplying the bulk of the power at the low voltage when the output current is high. The pulse-width modulation control is such that a voltage regulator is mechanized. The regulation point is controlled by an external analog voltage.

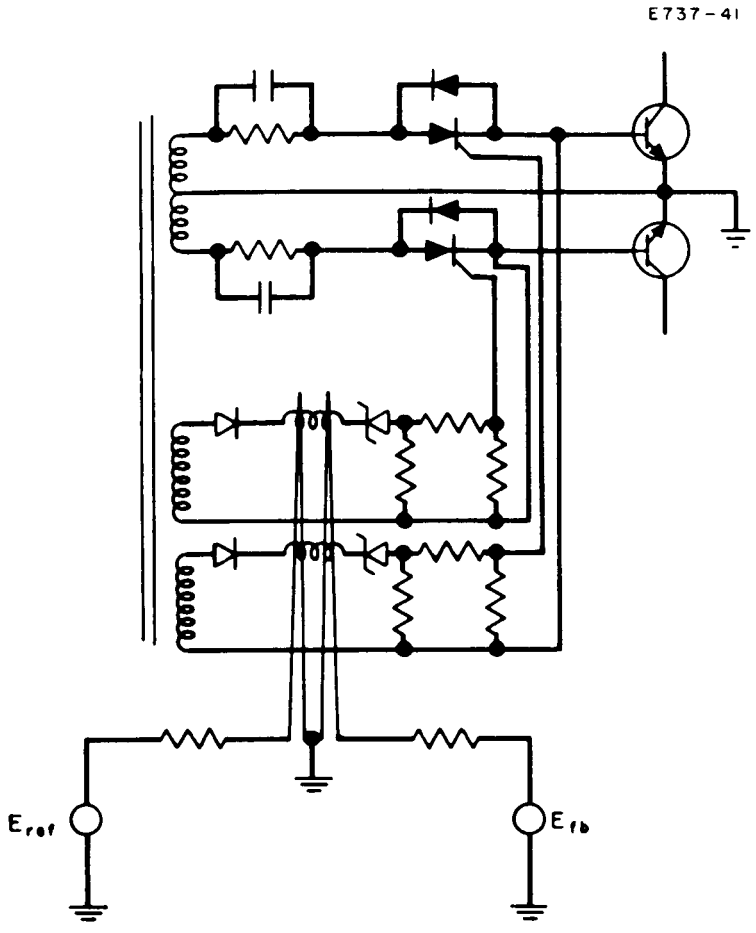

Fig. 18. Pulse-width modulation base drive circuit.

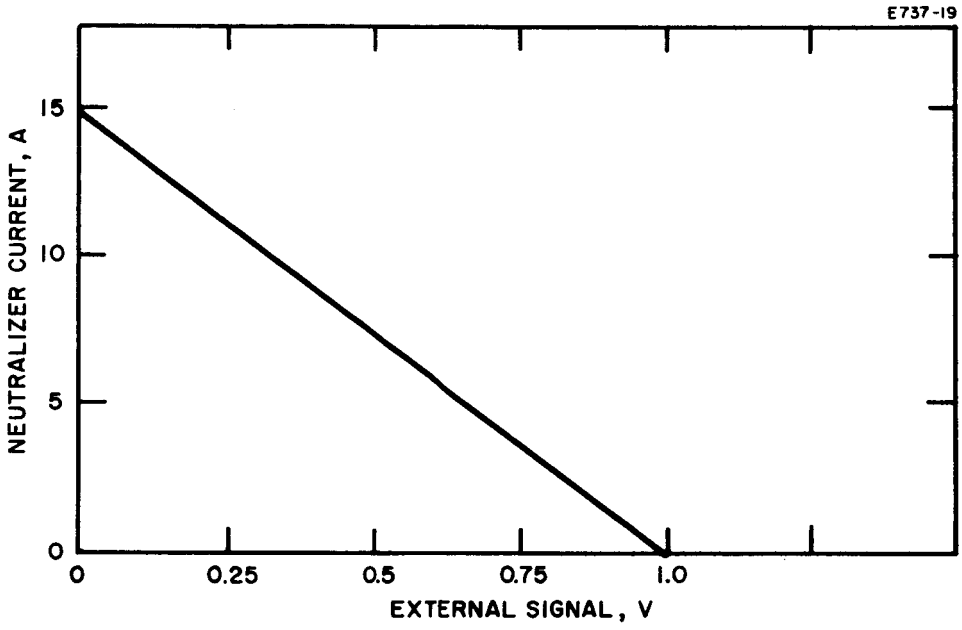

Fig. 23. Neutralizer control characteristics.

TABLE V

Ion Engine System Design Point and Control Specifications

Controller	Input				Output			
	Variable	Design Value or Range	Control Set-Point		Variable	Design Value or Range	Control Set-Point	
			Type	Value			Type	Value
Beam Current/ Cathode Heater	Beam Current	250 mA	Fixed	250 mA	Cathode Heater Current	25 - 50 A	Manually variable[a]	25 - 50 A
Arc Override/ Cathode Heater	Arc Current	2.5 A	Fixed	6.5 A	Cathode Heater Current	25 - 50 A	Manually variable[a]	25 - 50 A
Solar-Cell Override/ Cathode Heater	Solar-Cell Voltage	42 V	Fixed	40 V	Cathode Heater Current	25 - 50 A	Manually variable[a]	25 - 50 A
Arc Voltage	Cathode Heater Current	25 - 50 A	Fixed	25 A	Arc Voltage	30 - 36 V	Fixed	30 - 36 V
Vaporizer/Accel Current	Accel Current	2 - 5 mA	Manually variable[a]	2 - 5 mA	Vaporizer Heater Current	4 - 4.4 A	Manually variable[a]	4.0 - 4.4 A

[a]All manually variable control set-points are digital.

These control functions are mechanized by employing operational amplifiers and analog computer techniques. Analog signals representing the various inputs are available from the telemetry circuits of the power supply. These inputs are operated in accordance with the control characteristics to produce an analog voltage which is used by the power supply being controlled to establish its operating level. Each power supply is mechanized so that as its input analog control voltage rises from 0 to 7 V, its output is linearly reduced from 100% to 0. The linear controller uses microcircuit techniques in order to minimize size and maximize reliability. Each of the operational amplifiers employed is contained in a single TO-5 size transistor package.

The control of the cathode heater is as follows. Under normal operation, the cathode heater current will be determined by the beam current design point (250 mA). The upper set point for heater current is manually adjusted above that required for 250 mA of beam, the operating point will always be forced onto the sloping part of Fig. 24(a). If cathode deterioration causes the beam current to fall, the set point is raised discretely by external command.

If operation departs from normal for some reason (such as autocathoding), two override loops are provided. Figure 24(b) shows the arc override control function. Under normal conditions, arc current is 2.5 A. If the arc current exceeds 6.5 A, the cathode heater current will be reduced by the arc current signal, regardless of beam current.

Similarly, a second override loop is provided to accommodate a drop in solar-cell output voltage. The solar cell voltage is normally maintained at 42 V. If it falls below 40 V, the cathode heater current is reduced by the solar cell signal (Fig. 24(c)).

The arc voltage controller is designed to maintain a constant arc voltage, preset at a value between 30 and 36 V. In two situations, however, the arc voltage shall be other than the nominal design point value: (1) startup, and (2) autocathoding. During startup, in order to initiate the arc discharge, the arc voltage shall be increased to three times its normal value,

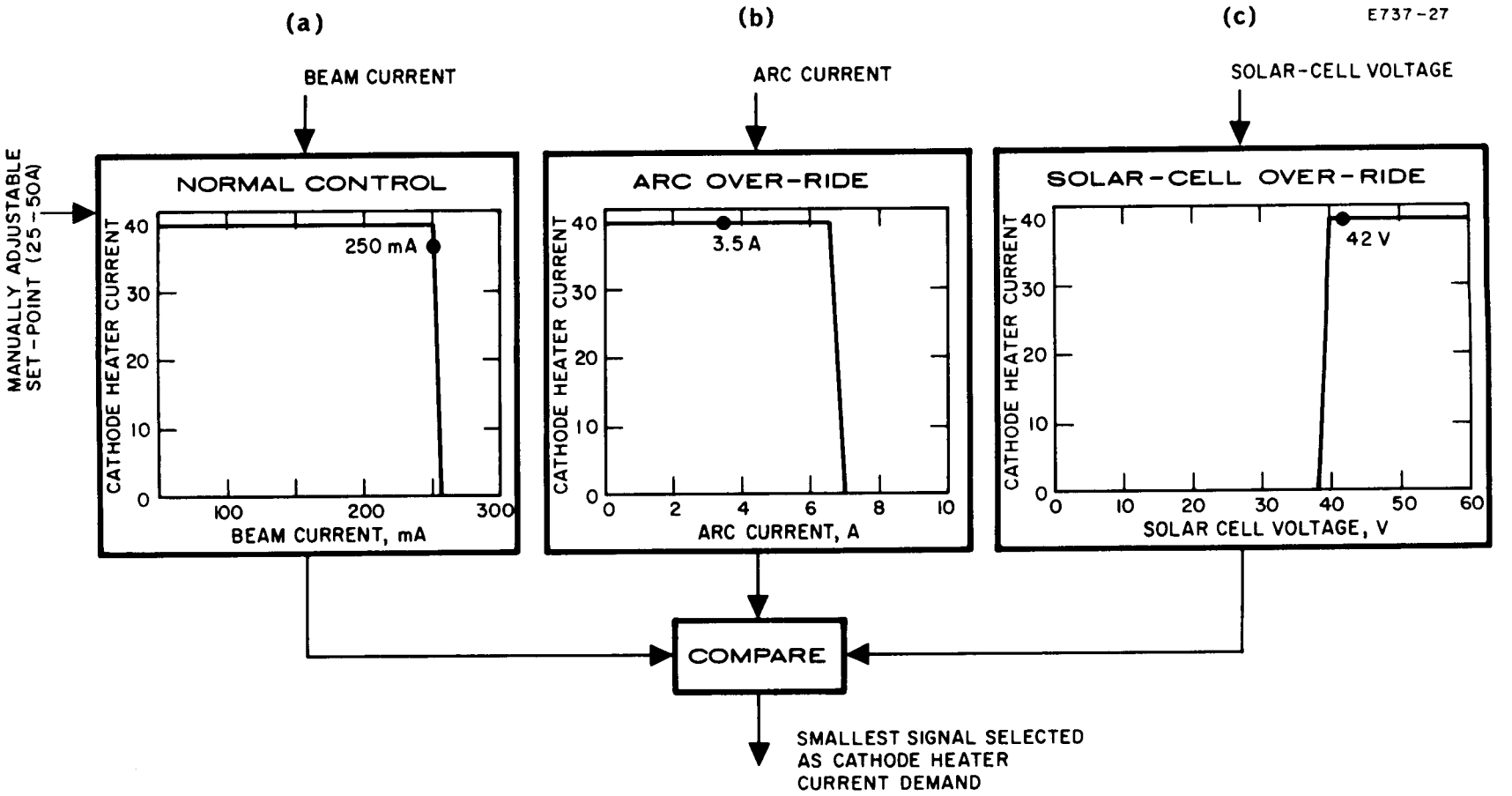

Fig. 24. Cathode heater current control logic and beam current control.

or 108 V. Tripling of the arc voltage is accomplished internally to the arc supply. While arc current is below 10 mA, the arc voltage is at the startup value of 108 V, regardless of any other system demand signals.

The other condition for departure from design point value of arc voltage is autocathoding. When cathode heater current falls below 25 A, an autocathoding situation is indicated and the arc voltage is reduced. The arc voltage demand falls to 5 V when the cathode heater current drops from 25 to 23 A.

The final control function employed in the system is the vaporizer heater control. The vaporizer heater current control is accomplished by maintaining a fixed value of accel drain current. This is accomplished in a manner similar to that used for cathode heater — beam current control. However, the vaporizer current controller differs somewhat because it has the capability for two-dimensional set-point adjustment (Fig. 22). Both the accel current operating point and upper set point of vaporizer heater current can be manually selected during the test.

The control loop may be used to maintain a relatively constant beam current through the relation between beam and accelerator drain currents. Although this control loop was implemented, it was decided in agreement with the JPL program manager that it would not be activated during the 500 hour test and that engine control would be maintained by the beam current to cathode power loop. The propellant flow rate during the test was set at the discrete vaporizer control point corresponding most closely to 80% propellant efficiency.

The neutralizer control (Fig. 23) was not employed (although the electronics were implemented), since no beam potential sensor was furnished.

2. Magnetic Component Design

Seventy-three magnetic components comprise 32 different and specially designed types used in the system. The basic system performance depends strongly on these magnetic-components because they make a substantial contribution to system weight, efficiency, and reliability.

A key parameter in minimizing the weight and maximizing the efficiency of the magnetics has been the inverter frequency. Limited by the switching speed of the transistors used, the upper frequency limit has been chosen as 10 kc at high, loaded line voltage. At this frequency it has been very advantageous to use ferrite cores instead of silicon steel, since the ferrites exhibit much lower hysteresis and eddy current losses at the same flux density.

One property of ferrites which has required special attention for this space application has been the relatively low Curie point compared with silicon steel. The ferrite alloy used (highest Curie point available) has been found to saturate at a flux density of 2 kG at 140°C core temperature. This characteristic permits a wide safety margin when operating at 2 kG and 85°C. This temperature which corresponds to a 15°C rise above the 70°C mounting base temperature, is easily obtained with 98% transformer efficiency. A particularly appropriate characteristic of the ferrite pot cores is the large, flat, ground, mounting surface of the core, permitting intimate thermal interface with the radiation mounting plate of the module. This efficient interface, combined with the ideal thermal configuration of the pot core, permits very low temperature gradients between transformer coil, core, and mounting. Thus the thermal limit of the ferrite core is completely compatible with the power transistors with which it must be in close proximity.

It should be noted that at a maximum ac flux density of 2 kG with square-wave 10 kc, ferrite core losses are negligible compared with those for silicon steel at this frequency and flux density, and less than half the copper loss when designed for 98% efficiency. Therefore, it is apparent that the ferrite transformer is substantially more efficient than a silicon steel transformer of the same weight.

Nickel-iron was considered as an alternative core material for the system. This material is available in two forms: tape toroids and laminations. The thinnest laminated material which can be used without fragile handling properties is 0.004 in. At this thickness, core losses are still higher than ferrite losses. On the other hand, the thin tape toroid requires that no dc unbalance be permitted in widings, since the absence of any effective air gap would result in core saturation becase of the narrow hysteresis loop. While this dc balance is obtainable in some circuits, it is impracticable in many others; therefore, ferrite is still preferable.

A particularly important, and formidable, design problem in transformers for this system is that of high voltage, since many transfomers require operation of one secondary at 3500 V relative to the primary and other secondaries. In connection with this requirement, the high voltage winding must be shielded to prevent engine arcs from capacitive coupling high voltage transients into low voltage circuits, with accompanying destruction. In contrast to this requirement for high voltage insulation, which suggests large separation of windings, is the requirement for low leakage inductance and tight coupling to provide fast rise times of the 10 kc square wave.

The design which represented the most suitable compromise of the above requirements, using a ferrite pot core, was a noninterleaved, layer-wound coil, with the high voltage secondary inside, next to the bobbin. This winding was then wrapped with six layers of epoxy-mica-mat (0.005 in. thick per wrap) and then shielded. The shield edges were insulated 1/8 in. back from the edge of the winding with 0.002 in. of bondable-teflon tape and wrapped again with one layer of 0.005 in. epoxy-mica-mat. Finally, the primary and other secondaries were put on. High voltage leads were brought out in teflon-sleeved, teflon-insulated wire. The finished transformer was wrapped with glass-tape and vacuum-formed with aluminum-filled epoxy. Transformers are high-potted at 5000 V before impregnation and again after impregnation.

Since transformers are mounted on the back surface of the module mounting plate (side away from space), the possibility of entrapped outgassing and associated intermediate pressure requires that high voltage terminals be hermetically sealed. This is accomplished by providing a potting cup, integral with the transformer, surrounding the high-voltage terminals, and filled with epoxy after lead termination at assembly.

To verify the adequacy of the high-voltage insulation, two main drive transformers which normally operate at 3500 V were high-potted to destruction. One unit failed at 15,000 V and the other at 17,000 V indicating a very adequate margin over normal stress.

3. Mechanical Design

An interesting feature of the modular power conditioning system is its physical geometry. The more conventional power supply would be packaged in a box shape, but the modular system takes on the appearance of a flat panel, which is desirable for a space environment in which cooling is accomplished by radiation only.

The components for each module are mounted on a thin plate whose size has been standardized at 3-3/4 in. by 7 in. This area is convenient for mounting the required number of parts and also provides sufficient radiating area to maintain the plate temperature at 70°C maximum (assuming operation at maximum power capability). Thus, with no cooling by conduction to the vehicle, a single module may be operated as a free body (from a thermal standpoint).

The individual module plates are mounted to an aluminum frame in a rectangular array. The thin webs which make up the frame employ 90° members to increase the bending moment. Since standby modules are used, all 24 modules are not operating at any one time. Because heat conduction is possible along the frame, the 3-3/4 in. by 7 in. area is effectively increased, which allows some conservatism in the 70°C maximum estimate. The frame is essentially all of the structure

required for the entire power conditioning system. It is necessary to attach this frame at only a few points on the vehicle; therefore, the design minimizes vehicle weight penalties in accommodating the power supply. The finished frame weighed only 2.5 lb. This design represents a minimum ratio of structure to component weight which has not been achieved before. The design was based upon meeting the shock and vibration requirements of a launch environment, although such testing was not part of the present program.

A very important aspect of the mechanical design is the manner in which high voltage integrity is assured. In order to eliminate high voltage breakdown caused by outgassing and the resultant intermediate pressure, and at the same time minimize the weight of potting compound required to seal high voltage connections, all exposed high voltage connections are located on the front face of the module plates. That is, they are located on the side exposed to space. A typical example of this is the front face location of the high voltage rectifiers. Since a number of magnetic components are operating at high voltage, the connections to these components are encapsulated in epoxy after module chassis wiring is completed.

The mechanical design considerations (including thermal) have proved to be as important as the electrical aspects in minimizing system weight. It is useless to establish some minimum weight of electrical components if massive mounting and cooling structures are then required. The features of this mechanical design (and subsequent verification by actual construction) demonstrate the manner in which the total weight of the vehicle has been considered in order to achieve an optimum.

4. Thermal Test

Since the thermal characteristics of the power supply are so important to its successful operation, a thermal test (in a vacuum) was performed on a single module prior to the system tests. A main

drive module was used as a sample, and the test was performed with the module suspended in the vacuum chamber by small wires (to minimize thermal conduction via the mounting structure) and radiating from one face to a LN_2 cryowall. The module was operated at full load, and the results of this test are presented in Fig. 25.

The test was assumed to have started at the time LN_2 was added. The module was not operated during the first 15 min, and the cooling curve may be seen. The module was then started and operated for 75 min, at which time thermal equilibrium was essentially established. It can be seen that all temperatures were relatively low. Therefore, on the basis of this test, it was concluded that the thermal design and performance were satisfactory. (This was later shown to be untrue, as discussed in a later section.)

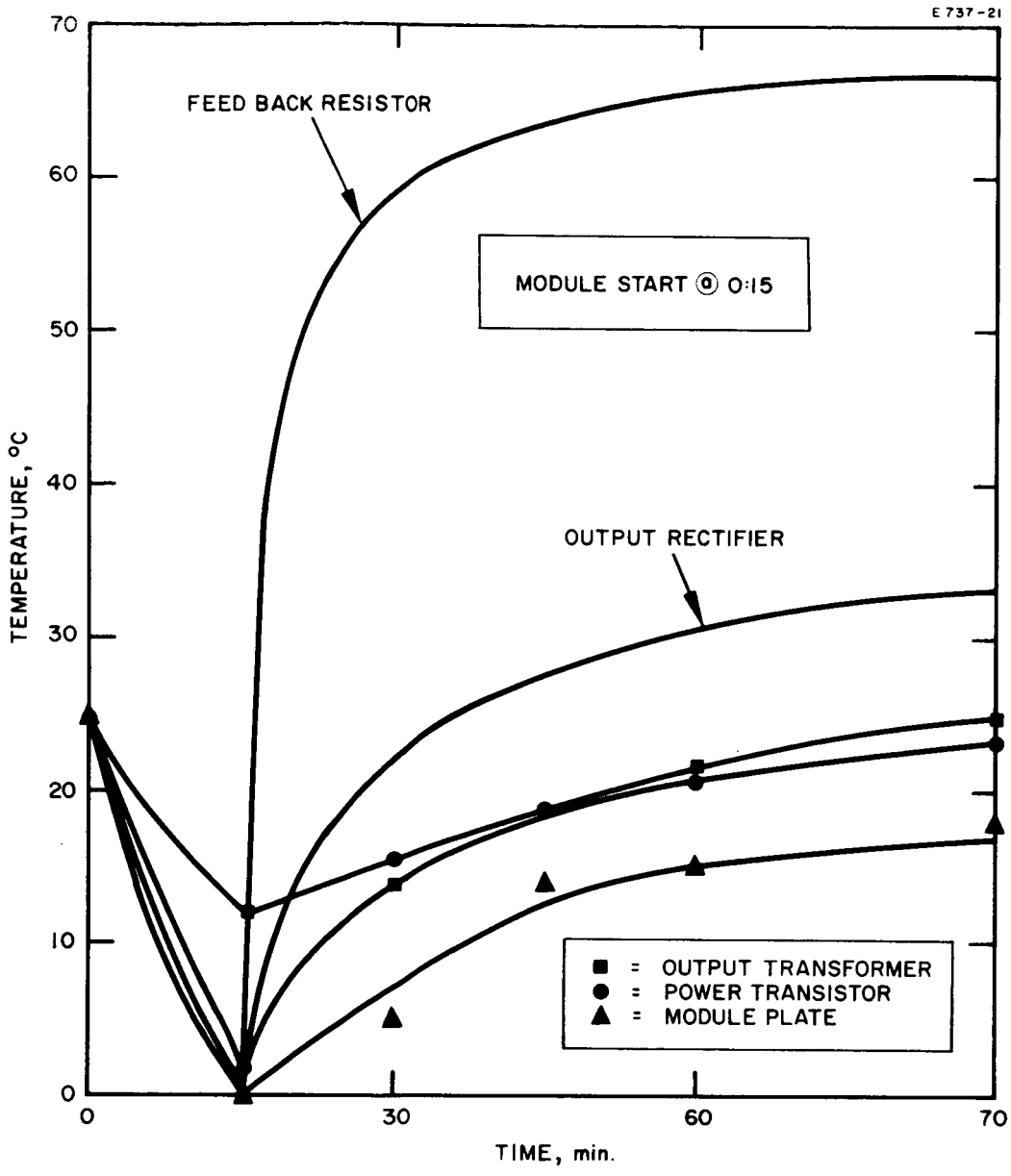

Fig. 25. Thermal vacuum test of single module (main drive).

SECTION VI

SYSTEM INTEGRATION

A. ELECTRICAL TESTS

The purpose of these tests was to establish compatibility between the power conditioning subsystem and the engine and feed system. These tests revealed the usual problems which accompany the integration of systems of this complexity. Although most of these problems were readily solved, three of them were particularly troublesome. They were

1. Transmission line drop encountered in handling low voltage, high current, high frequency, pulse-width modulated square waves for use by the cathode heater.
2. The resistance of the magnet winding when the engine was cold was found to be only half the operating (or hot) value.
3. The startup sequence could not be made to operate as originally specified.

1. Transmission Line Drop

Early in the integration tests, it was found that insufficient power was being delivered to the cathode in the engine. Measurements made directly at the power supply output terminals indicated that sufficient power was available but was not being transmitted to the cathode. This problem was aggravated by a situation peculiar to the test configuration. That is, not only was line drop a problem because of transmission length, but it was necessary to contend with two feed through drops in

in order to connect the power supply in one vacuum tank to the engine in another. In an attempt to minimize the line drop, the length was held to a minimum, heavy Litz wire was used to minimize reactive and resistive drop as well as any skin effect, and special low inductance feedthroughs were designed. After these improvements were made, a line drop measurement was made under the test condition shown in Fig. 26.

For this test, the cathode was replaced by a short circuit, and the voltage at V_1 was increased until rated (50 A) current was flowing. The voltages at the indicated locations were measured with a true rms meter for both the high frequency, pulse width modulated voltage applied at V_1 and for a 60 cycles sine wave applied at V_1. The results are presented in Table VI.

Table VI

Line Drop Data at 50 A RMS

V_1 Waveform	Voltage, V				
	V_1	V_2	V_3	V_4	V_5
High Frequency	2.71	2.41	1.77	1.08	0.46
60 Cycles	0.49	0.40	0.38	0.105	0.088

It can be seen that the total line drop was 2.7 V. Since the voltage available from the power supply has a maximum of 3.25 V, the nominal cathode power specification of 3 V, 50 A was not achievable at the cathode. Comparison of the high frequency and 60 cycle data shows that the line drop was primarily reactive.

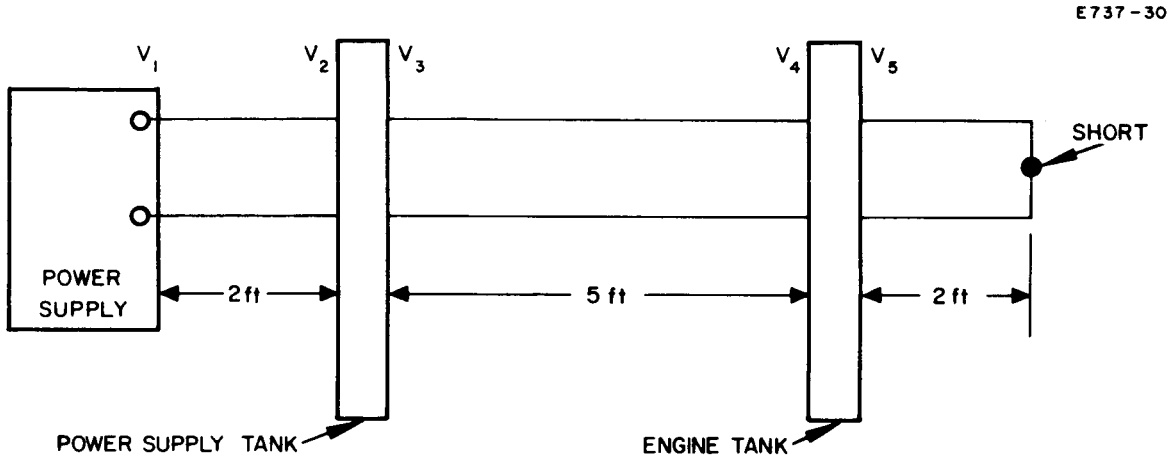

Fig. 26. Cable configuration.

The data given in Table VI can be used to compute the voltage at the 50 A load if the full 3.25 V power was applied at V_1. This calculation, which is made using a vector diagram and which assumes that the difference between the high frequency and 60 cycles data is pure reactance (i.e., no skin effect), indicates that only 1.4 V rather than the desired 3.0 V is available. It is interesting to note that if the feedthrough drops could be eliminated, 2.5 V would be available at 50 A. However, the combination of a difficult power transmission problem (low voltage, high current, high frequency) and a test configuration which required more connections in series with the line than would be encountered in an actual space application led to a solution in which the power transformer was moved to the engine tank.

With the cathode heater output transformer located in the engine tank, the transmission line problem was virtually eliminated. In this configuration, the major portion of the distance (including all feedthroughs) from the power supply to the cathode was covered at high voltage (80 V peak) and low current (2 A); only the last 12 in. or so were covered at 3 V, 50 A. It should be noted that even if the transmission line drop were such that rated power could be delivered to the cathode, the configuration with the transformer at the engine is far superior from a power factor standpoint. Therefore, locating the transformer at the engine will result in minimum power supply and transmission line weight.

Tests performed with this new configuration produced excellent results. Rated power plus some reserve was available at the cathode. The transformer core temperature was measured in this new environment and found to be around 75°C, which is considered to be a very mild thermal stress.

2. Magnet Resistance

As originally specified, the magnet supply provides unregulated power to what was to be an essentially constant resistance load. However, it was found that the resistance of the magnet winding was equal

to the specified value when the engine was hot, but that it was only half this value when the engine was cold. Therefore, the application of rated voltage to the magnet winding when the engine was cold resulted in a 100% increase over rated current. Since several minutes were required to bring the winding up to temperature, the magnet supply was subject to a heavy overload for a rather long time.

The following possible solutions to this problem were considered:

1. Redesign the magnet supply for double the original capacity or for current regulation.

2. Redesign the magnet winding for truly constant resistance.

3. Attempt long engine warmups with only the heaters operating in an attempt to raise the temperature of the winding prior to applying magnet power.

4. Warmup the magnet with solar panel simulator voltage turned low, increasing slowly as warm-up continues.

5. Insert a series impedance which varies with time to compensate for the magnet resistance variation.

Because alternatives 1 and 2 involved time-consuming changes to the completed hardware, they were rejected as not being consistent with the test objectives. Alternative No. 3 was tested but found to be ineffective. Alternative No. 4 was rejected because varying the solar panel voltage manually does not provide a realistic test, since the entire system would be subject to this variation (not just the magnet). Alternative No. 4 is also operationally cumbersome.

Alternative No. 5 was finally selected because it provided a solution which did not disturb the original hardware, did not pose operational problems, and did provide an essentially constant load to the power supply which was consistent with the original specification. In order to mechanize this alternative, several power thermistors

were operated in parallel in order to achieve the low impedance and high current level desired. They were also mounted on a metal plate and packaged in a foam block in order to give the assembly a thermal time constant approximately equal to that of the magnet winding. This assembly was mounted in the engine parameter meter console because it was necessary to operate at high voltage.

Alternative No. 5 proved to provide a satisfactory solution to the immediate problem. A future design would, of course, take this situation into account. At such time, alternatives 1 and 2 would be given serious consideration.

3. Startup Sequence

As mentioned earlier, the startup sequence did not operate as originally specified; the transient rating of the accel supply was inconsistent with the turn on sequence.

The original sequence called for turning on the arc supply (a voltage regulated supply) after the magnet was already on. Under this condition, the accel supply received a large transient current which was far greater than its rated value. The accel supply has a transient rating of 15 mA and a steady state rating of 10 mA (the actual steady state engine demand is only about 2.5 mA). Each time the startup sequence was attempted, the accel supply would trip. In order to determine just how much transient capacity was required of the accel supply, a laboratory high voltage supply with 50 mA capacity and a variable trip level was connected in place of the system accel supply. It was found that even with a trip level of 50 mA, this supply would trip each time startup was attempted. It then became apparent that the accel transient capacity would have to be increased to a level so far beyond its present capacity that this solution would be impractical.

Since it was clear that the existing sequence was placing an excessive demand on the accel supply, it was decided to change the sequence so that the transient demand would be reduced. One such sequence which was already established from past experience included turning on the magnet last. This, and other sequences were investigated:

1. Start vaporizer last
2. Start cathode heater last
3. Start arc with slowly rising voltage instead of step function
4. Reduce boost voltage on arc in attempt to minimize arc current surge at turn on
5. Increase accel trip time constant to 1 msec (maximum safe value)
6. Turn magnet on last with step function
7. Turn magnet on last with ramp function of current.

It was apparent that the nature of the problem was somewhat sophisticated because both the transient behavior of the engine during startup and the transient behavior of the power supplies were intimately involved. This situation, together with the necessity of finding an expedient solution, produced a result which was perhaps less than optimum. However, a solution was found which provided satisfactory engine-power supply performance while not sacrificing any of the test objectives.

While alternative No. 1 provided a smooth startup, it was objectionable from a time response standpoint. That is, in the event of an engine arc and system shutdown, the vaporizer would have to be held off for approximately 5 min before it could be turned on again; after it was turned on, another 5 min would be required to establish full beam current.

Alternative No. 2 also provided smooth startup and did not suffer from the very long time response of alternative No. 1. However, temperature cycling of the cathode each time an engine arc occurred was considered to be objectionable from the standpoint of cathode life.

Alternative No. 3 was attempted primarily because it could easily be mechanized electronically without major changes in the existing hardware. However, it was found that this method did not work because the voltage rose slowly until the arc ignited, and the same transients would be generated.

Alternative No. 4 has essentially the same defect as alternative No. 3.

Alternative No. 5 was easily mechanized but did not ease the problem. It probably can be concluded that since the laboratory supply was being tripped, and since this supply had a relay trip circuit with a long (compared to 1 msec) time constant, this alternative shows little promise.

Alternative No. 6 provided moderately satisfactory operation. However, it appeared that simply turning on the magnet with a step function generated some transients, so that several attempts usually were required before engine startup was accomplished. Furthermore, this mode of operation could not be easily mechanized with the existing hardware because the magnet inverter supplied the drive power to the arc inverter. Therefore, the magnet inverter could not be turned on after the arc inverter without a major modification. To mechanize this mode, it was necessary to place a switch in the output of the magnet rectifier. This alternative was finally abandoned because it was difficult to mechanize and provided only erratic performance.

Alternative No. 7 was finally adopted as most desirable from the standpoint of ease of mechanization and smooth operation. This mode was mechanized by placing a reactor in series with the magnet winding so that the combination of magnet load plus reactor provided a 50 msec time constant. The arc and magnet inverters were then turned on simultaneously (originally the arc was delayed by 5 sec) and the slow rate of rise of magnet current (50 msec time constant) provided smooth startup. Each time an engine arc occurred, the magnet and arc inverters were turned off and on simultaneously and a smooth restart always occurred. The reactor was mounted in the engine parameter meter console along with the thermistor assembly since it had to be at high voltage.

Alternative No. 7 could have been readily accomplished electronically early in the design by providing a current controlled magnet supply via a chopper regulator. This would allow the magnet current to be increased smoothly with an electronic time constant. This mechanization would also provide a solution to the problem of warming the cold magnet winding. However, converting the hardware at the integration testing stage would have caused unacceptable delays.

The startup sequence finally used could not be used with a permanent magnet for obvious reasons. Therefore, this problem should be investigated further when time permits. At present, it is believed that an arc supply with di/dt limiting may be the answer, but this solution must be studied carefully. Although the startup method which was finally chosen was probably not the ultimate optimum, it was sufficient temporarily. This sequence provided for full automatic operation and allowed the goals of a 500 hour life test to be met.

B. TRANSIENT AND THERMAL TESTS

The transient and thermal tests emphasized the two most critical parameters in the power conditioning subsystem. A power supply for operating an ion engine must be capable of withstanding the transients generated by engine arcing. The stress levels associated with these transients must be carefully examined to ensure reliable operation. The thermal stresses at which the power supply components must operate are equally important in assessing system reliability. Because the power supply must operate in a vacuum and be cooled by radiation only, the thermal characteristics of the supply provide an indirect measure of efficiency.

1. Transient

The major portion of transient data was gathered while the supply was operating into a dummy load and engine arcs were simulated with a variable arc gap in the various possible arcing paths. A peak reading voltmeter with fast response (< 1 μsec) and a digital memory was used

to monitor transients at various points in the system while the arc was simulated. This method provides a means of quickly and easily monitoring a large number of system locations and thereby provides a clear picture of the transient behavior on a broad spectrum.

In order to limit the di/dt available when an arc occurs, inductors were installed in series with both beam and accel supplies. The value of these inductors was determined experimentally using the peak reading meter. In order to detect possibly damaging transients before they occur, the arcing tests are conducted with an impedance in series with the arc to limit the intensity. This impedance is then gradually reduced to zero while the system is arced and monitored. An inductor may then be chosen which allows the high voltage to be safely arced into a short circuit.

The data corresponding to the final values of inductors used (0.5 H on beam, 0.4 H on accel) are presented in Figs. 27, 28, and 29. These are plotted in terms of the ratio of peak to nominal values. Therefore, a transient which caused the total voltage on the +6 V dc bias to be 9 V, would be recorded as 1.5. Not all of the monitored points are shown, but the items selected are considered to be key indicators of over-all transient performance.

It can be seen from the figures that the 40 V line does little more than rise to its open circuit value (1.5) when an arc occurs. The +6 V regulated is the output of the 6 V regulator; it can be seen that at some points this voltage rises as high as 10 V. However, the +6 V decoupled, which is the actual bus for the microcircuits, seldom rises above 8 V. (Microcircuits have a transient rating of 12 V for 1 sec.) These parameters behave in a manner which is typical of all parameters examined. On the basis of these measurements, it was concluded that sufficient transient safety factors existed and the system was immune to engine arcs. The test involved approximately 200 to 300 simulated arcs, and no failures took place. Observations made with the same meter while operating a real engine load have yielded the same basic results. Thus, it may be concluded that a valid transient simulation was achieved.

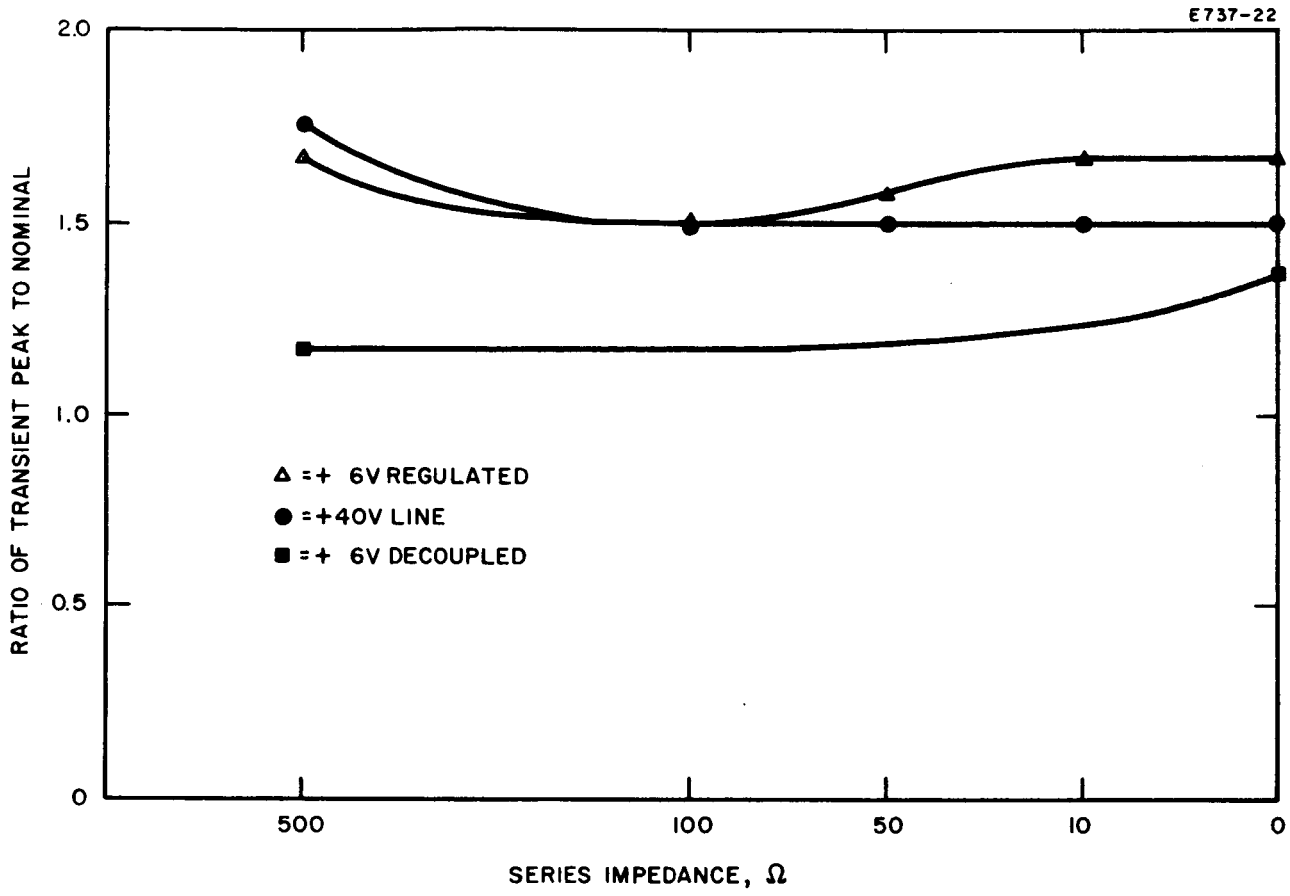

Fig. 27. Arcing — beam to ground.

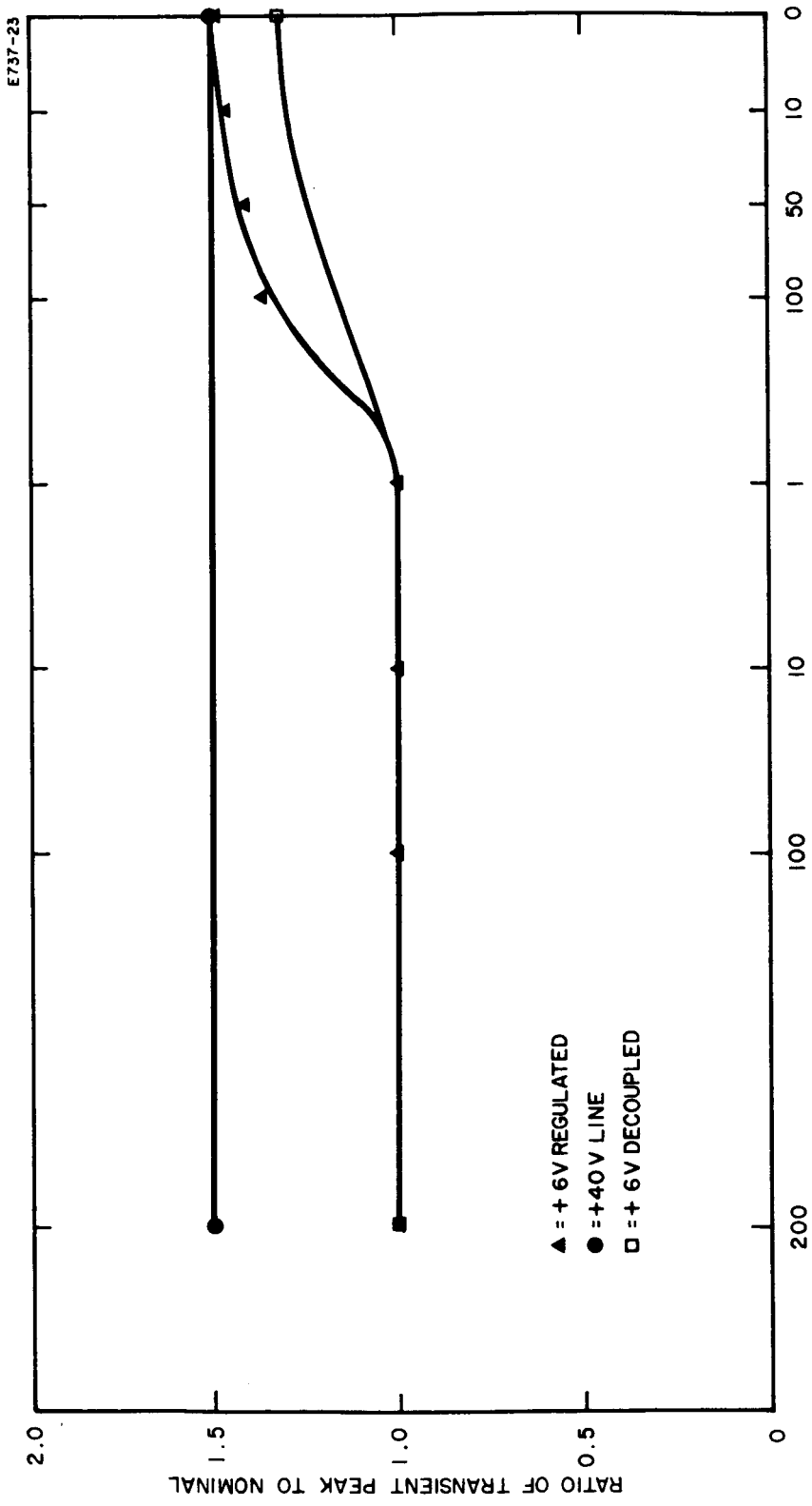

Fig. 28. Arcing – accel to ground.

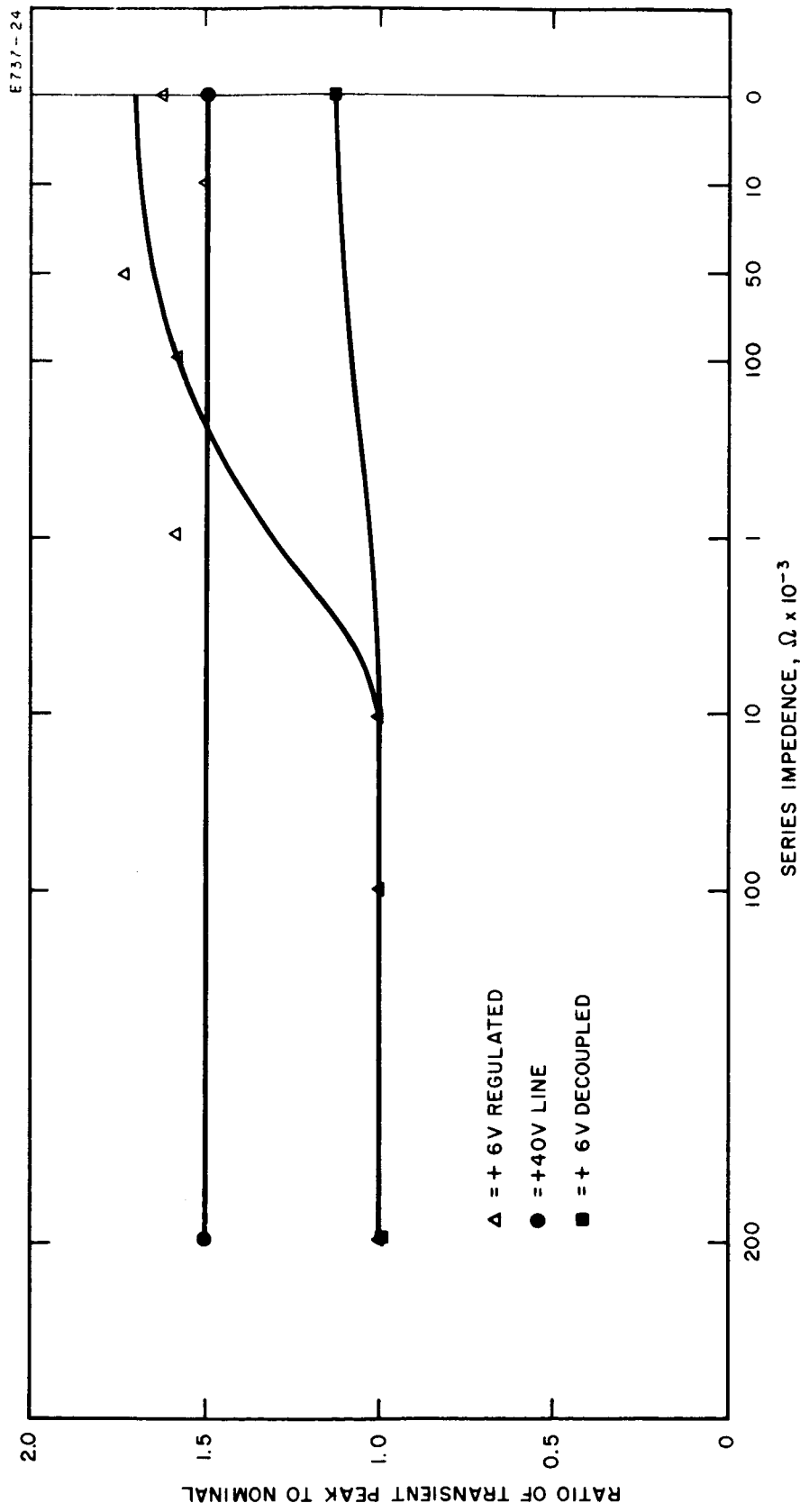

Fig. 29. Arcing – beam to accel.

2. Thermal

A thermal test was performed on the power supply prior to the initial engine test. For this test, the power supply was suspended in the vacuum tank so that it could radiate to a LN_2 cryowall. The dummy load was used, and a 2 hour run was made under full load. At the conclusion of this run, the following temperatures were recorded:

Location	Temperature, °C
Beam S/N 3 Plate	32
Beam S/N 4 Plate	9
Heater Inverter S/N 1 Feedback Resistor	190
Magnet Rectifier Plate	49
Heater Inverter S/N 1 Transistor	12
Arc Inverter Base Drive Resistor	41
Heater Inverter S/N Output Transformer	23
Arc Inverter Transistor	12
Magnet/Accel Inverter S/N 1 Plate	11
Cathode Controller Plate	9
Arc Rectifier Plate	25
Cathode Heater Inverter S/N 1 Transistor	—

From the above data, it may be seen that the feed system and neutralizer heater inverter feedback resistor was very hot. This is a wire wound component and is designed for high temperature operation. However, it was believed that this temperature was excessive and should be reduced. Since the original resistance value allowed sufficient base drive to supply a much higher peak current than was finally required, the resistance value was doubled. This reduced the dissipation to half its previous value. Tests also showed that the new value

of base drive was satisfactory for inverter operation. It was assumed that this 2 to 1 reduction of dissipation would decrease the temperature to a more acceptable value. (This later proved to be true.)

The cathode heater transistor temperature was not given because the module was turned off after 34 min of operation. At this time the temperature had reached 150°C and was still climbing. The module was turned off because it was felt that failure was imminent. At this time the backup cathode heater inverter was automatically turned on and operated successfully for the remaining 90 min of the test. The temperature of the backup module was not monitored, but it did not reach failure temperature. It was concluded that a marginal thermal situation existed in the cathode heater inverter and that some method of decreasing the dissipation in this module was necessary.

An examination of the cathode heater inverter circuit showed that the turnoff time (and hence the turnoff switching dissipation) could be improved by reducing the base drive. Such a reduction was justified when the transformer was moved to the engine because of the reduction of the ractive volt-amperes which resulted in a reduction of peak current. Reducing the base drive causes the turnoff time to decrease because the base junction is less heavily saturated. Therefore, the base drive was reduced to an optimum value (approximately 80% of original) which provided good turnoff time while still supplying ample drive to maintain transistor saturation. Room ambient temperature tests further verified that a definite improvement in dissipation was realized. As a final precaution, indium foil was placed in the interface between the module plates and the panel frame in order to provide better thermal conduction here. It was believed that these improvements would be sufficient to solve the cathode heater inverter problem; later tests revealed that the problem still existed, requiring further work.

Except for the resistor and transistor discussed above, all system temperatures were acceptable. After the improvements described above were made, the system was ready for the shakedown test. It should be pointed out that full load on the dummy load is not precisely equal to the engine load. However, the load was considered to be close enough for the thermal test. The actual test conditions of the dummy load are listed below:

Beam	E = 3.55 kV I = 210 mA
Accel	E = 2.2 kV
Neutralizer	No Load (this was done to accommodate thermocouples on the arc and magnet rectifiers)
Pressurizer	E = 5.2 V I = 3 A
Vaporizer	E = 4.9 V I = 4.2 A
Valve	No Load
Magnet	E = 3.0 V I = 16 A
Arc	E = 35 V I = 3.8 A
Cathode	E = 3.0 V I = 38 A

C. PRELIMINARY SYSTEM TEST

The preliminary system test was conducted so that any problems related to long term operation of the power supply-engine combination would be discovered before the 500 hour test. The test lasted for approximately 50 hours and adequately demonstrated the transient integrity and redundant switching circuitry in the power supply. The test revealed, however, that thermal deficiencies still existed in the system and had to be corrected prior to the 500 hour test. The test is briefly described below.

The test was started (power supply in a vacuum) and 250 mA of beam current was reached approximately 1-1/2 hours after initial turn on. The first hour was used for engine warmup and the beam reached full current 30 min after high voltage was applied.

Approximately 1 hour after full beam current, the No. 2 beam module indicated excessive input current. Failure appeared imminent, and the module was switched off. The No. 1 backup then switched on

automatically. Further tests with the No. 2 module indicated that it was drawing current but not producing output voltage. This suggested (as was later verified) that the output rectifier for this module had shorted.

Approximately 4 hours after full beam current, the No. 1 backup module failed and the No. 2 backup turned on automatically. The failure was not observed when it occurred, and the transition to the No. 2 backup was so smooth that the failure went undetected until it was noticed that this module was not operating.

After 6 hours, a count revealed that 12 trips and automatic restarts had occurred. The two beam modules which had failed up to this point did not fail at these trip times. (These failures appeared to be of a thermal nature.) Because no failures had been caused by transients, it was concluded that the supply demonstrated integrity in this environment.

After 24 hours, temperature data were recorded. This length of time was considered to be ample for establishing thermal equilibrium. The results of this measurement are given below:

	Temperature, °C
Beam S/N 3 Transistor	80
Beam S/N 4 Plate	40
Heater Inverter S/N 1 Feedback Resistor	90
Backup Cathode Heater Transistor (Not On)	—
Heater Inverter S/N 1 Transistor	20
Arc Inverter Base Drive Resistor	40
Heater Inverter S/N 1 Transformer	22
Arc Inverter Transistor	20
Magnet-Accel Inverter S/N 1 Plate	40
Cathode Controller Plate	25
Magnet-Accel Transformer	50
Cathode Heater Transistor	60-90
Cathode Heater Transformer (Engine Tank)	72

The above data indicated that the two thermal problems encountered during the initial test apparently had been solved. The heater inverter resistor was operating at a satisfactory temperature, and the cathode heater transistor had stabilized. The backup cathode heater was not on at this time, so that no data are given for it. The temperature range (rather than a fixed value) for the cathode heater transistor resulted because this module was being modulated as the $I_{Beam} - I_{Cath}$ loop demanded. Therefore, the module operated over a range of outputs and over a range of temperatures.

The temperature data indicated that the thermal behavior of the system was satisfactory, except for the beam transistor. The transistor was operating at a much higher temperature than was anticipated from previous plate temperature data. This seemed to indicate a thermal drop of around 40°C across the transistor-plate interface; this is very high considering that the transistor dissipates only 2 to 3 W. However, since the system operated satisfactorily for the first 24 hours (except for the two early failures of beam modules), the test was continued for another 24 hours.

After 47 hours it became necessary to increase the cathode power in order to maintain 250 mA of beam current. The cathode had been operated at 35 A up to this point, and a step increase to 37.5 A was commanded. Within minutes of this command, it was noticed that the cathode heater module had failed and that the backup had switched on automatically. Once again, the transition to the backup was so smooth that the failure was not noticed after the backup took over. An immediate check of the transistor temperature showed that the temperature at that time was 150°C indicating that the failure was caused by a thermal problem. The temperature of the backup cathode heater was then watched closely; within 20 min, it had reached 200°C. Since failure was imminent, the module was turned off and the entire test was terminated.

The test indicated satisfactory electrical performance, but some thermal design deficiency. On the basis of this test, it could be concluded that

1. The power supply and engine were electrically compatible
2. The power supply was capable of handling engine transients
3. Redundant switching was accomplished with no interruption of engine operation
4. The automatic control system performed satisfactorily in holding the engine at 250 mA of beam current
5. Thermal deficiencies still existed in the power supply.

Inspection of the system after removal from the vacuum chamber indicated that the beam module output rectifiers were overheating. These rectifiers had been mounted using a mylar insulator to provide maximum creepage distance from the high voltage connections to the plate, as shown in Fig. 30. Some of these insulators exhibited curling on the corners, as if they had been subjected to high thermal stress. In addition, the rectifier on the No. 2 beam module was found to have failed. It was concluded that it would be necessary to improve the thermal interface between the rectifier and the plate.

This improvement was made by attaching the rectifier to the plate with epoxy and eliminating the mylar insulator (see Fig. 30). This procedure provided intimate thermal contact and also maintained the large creepage distance because it was possible to construct a small dam of epoxy around the rectifier. The nylon mounting screw which was previously used to hold the rectifier to the plate was now eliminated since it was not needed to provide the tight mechanical connection for a good thermal interface. It was felt that the new mounting would have excellent thermal characteristics. The major objection to this improvement was that it would now be difficult to replace a rectifier in the event of failure. However, sacrificing maintenance ease for system performance seemed a reasonable tradeoff.

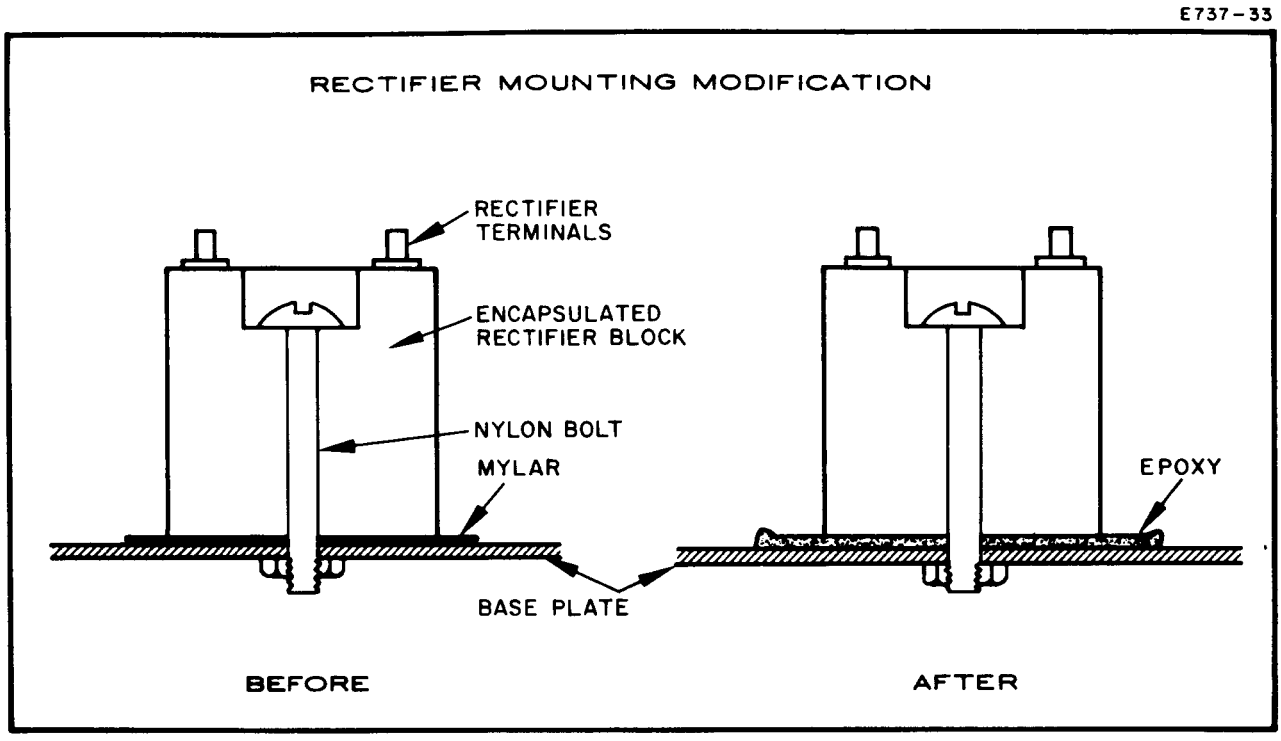

Fig. 30. Rectifier mounting modifications.

Inspection and examination of the cathode heater module (after replacing the transistor which failed) revealed no reason for failure. The thermal behavior in room ambient was satisfactory. After considering all of the available data, it was concluded that the failure was caused by a poor thermal interface between the transistor and the plate. The transistor was mounted (as shown in Fig. 31) using a mica washer to insulate the case from the plate. It was concluded that the poor thermal interface was caused by the inability to bring the surface of the transistor case and the plate into good mechanical contact. This problem is aggravated in a vacuum, where no air is present to fill in the small defects which might exist in the mechanical contact. Because it is not possible to make the surfaces perfectly flat, only a small percentage of the available surface area is actually in contact; therefore, high thermal resistance is found in a vacuum.

The problem area represented here was recognized early in the program. During a thermal vacuum test on a single module (as discussed earlier), the transistor case plate thermal drop was instrumented and found to be only 5°C. It was therefore concluded that the transistor mounting was satisfactory. However, the quality of the interface is somewhat random since it is determined by the amount of imperfection existing in the flatness of the two surfaces. Statistical evidence would probably have revealed this if more modules had been tested.

In order to solve this problem, indium foil was employed as a soft material which could cold flow and fill in the small voids. It was not possible to use a single piece between the transistor and the plate because the transistor case must be electrically insulated from the plate. To solve this problem, a hard anodized aluminum washer was used between the transistor and the plate with a piece of indium foil between the transistor and the washer and between the washer and the plate. The result (Fig. 31) was a mounting which provided both electrical insulation and good thermal conduction.

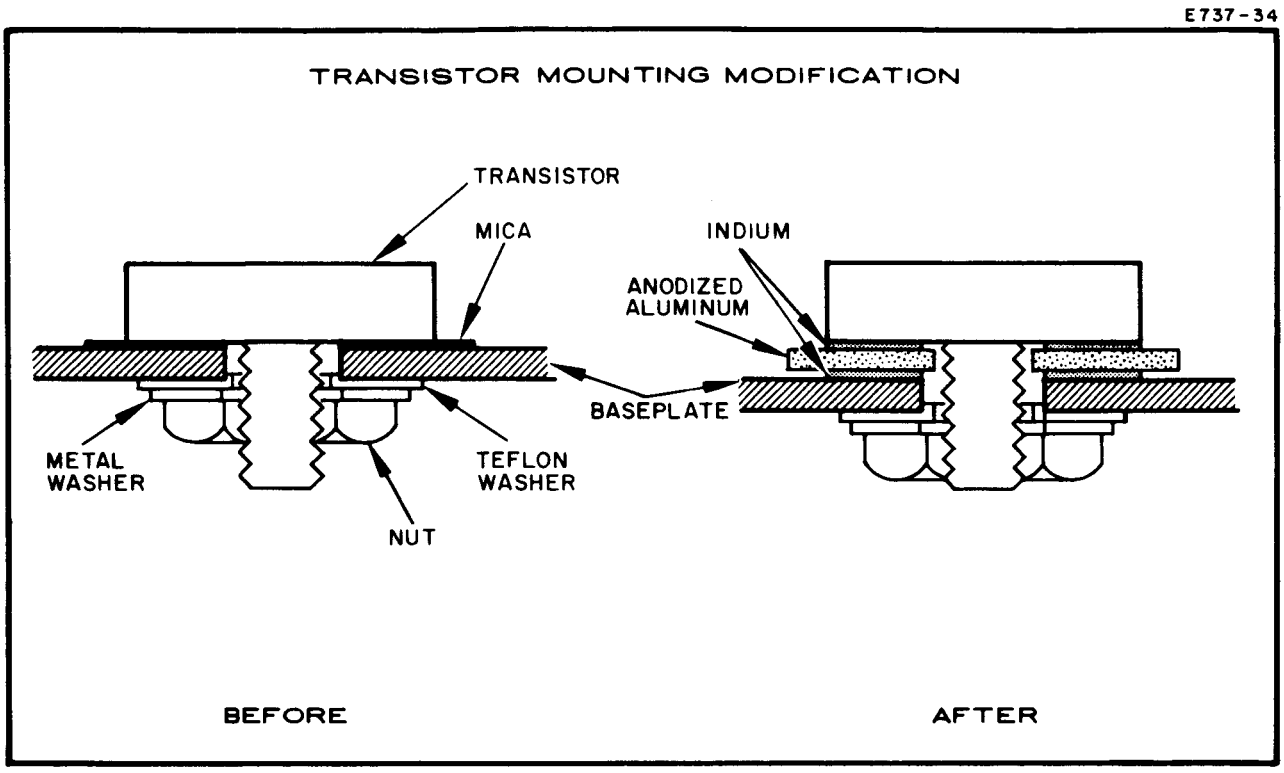

Fig. 31. Transistor mounting modification.

Although this thermal problem was measured only on the cathode heater, these latest considerations made all of the power transistor mountings suspect. It was not possible to monitor the case temperature for every transistor. Because of the uncertainty and because of the importance of the system thermal behavior, all of the power transistors were removed and remounted as described above. Note that no attempt was made to use grease as an agent to improve the thermal contact because of the uncertainty involved in long term vacuum exposure. There has recently been some mention of very low vapor pressure greases, but the data are inconclusive.

To verify the validity of this new improvement, another thermal vacuum test was run on the dummy load. An attempt was made to modify the dummy load so that the power supply could be run at increased stress on the cathode heater and beam supplies. The test lasted 4 hours and the results are given below:

	Temperature, °C
Beam No. 7 Transistor	32
Beam No. 7 Plate near Transistor	16
Beam No. 7 Plate near Rectifier	7
Beam No. 6 Transistor	35
Beam No. 6 Plate near Transistor	35
Beam No. 6 Plate near Rectifier	9
Beam No. 5 Transistor	32
Beam No. 5 Plate near Transistor	20
Beam No. 5 Plate near Rectifier	13
Backup Cathode Heater Transistor (not on)	15
Primary Cathode Heater Plate	30
Primary Cathode Heater Transistor	32
Beam No. 4 Transistor	33
Beam No. 4 Plate near Transistor	12
Beam No. 4 Plate near Rectifier	15
Beam No. 2 Transistor	42
Beam No. 2 Plate near Transistor	25

By comparing these data with those given earlier, it can be seen that the improvement was rather dramatic. Under the new conditions, the system temperatures are actually less than the values obtained in room ambient. Based on this test, it was concluded that the power supply performance was acceptable for the 500 hour test. The test conditions for the above data (using the dummy load) are listed below:

Beam	E = 3.5 kV
	I = 272 mA
Accel	E = 2.3 kV
	I = 8.1 mA
Neutralizer	E = 2 V
	I = 8 A
Pressurizer	E = 5.2 V
	I = 3 A
Valve	No Load
Magnet	E = 3.4 V
	I = 15.8 A
Arc	E = 35 V
	I = 3.4 A
Cathode	E = 3.4 V
	I = 49 A
Vaporizer	E = 4.6 V
	I = 4.2 A

SECTION VII

SYSTEM LIFE TEST

A. TEST SYNOPSIS

The operating characteristics of the engine system throughout the 500 hour test are summarized in Table VII. Except for the cathode power, all electrical parameters remained constant; however, a gradual increase in cathode power, cathode temperature, and arcing rate was observed (see Fig. 32). After 231 hours, a cold leak developed in the cryowall of the 3 ft tank which housed the power conditioning. This leak caused a pressure surge to 10^{-3} Torr, which in turn initiated a high voltage arc to ground inside the tank. Fuses in six power conditioning modules opened and the test was terminated temporarily while the tank was repaired and fuses replaced.

Both cathode performance and thruster arcing were attributed to an oil film on the inside of the test chamber walls. Oil incident on the cathode leaves a carbon deposit, which changes both the electrical and thermal emissivities. Oil on the vacuum chamber wall prevented the material sputtered from the collector from sticking to the chamber wall above the thruster, and small metallic flakes were observed to fall onto the electrostatic screen surrounding the thruster. To alleviate these problems, the tank was cleaned, a new cathode was installed in the thruster, and a shield was placed above the thruster. The test was restarted and continued with much improved cathode performance; the operating point is shown in Table VII. After 400 hours, an order of magnitude increase in the arcing rate (to ~20/hour) was observed. A 0.2 uF capacitor was inserted in the high voltage line and the test continued for a short time at reduced beam voltage.

TAB

Engine System Ope

Elapsed Time, hours	Beam Current, mA	Beam Voltage, kV	Accel Current, mA	Accel Voltage, kV	Beam Power, W	Accel Power, W	Discharge Current (at 36 V), A	Discharge Power, W	Cathode Heater Power, W
10	250	3.6	1.4	2.5	900	8	2.2	79	72
100	250	3.6	2.2	2.5	900	13	2.2	79	86
200	249	3.6	2.2	2.5	896	13	2.3	83	105
250[a]	251	3.5	1.4	2.5	880	8	2.5	90	55
300	251	3.5	1.4	2.5	880	8	2.6	94	69
400[b]	251	2.0	1.6	2.5	502	9	2.6	94	77
500	252	3.5	1.4	2.5	882	8	2.3	83	78

[a]New cathode installed at 231 hours.

[b]During period following high arcing, V_B temporarily reduced for 30 hours.

LE VII

rating Characteristics

Magnet Power, W	Feed System Power, W	Neutralizer Power, W	Total Power, W	Power Efficiency, %	Propellant Flow, equiv mA	Propellant Efficiency, %	Source Energy per Ion		Effective Impulse, sec
							Cathode Plus Discharge, eV/ion	Total, eV/ion	
51	26	18	1154	78.0	–	—	604	1005	4670
52	26	18	1174	76.6	340	73.5	644	1090	4600
51	26	18	1192	75.3	340	73.4	752	1180	4520
50	26	22	1131	77.7	305	82.4	577	1000	4950
50	26	22	1149	76.8	325	77.4	650	1060	4700
50	26	22	780	64.4	310	81.0	680	1110	3610
50	26	22	1149	76.8	310	80.6	640	1060	4760

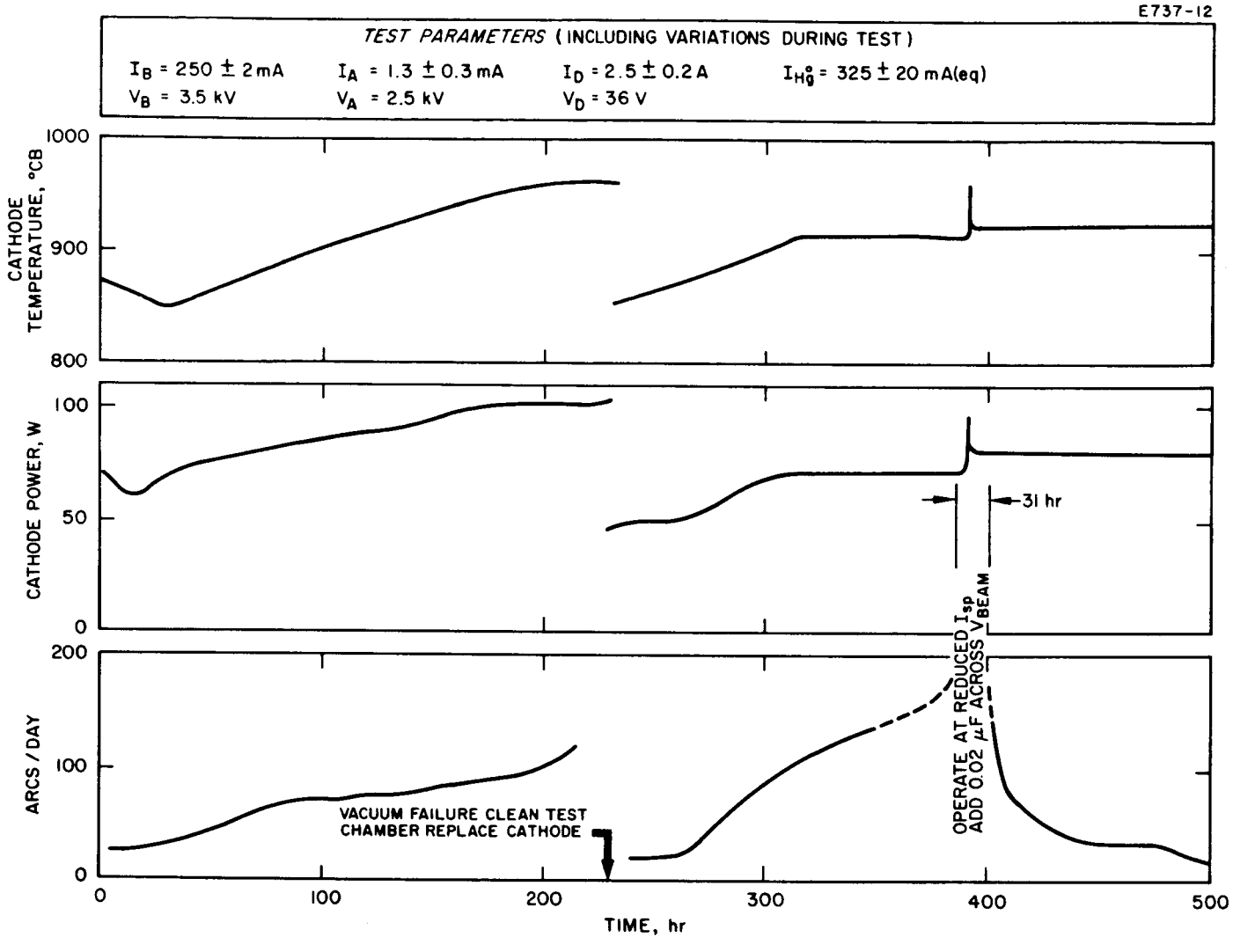

Fig. 32. System life test parameters.

The stored energy in the capacitor burned away the cause of the arcing so that the beam voltage could be increased to its original voltage in about 15 hours and the test could be continued at the original design point. Note that the cathode performance was much improved during the second phase of the test and that at the end of the test the arcing level had been reduced below that measured at the start of the test.

B. TEST SETUP

The physical test layout is shown in Fig. 33. The thruster and feed system (Fig. 34) were operated in a 9 ft by 20 ft high vacuum chamber lined over about 60% of the interior with a liquid nitrogen cooled surface. The pressure during the test was 1.5×10^{-7} Torr with the beam on and 8×10^{-8} Torr with the beam off. The original baffle design in this tank permitted small amounts of oil to creep into the chamber when it was cycled to atmosphere to install or remove components. The effect of oil contamination on the cathode was empirically evaluated with a 50 hour pretest and was estimated to be of negligible importance for the 500 hour life test. However, because of the continuous increase in required cathode power (e.g., see Fig. 33), the chamber was cleaned midway through the test when the test was briefly halted for other reasons, as discussed below. The baffle system has now been completely revamped so that future tests will be run in the cleanest possible environment.

The power conditioning panel was housed in a separate 3 ft by 5 ft vacuum chamber (shown in Fig. 35) equipped with a flat cryopanel which hangs approximately 2 in. away from the power conditioning panel. The blackened surface of this cryopanel serves to simulate the thermal environment of space. The power conditioning

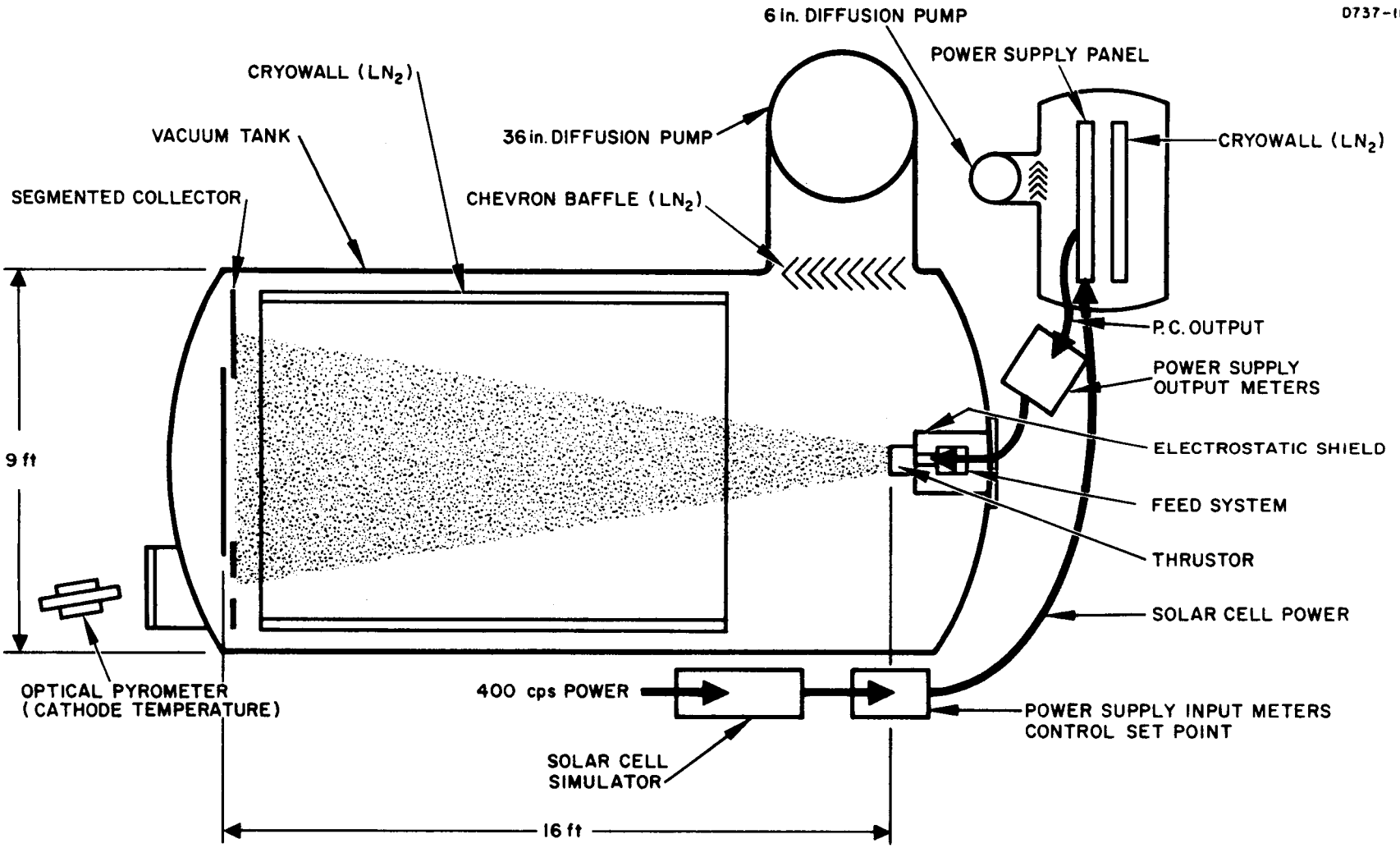

Fig. 33. Physical test layout.

M 4410

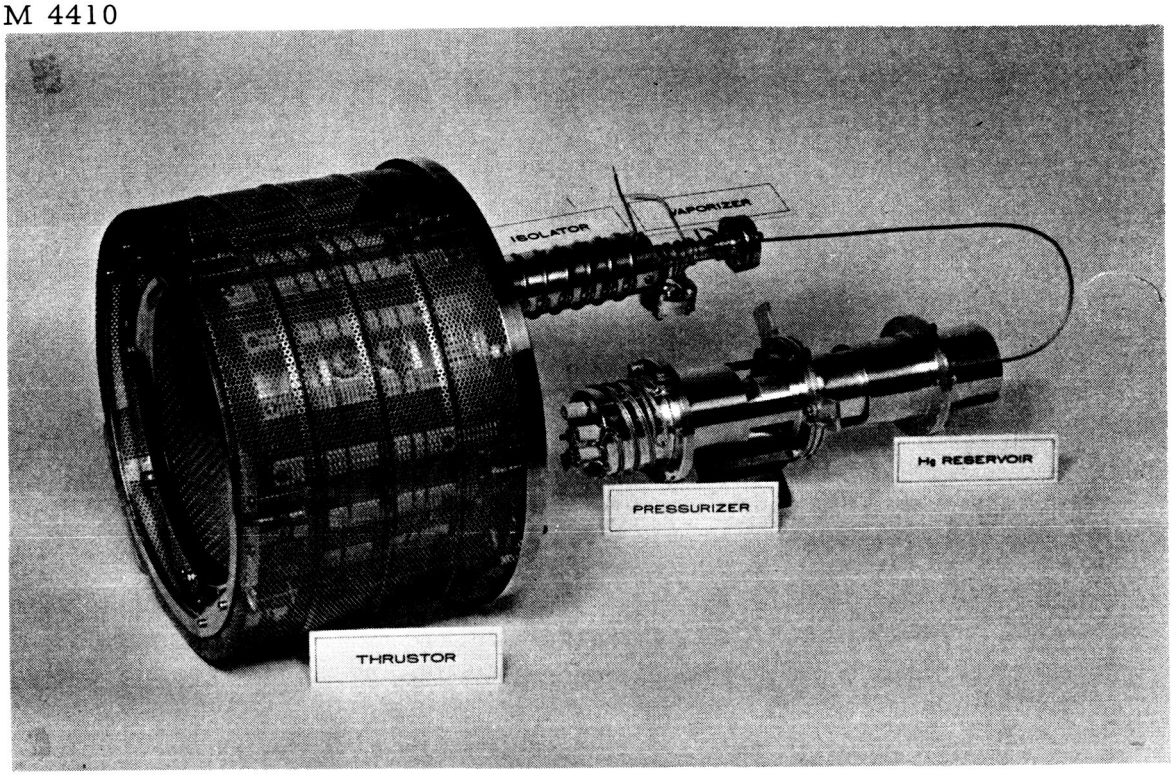

Fig. 34. Thruster and feed system.

M 4910

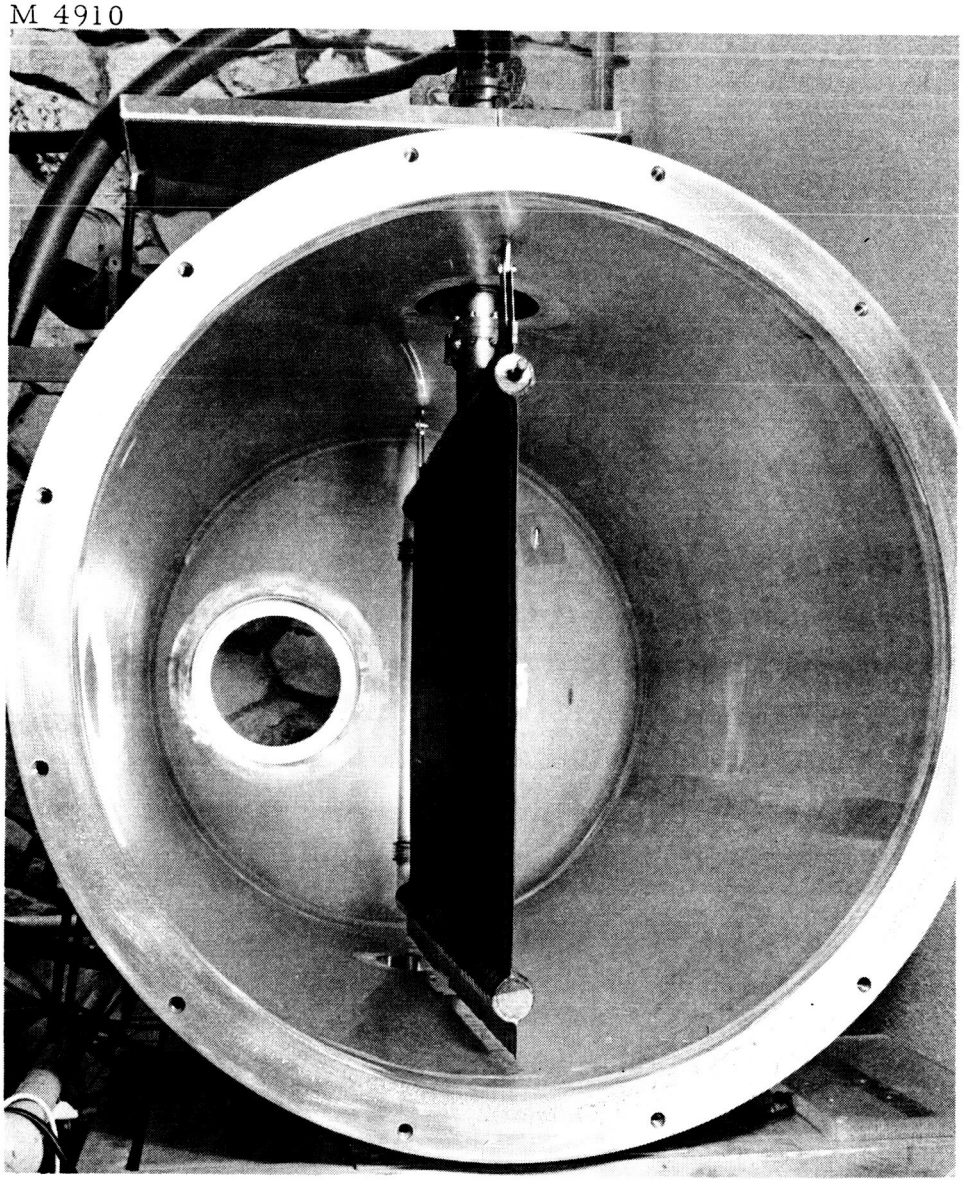

Fig. 35. Power conditioning system vacuum chamber.

and thruster were separated to reduce the effect of sputtered material on the power conditioning and to aid in the integration phase where minor changes required in the power conditioning could be performed in air with the thruster operating. As discussed elsewhere, the cryo-wall of the power conditioning tank developed a "cold leak" at the LN_2 inlet after 231 hours of test. This leak caused a pressure surge and subsequent high voltage arcing, which resulted in six blown fuses in the power conditioning modules. Both the power supplies and tank were readily repaired and the test restarted.

The electrical test setup is shown schematically in Fig. 36. It is designed to duplicate one unit of a flight system in all respects. Startup is automatic; after operation begins, adjustment of the control set points for the vaporizer, accelerator, and cathode power can be made only in a digital manner by "ground command" based on the information contained in the telemetry output signals. The meters were used here to provide an accurate measure of thruster and power supply performance independent of any calibration errors which might exist in the telemetry output signals.

C. TEST

At the beginning of the test, it was agreed with the JPL program manager that the best purposes of the test would be served by keeping the beam current as close to 250 mA as possible during the entire test. The control loop which links the accelerator current and propellant flow rate is designed to keep the accelerator current constant, rather than the beam current; therefore, it will not perform the desired task. The loop which links the beam current and cathode power has a 250 mA set point, and was therefore used as follows. The accelerator current and cathode current were set at 1.6 mA and

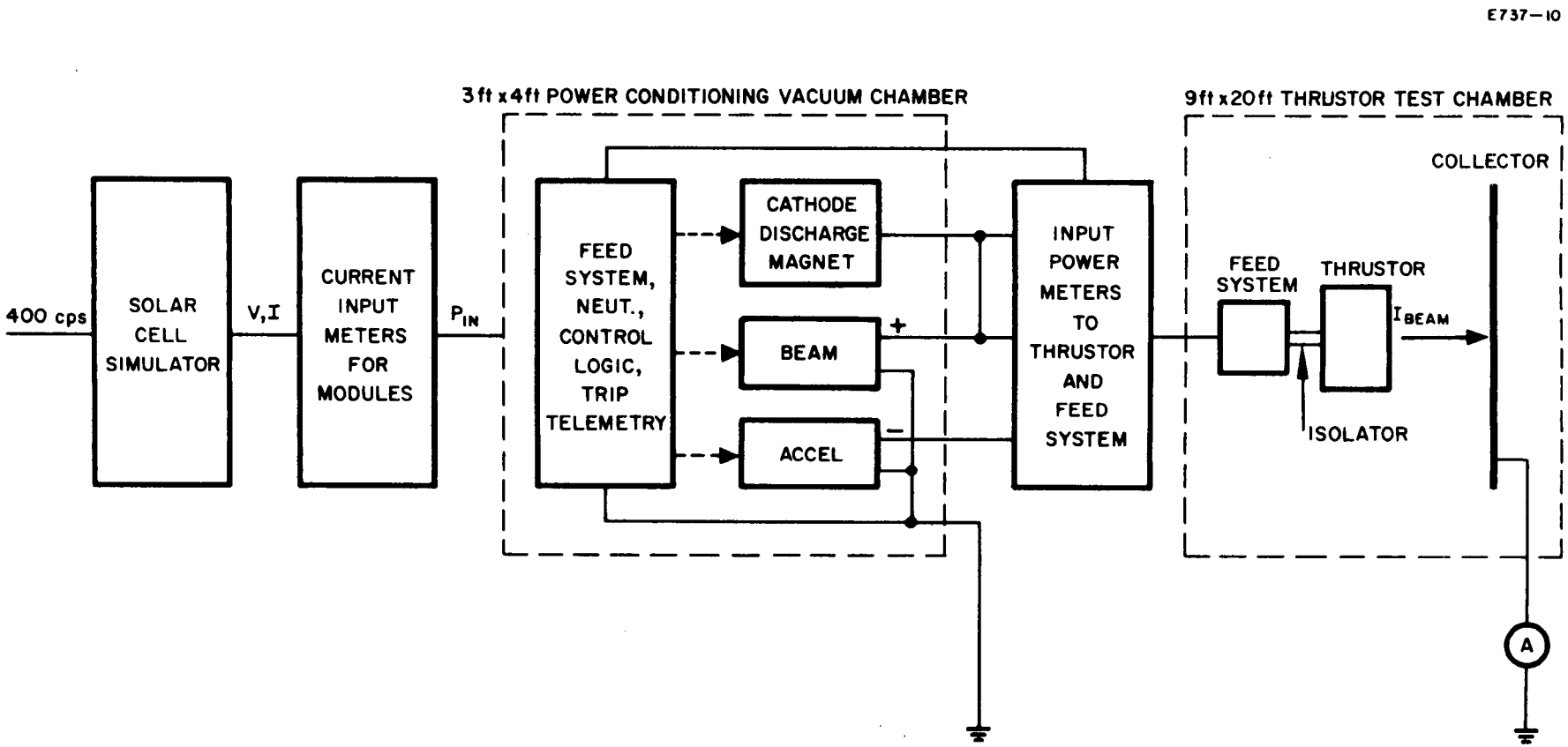

Fig. 36. Electrical test layout.

35 A, respectively. Both of these set points correspond to values above those required for operation of 250 mA and therefore hold the cathode and vaporizer supplies full on (see Figs. 20 and 22). The vaporizer set point was now set at 4.07 A, a value known to provide a flow rate of approximately 310 mA equivalent of neutral mercury vapor. As the vaporizer attained equilibrium temperature, the beam current rose to 250 mA, at which point the control loop reduced the cathode power to maintain the discharge current at the required level to produce 250 mA of ion beam current. The test was completed in this manner; the only changes were periodic adjustments in the cathode set point to assure that the cathode operating point would remain on the sloping rather than horizontal part of the control characteristic (see Fig. 20). Assuming that the future requirement will be for precise beam control, it will be desirable to modify the control philosophy in future systems.

Except for two incidents,* the test ran smoothly for the 500 hour period in this control mode at the nominal design point. The power conditioning performed without failure** and sustained approximately 1500 arcs during the test period. The maximum component temperature observed during the test was 50°C (transistor in a high voltage mode), which is 20°C below the design value (however, the power required was less than originally anticipated). A high arcing rate was observed after 390 hours. It was established that the arcing rate was very voltage sensitive and that the arcs were relatively small in magnitude (i.e., not large enough to trip a laboratory supply with nominal trip levels similar to those of the flight supplies). The

*See Test Synopsis

**Except during the vacuum failure which could not occur during a space mission. Here only the input fuses opened, as they should during an excessive overload.

high voltage was reduced to 2000 V by shutting off some modules at the input meter panel and placing a 0.2 μf capacitor across the output of the beam high voltage supply. The increased energy available during arcing gradually burned away the arc path, so that the high voltage could be gradually returned to its 3.5 kV level over a 15 hour period and the arcing rate subsided to its original level.

When the test was completed, the thruster was carefully disassembled to determine the location of the arcing. It was established by visual inspection (see Fig. 37) that there had been considerable surface breakdown on the inside of the glass wall of the isolator. Tracks were observed which shorted out all but one section of the isolator. Pits in the glass were visible where the high voltage arcs had burned themselves clear, and the high energies involved had locally heated the glass. The structure had not failed mechanically, however, and could not have leaked propellant.

Visual inspection after disassembly indicated a surface breakdown on the inner surface of the isolator, possibly caused by a surface contaminant. No such failure had been observed on any isolator operated prior to this time. The glass parts had been degreased, ultrasonically cleaned in alcohol, and washed in deionized water prior to assembly; the metal parts had been hydrogen fired. No evidence of oil or contaminant was present during the final glass-to-metal sealing operation. The mercury used was triple distilled and no anomalous operation of the vaporizer was observed, as would be expected if the mercury carried a contaminant. By heating the isolator jacket (using a heater installed during the integration period) it was established that the breakdown rate was not temperature sensitive, as would be expected if it were a result of simple mercury condensation. Therefore, it is not possible to establish by post examination the exact surface condition responsible for this breakdown. Possible causes of such contamination are impurities in the mercury, outgassing of the feedline upstream of the isolator, or contamination introduced during the final assembly phase when the last glass-to-metal seal was made.

M 4909

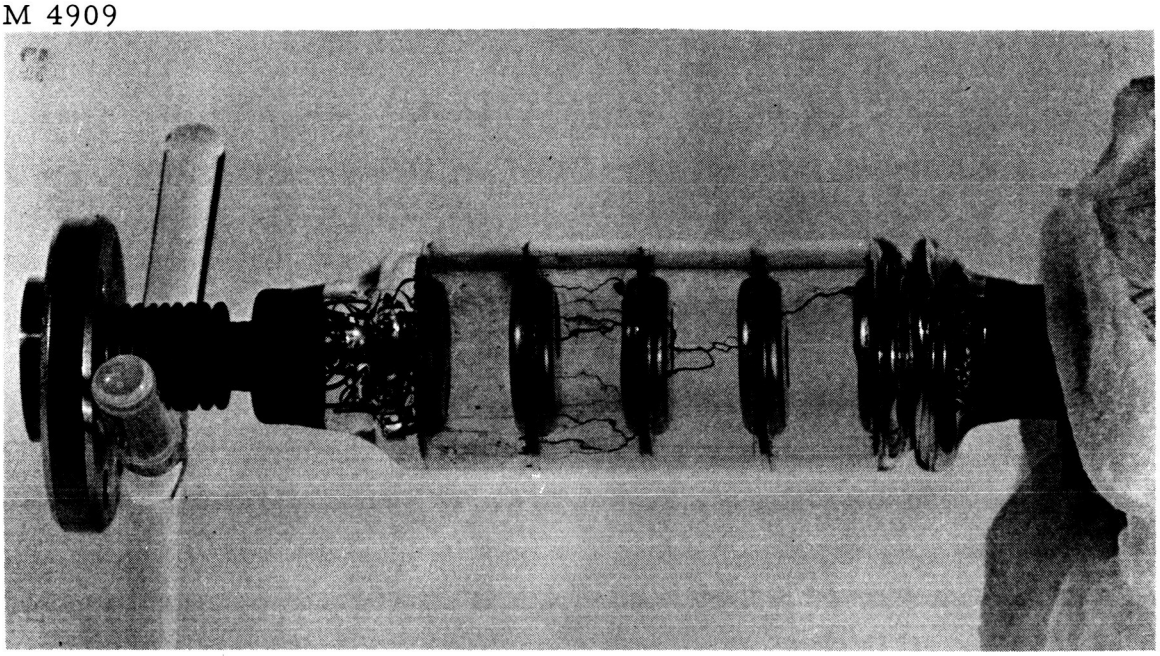

Fig. 37. Isolator after 500 hour test.

During the integration and test phase of this program an all ceramic and metal isolator (shown in Fig. 38) was fabricated for another program. The design criteria are the same; however, the glass has been replaced by alumina, and the glass-to-metal seals have been replaced by brazed joints. The complete structure is much more rugged, comes to thermal equilibrium faster, and can be vacuum fired just prior to installation to assure that all surfaces are clean. This isolator is currently part of an oxide cathode life test system working at an operating point which is similar to that of the 500 hour test. This test was run for more than 1000 hours, and no evidence of high voltage arcing has occurred.

Because of the many advantages of the ceramic design and its excellent performance during the cathode life test it may be used with confidence as a model for future designs.

The remainder of the feed system performed as specified in Section V-B during the life test. The piston position was monitored with a machinist's depth gauge calibrated in 0.001 in. increments. The dial was visible through a window in the vacuum tank. A plot of piston motion as a function of time indicated that the performance was smooth, continuous, and repeatable during the entire test period.

The Hughes cathode also performed as specified during the test period (see Fig. 32). In both temperature and power there was a gradual increase to a relatively high plateau during the first 231 hour period. This increase was attributed to contamination by the vacuum system. The second cathode used during the final 270 hours of the test period (after the tank was cleaned) showed a much reduced temperature rise and reached a very flat plateau in less than 100 hours. Severe arcing at the 400 hour point resulted in a new plateau which was 10°C higher. The eV/ion expended in the cathode (at a propellant efficiency of 80%) rose from 200 to 300 during the first 100 hours of cathode usage and then remained approximately constant during the remainder of the test.

M 5106

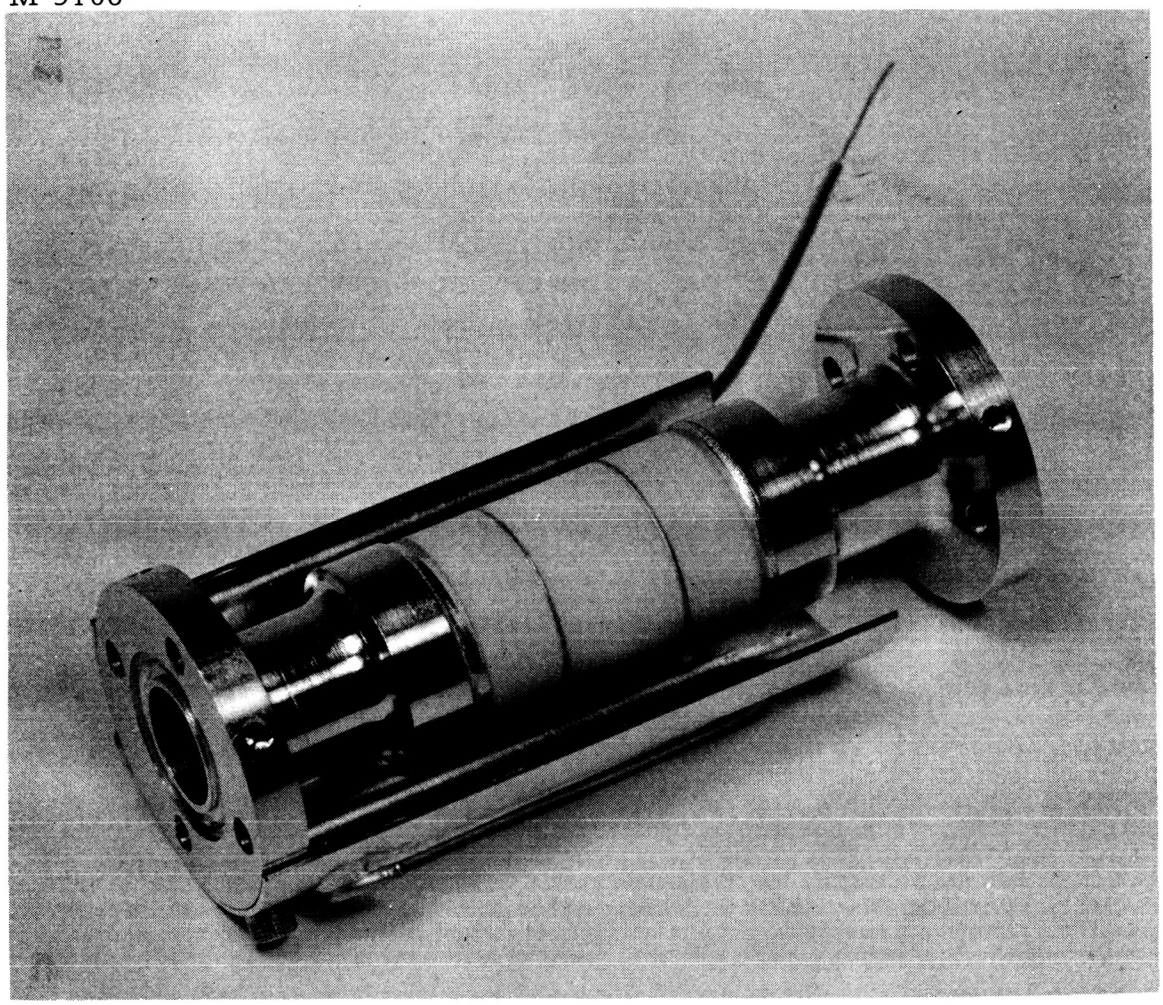

Fig. 38. Ceramic-metal isolator for mercury vapor feed system.

Weight measurements of the cathode taken before and after the run showed that 93 ±6% of the emissive material remained after the test. The relatively large error associated with the measurement exists because the corrections to the actual measurements resulting from loss of binder material and CO_2 during activation (25 to 30%), which are in part compensated by moisture absorbed from the atmosphere during the weighing process (~20%), are many times larger than the material loss resulting from sputtering. These measurements, plus visual inspection of the cathode after the test* (Fig. 39) indicate that the cathode life is much longer than the test duration but do not provide a quantitative lifetime prediction.

D. OPERATION OF POWER CONDITIONING AND CONTROLS

The performance of the power supply subsystem was excellent during the entire life test. In the two key areas of thermal and transient behavior, the subsystem performance demonstrated that all of the problem areas previously encountered had been satisfactorily dealt with and that all subsystem interfaces (thermal and electrical environment) were well under control. There were no component failures during the test and no standby modules were actually needed. The highlights of the test as they concern the power supply are described below.

1. Thermal Characteristics

The thermal characteristics of the power supply were essentially as predicted by the final dummy load test. After the initial difficulties centered around the thermal performance, the life test ran smoothly.

*See Fig. 4 for photograph of unused cathode

M 4908

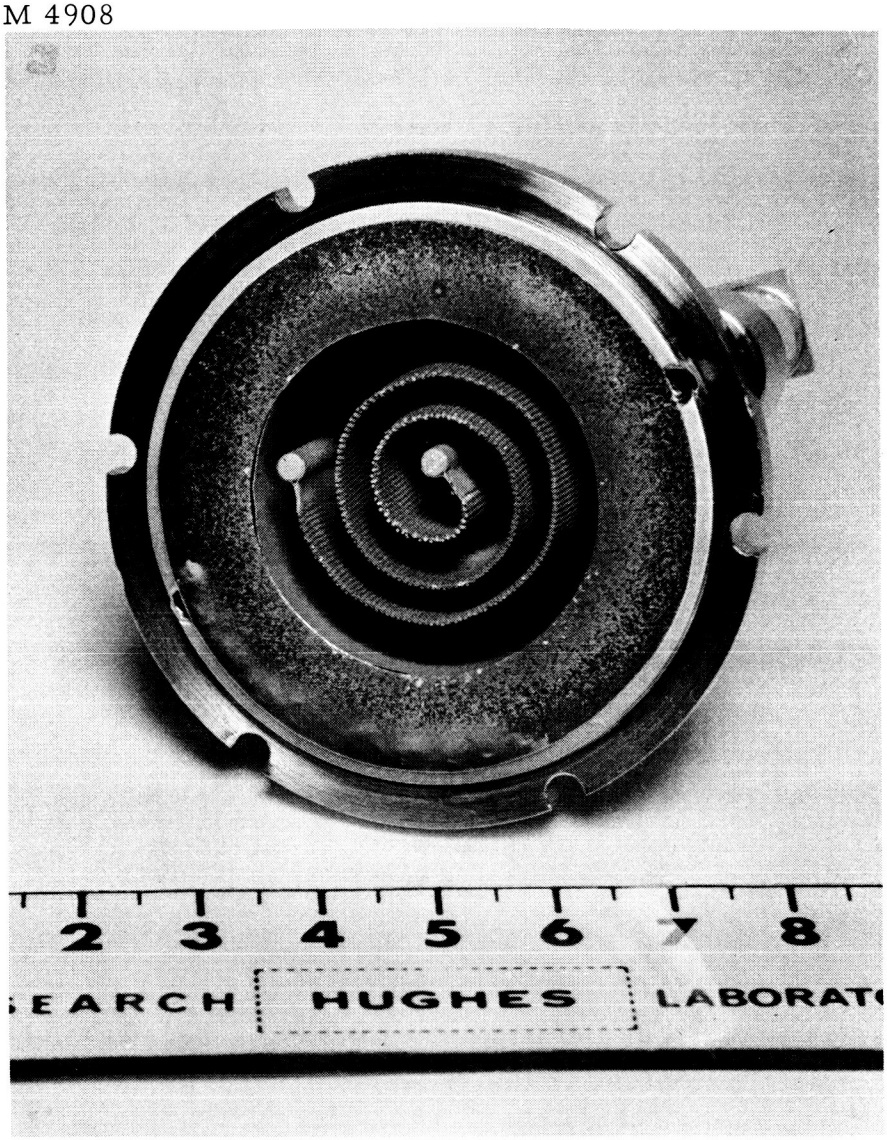

Fig. 39. Cathode after test.

The temperatures stabilized after about 8 hours and remained virtually constant throughout the test. The values given below were recorded at the 515 hour point; except for variations of 1 to 2°C, they are the temperatures which were maintained throughout the test.

	Temperature, °C
Beam No. 7 Transistor	30
Beam No. 7 Plate near Transistor	39
Beam No. 7 Plate near Rectifier	28
Beam No. 6 Transistor	36
Beam No. 6 Plate near Transistor	38
Beam No. 6 Plate near Rectifier	33
Beam No. 5 Transistor	31
Beam No. 5 Plate near Transistor	47
Beam No. 5 Plate near Rectifier	38
Backup Cathode Heater Transistor (Not On)	5
Primary Cathode Heater Plate	28
Primary Cathode Heater Transistor	21
Beam No. 4 Transistor	32
Beam No. 4 Plate near Transistor	41
Beam No. 4 Plate near Rectifier	37
Beam No. 2 Transistor	39
Beam No. 2 Plate near Transistor	47
Cathode Heater Transformer (in Engine Tank)	75

It can be seen from the above data that the thermal characteristics of the power supply were excellent. As was pointed out earlier, the power conditioning was not operating at its power or thermal limit; therefore, it was decided to make a higher power test at the conclusion of the 500 hour life test. The high power test was conducted with no changes made to accommodate the increased power level. Therefore, it was expected that inverter performance

would not be optimum because base drive and base storage had been selected to maximize performance at the original operating point. Furthermore, indium foil had not been used for the module plate-frame interface (except for the cathode heater) because it was not required for the original operating point. For this reason, radiating area sharing (with nonoperating standby modules) was not expected to have maximum effectiveness. Therefore, the thermal results of this test were somewhat conservative. Some redesign would be incorporated if operation at higher power were indicated. In spite of nonoptimum performance, however, the results showed that significantly higher power capability was available with no increase in weight.

The parameters of this increased power test are given in Table VIII. The key values of E_{Beam} = 3600 V and I_{Beam} = 340 mA corresponds to operation at approximately 1.3 times the original power level. Operation at this level was somewhat critical, since the beam trip level was originally set at 350 mA. However, about 1 hour of operating time at this level was obtained, and this time interval was sufficient to establish thermal behavior. The temperature data for this run are also given in Table VIII.

It was not possible to operate at a higher level than 340 mA beam current because of trip level limitations. Changing the trip level required a hardware change which was beyond the scope of the test. From the above data, it may be seen that operation at higher outputs would have been possible. The thermal limit was being approached, however, as may be seen from items 8, 16, and 17. For high reliability operation, 100°C plate temperatures are considered to be maximum. At the conclusion of the high power test, the system was returned to the original operating point to verify that there had been no degradation of power supply performance. System temperatures returned to the values shown for the life test, and the supply was operated in this mode for approximately 2 hours prior to final test termination.

TABLE VIII

Performance at Increased Power

Thruster					
Beam Current, mA	250	288	300	330	340
Beam Voltage, kV	3.90	3.74	3.68	3.62	3.60
Accel Current, mA	1.5	1.3	1.3	1.9	1.7
Accel Voltage, kV	2.7	2.7	2.7	2.7	2.7
Beam Power, W	975	1078	1105	1195	1250
Accel Power, W	10	8	8	13	12
Discharge Power (at 36 V), W	79	101	108	126	133
Cathode Heater Power, W	80	85	87	90	91
Magnet Power, W	60	60	60	60	60
Feed System Power, W	26	26	26	26	26
Neutralizer Power, W	22	22	22	22	22
Total Power to Thruster	1252	1380	1416	1532	1594
Power Conditioning Temperature, ^{o}C					
Beam No. 7 Transistor	34	42	50	68	71
Beam No. 7 Plate near Transistor	43	51	60	71	75
Beam No. 7 Plate near Rectifier	31	38	42	48	50
Beam No. 6 Transistor	41	50	59	71	75
Beam No. 6 Plate near Transistor	43	50	59	67	70
Beam No. 6 Plate near Rectifier	38	43	49	53	57
Beam No. 5 Transistor	36	44	57	71	75
Beam No. 5 Plate near Transistor	51	60	68	80	82
Beam No. 5 Plate near Rectifier	41	49	53	59	62
Backup Cathode Heater Transistor (Not On)	11	13	17	19	22
Primary Cathode Heater Plate	31	37	40	40	41
Primary Cathode Heater Transistor	28	33	36	37	40
Beam No. 4 Transistor	37	45	33	68	71
Beam No. 4 Plate near Transistor	47	59	62	71	73
Beam No. 4 Plate near Rectifier	42	49	52	59	61
Beam No. 2 Transistor	42	51	63	81	88
Beam No. 2 Plate near Transistor	52	59	68	80	83

It may be concluded from both the life test thermal data and the increased power test thermal data that the power supply was not overstressed, and therefore provided a high degree of confidence in its basic reliability. Furthermore, the low operating temperatures are a direct measure of internal dissipation; therefore, the thermal data serve to demonstrate the high efficiency of the supply.

2. Transients

During the life test, the power supply was subjected to over 1500 engine arcs. There were no component failures as a result of these arcs. Furthermore, the supply continually demonstrated the ability to turn off the required voltages and to automatically restart the engine after each arc. After 231 hours, there was a leakage failure in the vacuum chamber which contained the power supply. This failure subjected the supply to a partial pressure while it was still operating at high voltage. Ordinarily this situation would be expected to be catastrophic since breakdown paths would exist to almost every point. However, the supply again demonstrated its inherent transient integrity and no component failures took place. Following this difficulty, close inspection revealed that the only consequence was that six fuses had to be replaced.

The power conditioning system has clearly demonstrated its transient integrity during both integration and life testing. Excellent performance in this difficult design area is essential to successful ion engine operation.

3. Efficiency

Estimates based on theoretical calculations and laboratory measurements of module performance have resulted in a 90% figure for total system efficiency. The excellent thermal behavior of the system described earlier has given a high degree of confidence in this estimate. During the test, an attempt was made to compute

efficiency from measured input and output parameters. The efficiency calculation was based on data taken at the 235 hour point, and the computation is made simply by multiplying all voltages and currents and adding the result to obtain the total power input and output. Based on the data mentioned above, the following is found:

$$\text{Power Out} = 1122 \text{ W}$$
$$\text{Power In} = 1340 \text{ W}$$

The Power In value contains power lost in intercabling and test monitoring, and this loss must be subtracted before the power conditioning system efficiency is computed. This loss is substantially higher than would be expected in vehicle wiring because of the necessity for extensive monitoring (and therefore excessive cable length, meter drops, etc.). All line drops were measured, and the drops were converted to a power loss by multiplying by the various currents. This number was found to be 83 W at the power level used in this efficiency calculation. Therefore, the net Power In to the power supply is given by

$$\text{Power In (Net)} = 1340 - 83 = 1257 \text{ W},$$

and efficiency is given by

$$\eta = \frac{1122}{1257} = 89.8\%$$

This result agrees quite closely with the predicted value. However, there is at least a ±2% uncertainty in the measured value because it is obtained by subtracting two large numbers. Therefore, any error in measuring either of the large numbers can have a significant effect on the calculation. Nevertheless, the close agreement with the prediction coupled with the thermal behavior provides a high degree of confidence in the 90% value.

SECTION VIII

CONCLUSIONS AND RECOMMENDATION

A. CONCLUSIONS

The successful design, fabrication, and life test of an ion engine system built to the specifications assumed in the study phase of the JPL program demonstrates that these systems can be considered as current state of the art. In particular, it has been demonstrated that the power conditioning design is conservative from a weight standpoint. Future systems can be built with no sacrifice in reliability or efficiency at a specific weight of less than 13 lb/kW, depending on the thruster power level (as low as 7 lb/kW at the 3 kW level). In addition to the demonstration of the required system weight and electrical requirements, several other specific observations are worthy of note.

1. Thruster

- The ion optical system showed minimal erosion, indicating an estimated lifetime of roughly one year.
- The HRL flower cathode functioned well throughout the test. After approximately 150 hours, during which time the thermal emissivity was modified by the test environment, the power consumption and temperature remained constant.
- The specified control loop which linked accelerator current and propellant flow was undesirable (see Recommendations).

2. Feed System

- The concept of an electrically isolated feed system was demonstrated. A severe arcing condition developed in the isolator after 400 hours of operation, and improvement in the design of this component is required (see Recommendations).
- The entire feed system performed as specified. Flow control with the simple screen type of vaporizer was adequate.

3. Power Conditioning

- The power conditioning system delivered the 1200 W of power required by the thruster and feed system at operating temperatures well below allowable (40°C versus 70°C design goal).
- No difficulty was experienced with high voltage breakdown due to outgassing.
- No damage due to engine arcs was observed.
- During 50 hour preliminary system test, redundant circuitry replaced faulted modules with no interruption in engine operation.
- Closed loop engine operation holding beam current constant was stable, and overrides functioned as planned.
- Over-all power efficiency of 90% was obtained as estimated.
- System weight of 25 lb for original 1500 W output specification yielded 16-1/2 lb/kW, only slightly over 15 lb/kW target. Target would be easily met with feed system designed for grounded operation, which is now proved feasible. In addition, a total power conditioning capability of 1.8 kW was demonstrated in

short term high power tests providing 14 lb/kW. No failures were experienced in the 500 hour life test of the system after the thermal problems experienced in the 50 hour shakedown were corrected; this verified system reliability estimates. A subsequent detailed reliability analysis of the existing system (to be reported under separate cover) yielded a value of 0.85 reliability for 10,000 hours. It was shown that this could be increased to 0.97 with slight modifications in system design and no weight penalty.

B. RECOMMENDATIONS

This program has revealed there are several areas in which changes in mechanical design or design philosophy would benefit the over-all system. In some cases changes are desirable because it was shown that the initial design was conservative; in some areas, the state of the art has progressed since the system design freeze, and the newer innovations should be considered in future designs. Possibly the most serious deficiency in the total system is the lack of a proven neutralizer which is compatible with this type of thruster. The above and other specific points are listed below.

1. Thruster

- Other control systems should be investigated. A loop which links beam current directly to the propellant feed rate would be particularly desirable to optimize propellant efficiency.
- The suitable neutralizer and the associated control circuitry should be designed and tested.

- The feasibility of using permanent magnet thrusters on spacecraft should be assessed. Permanent magnets would reduce the power consumption here by 50 W (~200 eV/ion), but would require the development of a slightly different startup sequence.
- Once the sizes of the individual thrusters and feed systems are determined, considerable weight and structural improvements may be made in both the thruster and feed system components.
- Long term life tests on cathodes of the type to be used in the final system and under typical operating conditions are desirable to determine life, failure modes, and the range over which control circuits must be expected to function.

2. Feed System

- The present isolator design should be replaced by a metal ceramic model (possibly of a single gap design). This can be vacuum fired for cleaning prior to installation, and will have better thermal characteristics than the glass design.
- A commercial valve may be substituted for the one used here. It would be desirable to use a latching design to reduce power consumption to zero during the running period.
- A feed system recently has been designed and fabricated in which the pressurizer was replaced by a constant force spring. At little or no increase in weight this design eliminates the pressurizer, power supply, and associated temperature controller and also eliminates potential failures caused by ruptured or leaky elastomeric bellows in the pressurizer. The scalability and mechanical properties of large constant force springs should be investigated.

C. SUMMARY

These conclusions and recommendations summarize the most important discoveries of this portion of the program. The program was successful in meeting the initial goals set forth in the RFQ and also in incorporating many novel features as it became desirable to do so during the contract period. The more complete understanding of the system gained from the detailed design and test programs also uncovered several system simplifications and defined areas which require further investigation. The work performed here formed a firm basis for the design of particular propulsion systems for actual space missions.

APPENDIX

OPTIMIZED 1200 W SYSTEM

Figure 40 shows an assembly of modules optimized for the 1200 W demand of the 15 cm engine. This array would be 21 in. by 25 in. by 3 in. deep and would weigh 15.5 lb or 12.9 lb/kW total, including frame, redundancy, and control.

It should be noted here that original NASA estimates of the power demand of the 15 cm engine indicated a total of 1600 W. This requirement, plus the need to demonstrate techniques applicable to larger engines (i.e., 6 kW), resulted in a demonstration system on this contract, capable of 2 kW output, with only 1200 W demand. Hence, the optimized system illustrated results in substantial reduction in size and pounds per kilowatt demand for the demonstration system.

In addition to improvements resulting from optimization for the actual load demand, the optimized system would incorporate weight reductions made possible by a grounded feed system, use of improved transistors (higher frequency), and higher solar cell voltage (60 to 90 V, or original 40 to 60 V). Table IX indicates the wide variation in weight/power ratio for the various supplies required, resulting from varying requirements of control, rectification, filtering, and percent redundancy.

It is particularly interesting to note from Table IX that while the beam supply required 73% of the total power, it accounted for only 38.6% of the weight; the arc supply required only 7.5% of the power and accounted for 13.5% of weight.

The estimated efficiency of the total system is 91%; based on the measured efficiency of the prototype system, this estimate should be reasonably accurate. This number is extremely important

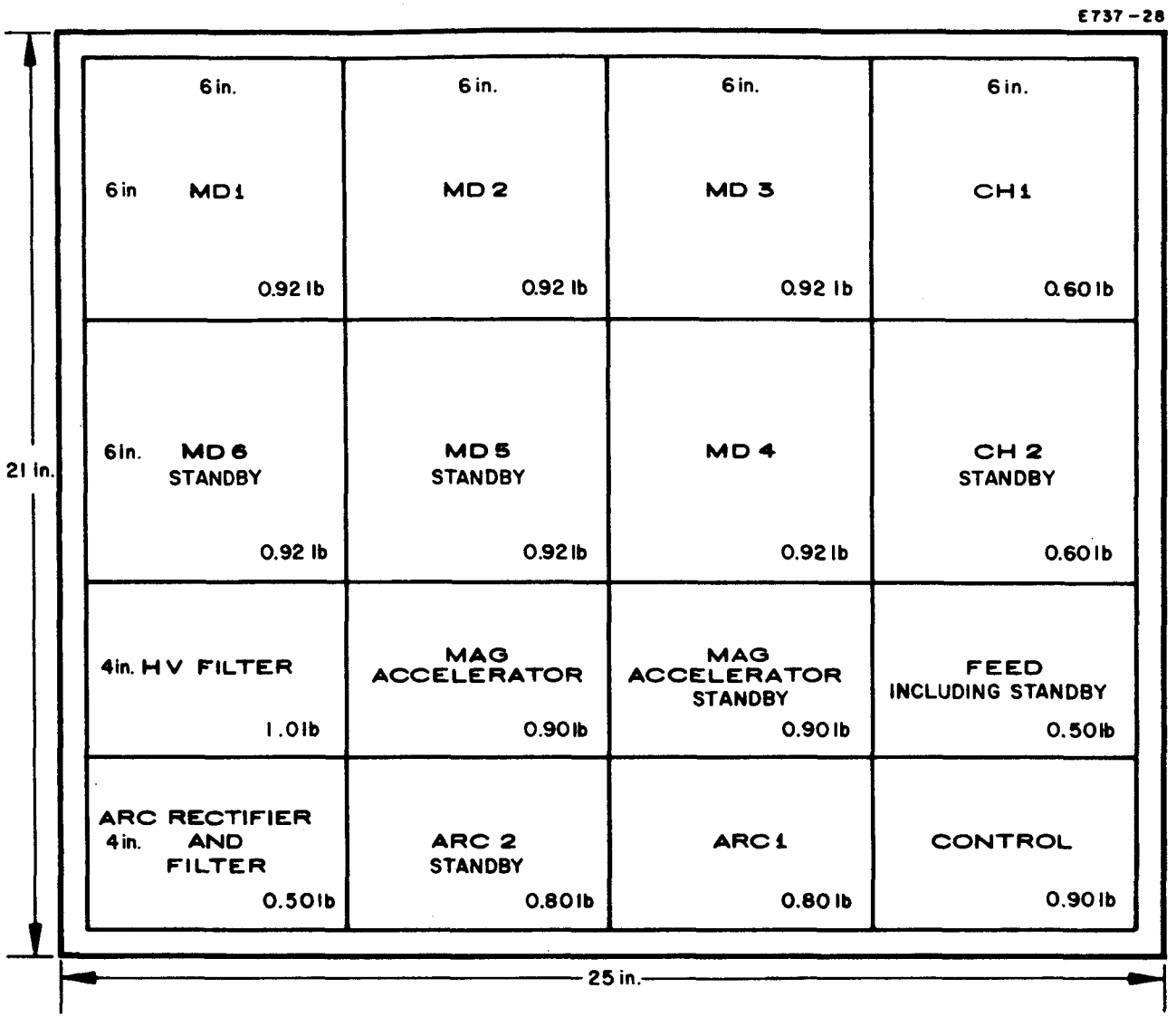

Fig. 40. Assembly of modules for 1200 W demand of 15 cm engine.